If the wise man listens, he will increase his learning,
and the man of understanding will acquire skill

Proverbs

Chapter 1

Verse 5

STUDIES IN NON-DISPERSIVE ATOMIC FLUORESCENCE SPECTROMETRY.

by

Richard Peter Mounce, B.Sc. (London)

A Thesis submitted for the degree of
Doctor of Philosophy of London University.

June 1974

Chemistry Department,
Imperial College of Science and Technology,
London, SW7 2AZ.

ABSTRACT

The first part of this thesis describes the brief history and theory of atomic fluorescence, in terms of the Voigt profile, and derives an expression for the analytical growth curve for a narrow line source. Theoretical comparisons are made between AA and AF techniques and flame and non-flame cells.

Two non-dispersive systems, employing a solar-blind PMT, are described. These were designed to make full use of the fluorescence process.

A comprehensive review is reported on the preparation and operation of electrodeless discharge lamps. Detailed studies are made for a number of difference EDLs, to obtain the optimum brightness.

Each system is rigorously studied to obtain the optimum conditions for the determinations of several elements. The analysis of real smaples, for bismuth and lead, has been successfully completed using the non-dispersive system.

ACKNOWLEDGEMENTS

The work described in this thesis was carried out in the Department of Chemistry, Imperial College of Science and Technology, between October 1971 and June 1974. It is original except where due reference is made and no part has been submitted for any other degree.

I wish to express my thanks to my supervisors, Professor T.S. West, Dr. B.L. Sharp and Dr. R.M. Dagnall for their assistance and encouragement throughout this project, and to the other members of the Analytical Department for their helpful suggestions and discussions, in particular G. Thompson.

I am indebted to the Ministry of Defence for its financial support of this work.

Finally, I would like to thank both Rosemary Parker and John Moore, for the significant moral support they have given to me over this period.

CONTENTS

Chapter 1

1.1. History of atomic fluorescence spectroscopy.

The full potential of atomic fluorescence spectrometry as an analytical technique was not fully appreciated until the first investigation by Winefordner et al in a series of papers starting in 1964 (21, 22, 23, 24). They used metal vapour discharge lamps as irradiating sources and nebulised solutions into flames maintained on total consumption burners. They were able, with perhaps not the most ideal conditions to obtain detection limits for certain elements (Zn, Cd, Hg) below those obtainable in atomic absorption spectrometry. Also at this time, completely independent work in atomic fluorescence was being carried out at this college by West et al (26).

The first atomic fluorescence was reported as early as 1904 by Woods (1). This worker excited atomic fluorescence of the sodium D lines by irradiating the metal vapour, enclosed in a glass vessel, with atomic line emission from a flame containing sodium chloride. Prior to this work only banded molecular fluorescence spectra had been observed, although classical atomic theory (2) predicted that fluorescence should follow absorption for atoms in the gaseous state.

Following this work, the atomic fluorescence of lithium (3), caesium (4), mercury (5), cadmium (6), zinc (7), thallium, lead, bismuth, antimony (6), and manganese (8), was observed. In each instance the element concerned was sealed into an evacuated quartz vessel and its vapour pressure controlled by the temperature of a containing oven. The sources of excitation were generally vacuum arcs of either the type described by Elett (9), in which the metal is held in the side arm and its vapour pressure maintained by an oven, or the Schuller tube (10) which is a fore-runner of the present day hollow cathode lamp. However, vapour discharge lamps (1, 6, 7,) and flame sources (1, 3) were also used.

The spectroscopic data and scope of this early work were limited to those elements with vapour pressures about 10^{-4} torr at the maximum furnace temperature available (less than 1200 C):this allowed a detailed examination

of the fluorescence process to be made. An excellent summary of much of this work has been made by Mitchell and Zemansky (2).

Until 1966, atomic fluorescence spectroscopy, like atomic absorption spectroscopy, had been primarily used in astrophysics for the study of the composition of gaseous atmospheres associated with stellar bodies. However, a few workers in the interim period had extended the range of the technique, by showing that flames could also serve as suitable atom reservoirs and it is this discovery that has led directly to the exploitation of atomic fluorescence spectroscopy as a spectrometric technique for trace analysis.

The first study of this nature was made by Nichols and Howes (11) in 1923 in the course of a qualitative examination into the fluorescence of several elements, and they obtained weak signals from high concentrations of sodium, lithium, calcium, strontium, and barium. Later studies in the same field were made by Badger (12) and Mankopff (13). However, in this and more recent work by Boers' Alkemade and Smit (14), Robinson (25), Hooymayers and Alkemade (15) and Jenkins (16, 17, 18, 19, 20) the primary objective was to obtain information about excitation mechanisms (11, 15) or fluorescence quantum efficiencies (14, 15, 16, 17, 18, 19, 20). As such these spectroscopy studies were the precursors of modern atomic fluorescence spectrometry.

In 1962 at the Colliquium Spectroscopicum Internationale, Alkemade (27) gave a paper on mechanisms of excitation and deactivation of atoms in flames. He described the use of an atomic fluorescence method for the determination of quantum yields and indicated the same method as having possible analytical application, which was firmly established for analytical use by Winefordner.

Since then, the technique has developed very rapidly in an effort to lower the detection limit, expand the analytical linear range and the number of elements that can be determined by atomic fluorescence spectrometry.

Various sources have been used; in the early developments D.C. arcs, vapour discharge lamps and continium xenon arcs were used. Hollow cathode lamps, especially the high intensity variety were tried but electrodeless discharge lamps are now generally accepted as the most commonly available

intense atomic line sources. These may well be replaced by lasers, when their spectral range is extended and their high cost is reduced.

During the development of atomic spectrometry various atom reservoirs have been used. In the earliest stages of the technique total consumption burners were used. But they were soon replaced by premixed laminar flow burners supporting various gas compositions eg air/propane, air/acetylene and nitrous oxide/acetylene. Further improvements were gained by the development of capillary burner heads, as various flame geometries could be obtained (retangular, circular) compared with the former single slot burner. This type of head provided further improvement as the flame's primary reaction zone can be separated from the secondary zone, first developed in this department. Low noise flames of high luminosity and also diffusion flames have found particular application in atomic fluorescence.

During the same period, considerable advances were made in entirely different kinds of atom reservoirs. The non-flames, reviewed recently by Kirkbright (102), commonly produce atomisation in an inert gas medium from some form of electrically powered heating device. The L'vov cell, King/Massmann tube and West filament all used carbon and an inert support gas to develop the necessary temperature for atomisation. Hwang, used a tantalum strip and other workers using a hot-wire loop made use of metallic materials electrically heated in an inert support gas.

The detection of the signal is usually made by a photomultiplier tube (PMT) housed in a monochromator which restricts the spectral region viewed. The signal developed can be treated in several different ways. Direct current measurements with amplification have been extensively used. Some advantage can be gained by the use of alternating current measurements using lock-in-phase sensitive amplification for steady state signals. Other workers have used various forms of integration on D.C. transient signals, including the photon counting technique. Recent developments have been made, where the signal is not dispersed by a monochromator but viewed directly with a solar blind PMT, photodiodes, or silicon vidicons.

1.2. Atomic Fluorescence Spectrometry.

1.2.1. Types of fluorescence.

In atomic fluorescence spectrometry, atoms are excited by the absorption of radiation of the requisite frequencies and then deactivate by the emission of radiation of the same or lesser frequency. The frequency of the radiance indicates the type of atomic fluorescence transitions taking place:-

1) Resonance fluorescence (Zn) in which the same lower and upper levels are involved in the excitation-de-excitation processes.

2) Direct line fluorescence (Sb) in which the same upper level is involved in the radiational excitation-de-excitation processes.

3) Stepwise line fluorescence (Na) in which different upper levels are involved in the excitation-de-excitation processes.

4) Sensitized fluorescence where one species is excited (donor) (Tl/Hg) and transfers excitation energy to an atom of the same or another (acceptor) either of which de-excites radiationally;

5) Multiphoton fluorescence, where two (or more) identical photons excite an atomic species which then radiationally de-excites.

If the excitation energy is greater than the fluorescence energy then this type of fluorescence is termed Stokes, and if the fluorescence energy is greater than the excitation, then this type of fluorescence is termed anti-Stokes. If the radiational excitation and radiational de-excitation (fluorescence) process involves only excited states, then the fluorescence process is said to be excited. The process could be called unexcited when the ground state is involved in both excitation and fluorescence; however it is unnecessary since most AF studies involve the ground state. If the excitation process involves a collisional excitation following the radiational excitation process, then the process is said to be thermally assisted (Bi), In fig. (1) all possible types of AF processes are described. Most of the processes described have been or should be of analytical use especially with laser excitation (28).

1.3.1. Theory of atomic fluorescence spectrometry.

1.3.2. General.

The frequency of the emitted radiation (fluorescence) is also characteristic of the absorbing atoms and the intensity of this emission may be used as a measure of their concentration. The intensity of the emitted radiation should be dependent on the fraction of exciting radiation absorbed, on the efficiency of conversion of absorbed radiation to emitted radiation, on the fraction of emitted radiation self-absorbed by similar ground state atoms, and on the brightness of the radiation from the source of excitation.

Thus atomic fluorescence has characteristics that resemble atomic aborption. However, we have to consider the extra factor when dealing with atomic fluorescence, that is the quenching factor p.

fig.1

TYPES OF ATOMIC FLUORESCENCE TRANSITIONS

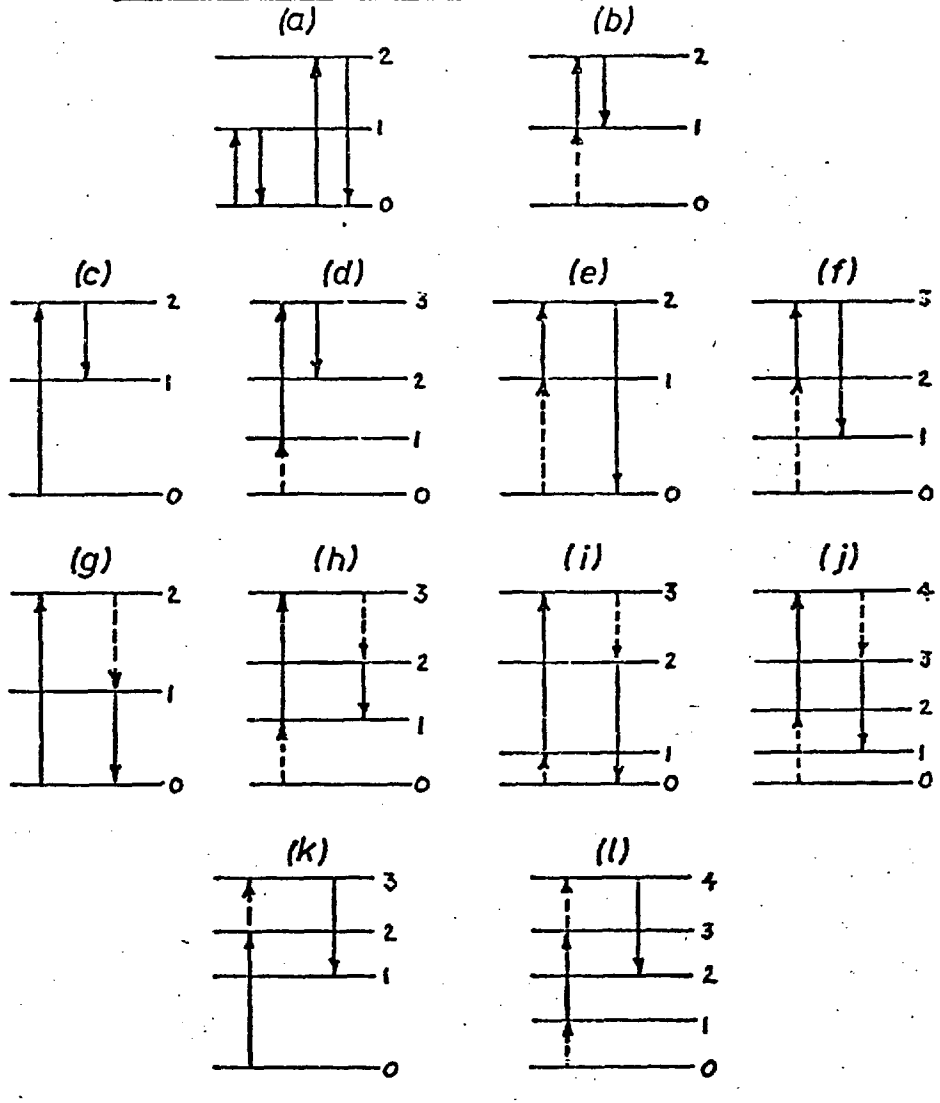

a) resonance (either process)
b) excited state resonance
c) Stokes direct line
d) excited state Stokes direct line
e) anti-Stokes direct line
f) excited state anti-Stokes direct line
g) Stokes stepwise line
h) excited state Stokes stepwise line
i) anti-Stokes stepwise line
j) excited state anti-Stoke stepwise line
k) thermally assisted stepwise line
l) excited state (k)
m) sensitized
n) two photon excitation

Where p is the probability that an excited state will undergo radiational de-activation before being deactivated by collisions, thus giving the energy up to other species eg CO, N_2, H_2, in vibrational/electronic transitions. The same, of course, applies to atomic emission but normally we do not consider p since we have little control over it. However, in fluorescence, particularly non-flame fluorescence we can choose an appropriate gas to keep p high.

1.3.3. Discussion of establishing the model.

A general expression will be derived under idealised conditions for the integrated resonance fluorescence intensity that is emitted in the direction perpendicular to the existing light beam and flame axis (29). Consider an idealised shielded flame which has a uniform temperature throughout its bulk, and calculate the total or integrated fluorescence flux emitted into the small solid angle d at right angles to the incident radiation. The treatment will be for the Voigt profile for which the crucial parameter is the damping ratio a.

$$a = \frac{\Delta\nu_L}{\Delta\nu_D}\sqrt{\ln 2} \qquad \text{eqn.(1)}$$

where a is the damping parameter

$\Delta\nu_L$ is the Lorentz half-width $sec.^{-1}$

$\Delta\nu_D$ is the Doppler half-width $sec.^{-1}$

The Voigt profile represents the most common profile under analytical conditions, and is the mathematical result of the convolution of the Doppler and Lorentz profiles.

The width of a line depends on a number of factors:-

1) The natural line width due to the finite time that the atom is in the excited state.

2) Doppler broadening due to the random thermal motions of the atoms.

3) Lorentz broadening due to the collisions between atoms and foreign support gas, atoms and molecules.

4) Holtzmark broadening due to collisions between atoms of the same kind.

5) Stark broadening due to electric fields which may be internal (ions or

electrons) or external. For flames, and particularly non-flame atom reservoirs we may ignore all but Doppler and Lorentz broadening.

Also we will consider that the flame or atom cell has uniform ground state distribution. Let the exciting beam be parallel and homogeneous and have a cross sectional area A = 21 x 21' (21' goes down into the page see fig. 2).

The flux contribution from re-emission of self absorbed fluorescence radiation will be ignored. Also, only a single absorption line is considered. The hyperfine structure as a result of the presence of several isotopes absorbing radiation at slightly different wave lengths is ignored as is the contribution to the broadening made by the Holtzmark and the Stark effects.

1.3.4. Spectral flux; general equation.

From Beer's law :-

$$I = I_0 . \exp^{-\alpha.c.x} \qquad \text{eqn.(2)}$$

we know that

$$I_\nu.(x) = I_\nu\ (o).\exp.^{-k_\nu.x} \qquad \text{eqn.(3)}$$

where I is intensity of radiation at plane (x) watts.m^{-2}

I_0 is incident intensity watts.m^{-2}

α is absorptivity

x is length of the absorption cell m

c is concentration $g.l^{-1}$

where I_ν is intensity of radiation at frequency ν/unit freq. interval at plane (x) watts.m^{-2}.sec.

$I_\nu(o)$is incident intensity of radiation at freq. ν /unit freq. interval at plane (o) watts.m^{-2}.sec.

fig.2

a) IDEALISED FLAME CROSS SECTION (FROM ABOVE)

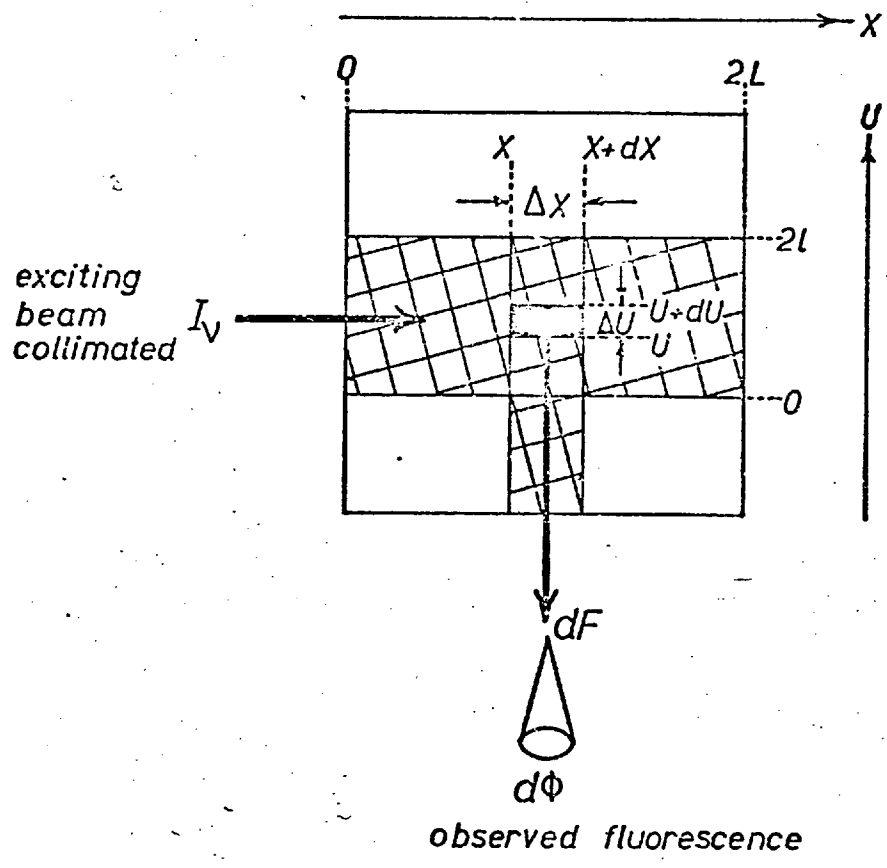

b) ANALYTICAL CURVES FOR NARROW LINE SOURCE

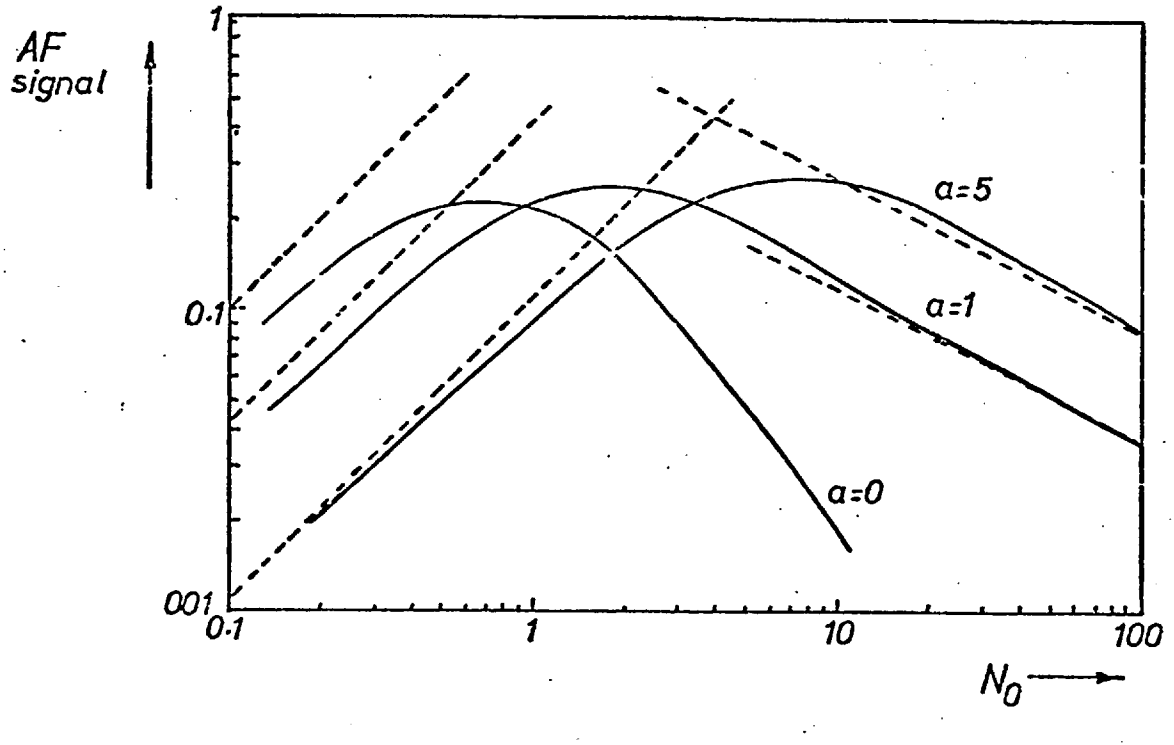

k_ν is absorption coefficiency at freq. ν $\quad m^{-1}$

x is length of absorption cell $\quad m$

Thus the intensity of the beam at the plane x is given by:-

$$I_\nu . \exp^{-k_\nu . x} \qquad w.m^{-2}.s \qquad \text{eqn.(4)}$$

since we are dealing not with integrated intensity but with the intensity per unit frequency interval in the interval $\nu \rightarrow \nu + d\nu$. Now we know also from Beer's law that the decrease in energy of a beam is

$$-dI_\nu = k_\nu . I_\nu . dx \qquad w.m^{-2}.s \qquad \text{eqn.(5)}$$

or $$-dI_\nu = k_\nu . A . I_\nu . dx \qquad w.s. \qquad \text{eqn.(6)}$$

where $$A = du.2l' \qquad m^2$$

now we have

$$I_\nu = I_\nu(o) . \exp^{-k_\nu x}$$

Thus the energy absorbed in the element dx. A or (dx. du. $2l'$) (which will be positive in sign rather than negative when refered to the element) is:-

(flux) $$dF_\nu = k_\nu (du.2l').I_\nu \exp^{-k_\nu x} dx \qquad w.s. \qquad \text{eqn.(7)}$$

Now we are interested the integrated energy absorbed per second over all frequencies by the layer of absorbing atoms.

Therefore $$dF = du.2l'.dx. \int_o^\infty k_\nu I_\nu . \exp^{-k_\nu x} d\nu \qquad w. \qquad \text{eqn.(8)}$$

We require the flux dF emitted at right angles to this volume through a small solid angle $d\phi$. Of course all the flux is not emitted, a fraction p (fluorescence yield factor) comes into it to allow for quenching. The self-absorption can be taken account of by merely carrying out the same calculation as above using the atomic emission generated by the initial absorption process. Thus let us define atomic emission by its profile $\alpha_{\nu'} = f(\nu')$

where $\alpha_{\nu'} . d_{\nu'}$ is the fraction of photons that have energies in the

range $\nu' \rightarrow \nu' + d\nu'$ and as usual :-

$$\int_0^\infty \alpha_{\nu'} . d_{\nu'} = 1 \qquad \text{eqn.(9)}$$

Where this is the normalised shape of the spectral line not distorted by self absorption. Now we must note that $\alpha_{\nu'}$ is independent of I_ν the shape of the exciting line, ie the fluorescence line profile is independent of the shape of the exciting line except at a very low pressure, where collisional processes do not have a chance to redistribute the profile over all the Doppler and Lorentz intervals. Note we are now using ν' since $I_\nu(o)$ and $k_\nu(o)$ may be located at differenct points in ν eg ν'.

The total energy absorbed as calculated in watts is equivalent to B_0 The fraction of this that will be emitted in the wavelength interval ν' to $\nu' + d\nu'$ into each steradian is:-

$$dF_{\nu'} = \frac{d\phi}{4\pi} B_0 \, p \, \alpha_{\nu'} \qquad \text{eqn.(10)}$$

where $dF_{\nu'}$	is flux/intensity at a particular freq.	$w.st^{-1}$ s.
$\frac{d\phi}{4\pi}$	is the solid angle of viewing	st.
B_0	is the total energy absorbed	w.
p	is fluorescence yield factor	
$\alpha_{\nu'}$	is the emission profile	s.

The self absorption can be calculated simply from Beer's law at the frequency ν considering the flux at the edge of the flame due to the excited segment. Now the emission profile and the absorption profile will be the same ie

$$\alpha_{\nu'} = k_{\nu'} \qquad \text{eqn.(11)}$$

where $k_{\nu'}$ absorption coefficient at freq. ν' $cm.^{-1}$

Now $$\int k_{\nu'} d\nu' = \frac{\lambda_o^2 \cdot g_k \cdot A_{ki} \cdot N_o}{8\pi \cdot g_i} \qquad \text{eqn.(12)}$$

where λ_o central wavelength of emitted flourescence radiation m^{-1}

N_o ground state atom concentration $g\ l^{-1}$

A_{ki} transition probability for the transition under consideration s^{-1}

and $$\int \alpha_{\nu'}\, d\nu' = 1 \qquad \text{eqn.(13)}$$

therefore $$\int k_{\nu'}\, d\nu' = c \int \alpha_{\nu'} d\nu' \qquad \text{eqn.(14)}$$

$$= \frac{\lambda_o^2\ g_k\ A_{ki} N_o}{8\pi\ g_i} \int \alpha_{\nu'} d\nu'$$

therefore $$\alpha_{\nu'} = \frac{k_{\nu'} 8\pi\ g_i}{\lambda_o^2\ g_k\ A_{ki}\ N_o} \qquad \text{eqn.(15)}$$

where g_{ki} are the statistical weights of the ground (i) and upper (k) energy levels involved in the absorption transitions respectively.

The brightness at the edge of the flame due to the excited segment is given by Beer's law as :-

$$B_{\nu'} = \alpha_{\nu'} \exp^{-(k_{\nu'}[L-l+u])} \qquad \text{eqn.(16)}$$

$w.st^{-1}.s$

for the interval $\nu' \rightarrow \nu' + d\nu'$. Thus taking all frequencies :-

$$\int B_{\nu'} = \int_o^{\infty} \alpha_{\nu'} \exp^{-(k_{\nu'}[L-l+u])}\, d\nu' \qquad \text{eqn.(17)}$$

$w.st^{-1}$

where $(k_{\nu'}[L-l+u])$ accounts for the loss in fluorescence intensity due to self absorption in the flame.

Making the relevant substitutions we obtain the total flux dF emitted into the small angle $d\Phi$.

$$dF = \frac{d\phi}{4\pi}\left[\frac{du\, 2l' dx\, p 8\pi g_j}{\lambda_o^2 g_k A_{ki} N_o}\int_o^\infty k_\nu I_\nu\, e^{-k_\nu x} d\nu\right]\left[\int_o^\infty k_{\nu'} e^{-k_{\nu'}(L-l+u)} d\nu'\right] \qquad \text{eqn.(18)}$$

This is the flux contibution from $\Delta x . \Delta u$ but of course all elements within the beam will be emitting and absorbing radiation simultaneously and therefore to obtain the total flux from the illuminated segment we must integrate

$dx \qquad 0 \longrightarrow 2L \qquad$ and $\qquad du \qquad 0 \longrightarrow 2l$

Thus the total outgoing flux of fluorescent radiation observed is :-

$$\int_0^{2L}\int_0^{2l} dF dx du = \frac{d\phi 2l' p 8\pi g_j}{4\pi\lambda_o^2 g_k A_{ki} N_o}\left[-\int_o^\infty I_\nu \frac{k_\nu}{k_\nu}(e^{-k_\nu x})_0^{2L} d\nu\right] \text{-----} \qquad \text{eqn.(19)}$$

$$\text{----}\left[\int_o^\infty \frac{k_{\nu'} e^{-k_{\nu'}(L-l)}}{k_{\nu'}}(e^{-k_{\nu'} u})_0^{2l}\, d\nu'\right]$$

$$= \frac{d\phi 2l' p 8\pi g_j}{4\pi\lambda_o^2 g_k A_{ki} N_o}\left[\int_o^\infty I_\nu(1-e^{-k_\nu 2L}) d\nu\right]\left[\int_o^\infty e^{-k_{\nu'}(L-l)} e^{-k_{\nu'}(L+l)} . d\nu'\right] \qquad \text{eqn.(20)}$$

1.3.5. Equation in terms of the Voigt profile.

Now this is a general expression and does not relate to the profile of either I_ν or k_ν . It is convienient to express k_ν in terms of the Voigt profile, (30,31) which we know represents most common analytical conditions.

$$V(a,w) = B_\nu d_\nu \qquad \text{eqn.(21)}$$

We can write the absorption profile in the form

$$k_\nu = k_0 \qquad \text{(distribution function)}$$

$$k_\nu = k_0 B_\nu d_\nu = k_0 V(a,w) \qquad \text{eqn.(22)}$$

$$k_\nu = k_0 \frac{a}{\pi}\int_{-\infty}^{+\infty} \frac{e^{-y^2} dy}{a^2+(w-y)^2} \qquad \text{eqn.(23)}$$

where the integration variable

$$y = \frac{2\delta\sqrt{\ln 2}}{\Delta\nu_D}$$

where δ is the frequency difference

The damping parameter $$a = \frac{\Delta\nu_L \sqrt{\ln 2}}{\Delta\nu_D}$$

$$w = \frac{2(\nu - \nu_0)\ln 2}{\Delta\nu_D} \qquad \text{eqn.(24)}$$

The variable is now w instead of $(\nu - \nu_0)$

Substituting for $V(a,w)$ instead of I_ν , k_ν and noting that

$\int_{-\infty}^{+\infty}$ symmetrical function = $2\int_0^\infty$ symmetrical function

The Voigt profile is symmetrical - observed profiles are not. We have:-

$$dF = \frac{d\phi\, 2l' p\, 8\pi\, g_j}{4\pi\lambda_0^2 g_k A_{ki} N_0}\left[2\int_0^\infty I_w(1-e^{-k_0 V(a,w)2L}dw\right]\text{----} \qquad \text{eqn.(25)}$$

$$\text{----}\left[2\int_0^\infty e^{-k_0 V(a,w')(L-l)} - e^{-k_0 V(a,w')(L+l)}\, dw'\right]$$

We may note at this point that whilst the exciting beam profile k_ν or I_ν was independent of the emitted profile $k_{\nu'}$ or $B_{\nu'}$, that k_0 is in fact the same value for both, since similar atoms are involved. k_0 is the absorption coefficient at the line centre due to the purely Doppler broadened line. The centre of the Voigt line is best represented by a Doppler profile. Thus:-

$$k_0^D = \frac{N_0\sqrt{\ln 2}\ \lambda_0^2 A_{ki} g_k}{16\pi^{3/2}\ \xi_0\ \Delta\nu_D\, g_j} \qquad m^{-1} \qquad \text{eqn.(26)}$$

Where ξ_0 is the permitivity of free space and converts c.g.s. theory to s.i. units.

Using a dimensionless variable $k_0 = \xi = \text{constant}\ L\, N_0$ eqn.(27)

Thus substituting yields :-

$$dF = \frac{d\phi\ \delta\ p \ln 2\ 4L}{4\pi\ \xi\ l\ \varepsilon_0 \Delta\nu_D \pi^{1/2}}\left[\int_0^\infty I_w(1-e^{-k_0 V(aw)2L})dw\right]\text{----} \qquad \text{eqn.(28)}$$

$$\text{----}\left[\int_0^\infty e^{-k_0 V(a,w')(L-l)} - e^{-k_0 V(a,w')(L+l)} dw'\right]$$

where $\delta = 2l.2l'$ is the cross sectional area of the beam. This is the final expression for a generalised exciting beam and Voigt absorption profile. The evaluation of dF is difficult because we do not always know I_w and, if we do, the mathematics is still complex. However we can consider limiting cases.

1.4.1. Analytical growth curves for narrow line sources.

Narrow line sources $\Delta\nu_E \ll \Delta\nu_A$

In the case of a narrow line exciting source we essentially deal only with the centre of the exciting line as the half width is small compared to the absorption line half width and therefore we do not concern ourselves with $V(a,w)$ but $V(a,o)$.

ie

$$V(a,\sigma) = \frac{a}{\pi}\int_{-\infty}^{+\infty}\frac{e^{-y^2}}{a^2+y^2}\,dy \qquad \text{eqn.(29)}$$

$$= \frac{1}{\sqrt{\pi}}\int_o^{\infty} e^{-az-\frac{z^2}{4}}\,.\,dz$$

$$= e^{a^2}(1-\operatorname{erf} a)$$

where $$\operatorname{erf}(a) = \frac{2}{\sqrt{\pi}}\int_0^a e^{-t^2}dt \qquad \text{eqn.(30)}$$

and, $\operatorname{erf}(a)$ is the error function ie the Gaussian integral to limit a unsolvable except by tables of normal distribution.

Also we can deal with $I = \int_o^{\infty} I_\nu\, d_\nu$ rather than I_ν or I_o

Now under these circumstances the $\Delta\nu_D$ of the equation disappears and we have

$$\frac{dF}{\frac{d\phi\,l\,\delta\,p\,4}{4\pi\,\varepsilon_o}} = \frac{L}{\pi\,\xi\,l}(1-e^{-V(a,o)zg\,\varepsilon_o}) \qquad \text{eqn.(31)}$$

$$\int_o^{\infty}\left(\left[1-\exp\{-V(a\,w)\xi(1+l/L)\}\right]-\left[1-\exp\{-V(a\,w)\xi(1-l/L)\}\right]\right)dy$$

Thus dF can be calculated using the tabulated values of Van Trigt (47) who derived the growth curves for $l/L = 0.25$ for $a = 0,1,5$. We should note that we still have $V(a,w)$ for the emission line which is unaffected by the exciting line shape. Again the low density case has a simpler solution than the general case.

1.4.2. Low density case.

Using the first terms of e^x again we have:-

$$dF / \frac{d\phi \, l \, \delta p \, 4}{4\pi \, \varepsilon_0} = \xi \, V(a,o) = \xi (e^{a^2}(1-\mathrm{erf}\, a) \qquad \text{eqn. (32)}$$

when $a \ll 0.1 \qquad (e^{a^2}(1-\mathrm{erf}\, a) \simeq 1$

$a \gg 5.0 \qquad (e^{a^2}(1-\mathrm{erf}\, a) \simeq 1/a\sqrt{\pi}$

Therefore for narrow line absorption:-

$$dF / K' = \xi = N_0 \, L \, \text{const.}$$

where K' is a constant.

ie

$$\underline{\underline{dF \propto N_0}}$$

The atomic fluorescence signal is proportional to the ground state atom concentration in the flame.

However, when the absorption line is broader, k_0 drops off (large a values associated with broad absorption lines).

since $\int_0^\infty k_\nu \, d_\nu$ is independent of line width.

Thus the initial absorption is less and so is the corresponding fluorescence which we can see since :-

$$dF / K' = \xi / a\sqrt{\pi}$$

1.4.3. High density case.

Again we use the same approximation as above. Thus for small a

ie $$e^{a^2}(1-\text{erf } a) = 1$$

$$dF/K' = \frac{L}{\pi l \xi} \xi^{1/2} a^{1/2} \pi^{1/4} ((1+l/L)^{1/2} - (1-l/L)^{1/2}) \qquad \text{eqn.(32 a)}$$

Therefore $$dF/K' = \frac{a^{1/2}}{\xi^{1/2}\pi^{3/4}} (1 + (l/L)^2 + \cdots\cdots) \qquad \text{eqn.(33)}$$

For $l/L = 0.25$ the expression approximates to :-

$$1/2.\ a^{1/2} / \xi^{1/2}\pi^{3/4}$$

In the limiting case of $l/L = 1.0$ we have,

$$dF/K' \approx \frac{a^{1/2}}{z^{1/2}\xi^{1/2}\pi^{3/4}} = \frac{\text{const.}}{\sqrt{\xi}} \qquad \text{eqn.(34)}$$

Therefore dF/K' is proportional to $N_0^{-1/2}$

ie curve slopes down with a log log plot having a slope of - 0.5.

Because ξ = const. N_0 and that with narrow line sources the absorption of exciting radiation apporaches 100 percent and thus becomes independent of N_0, it can be seen from the results that for a constant amount of absorbed energy the outgoing resonance fluorescence flux behaves for $a \neq 0$ as $1/N_0$ for N_0 tending to infinity.

1.4.4. Other factors effecting the growth curve.

The equations for the limiting case also reveal the direct proportionality between 1) Fluorescence efficiency

2) Source intensity

3) Solid angle over which the fluorscence is stimulated and measured

4) Absorption line oscillator strength

and 5) Path length in the atom cell.

It is, therefore, possible to optimise these papameters to obtain greatest radiant power of fluorescence at the detector (32).

The analytical curve, ie the plot of log S versus log C, where S is the instrumental signal due to the total flux dF, and C is the analyte concentration

introduced into the atomiser cell, has essentially the same shape as log dF *vs.* log N_0 (fig.2b). However some deviation from log dF *vs.* log N_0 may result at low concentrations owing to ionization of analyte atoms, and at high concentrations owing to decreased sample introduction rate into the atomiser, *eg* flame studies, reduced solute vaporisation rate, and reduced nebuliser yield. Also incomplete illumination of the cell, incomplete measurement of atomic fluorescence over the cell area towards the detector, non-parallel exciting or fluorescence radiation, and cell shapes other than rectangular shape will all contribute to the experimental analytical growth curves deviating from that calculated from the theoretical model (33).

1.5. Analytical sensitivity of atomic fluorescence.

The sensitivity of atomic spectrometry for the determination of a particular element may be defined in relation to the analytical signal to noise ratio obtained with optimised conditions, (32). If such a ratio is evaluated for atomic emission, AE, atomic absorption, AA, and atomic fluorescence, AF, then comparison of relative limits of detection obtained with these three methods is possible. Assuming that the same resonance line of the same atom is measured by the same instrumental system and that the same atomiser is used for all three methods, then it can be shown that AE should result in lower limits of detection than AF and AA for atoms with resonance lines above approximately 400nm and AF (and sometimes AA, especially for high temperature flames) should result in lower limits of detection than AE for atoms with resonance lines below approximately 300nm. All methods should give similar results for atoms with resonance lines in the intermediate region 300 to 400nm (see fig. 3a).

fig.3

a) THEORETICAL PREDICTION OF WAVELENGTH RANGE OVER WHICH VARIOUS ATOMIC FLAME SPECTROSCOPIC METHODS ACHIEVE LOWEST LIMITS OF DETECTION.

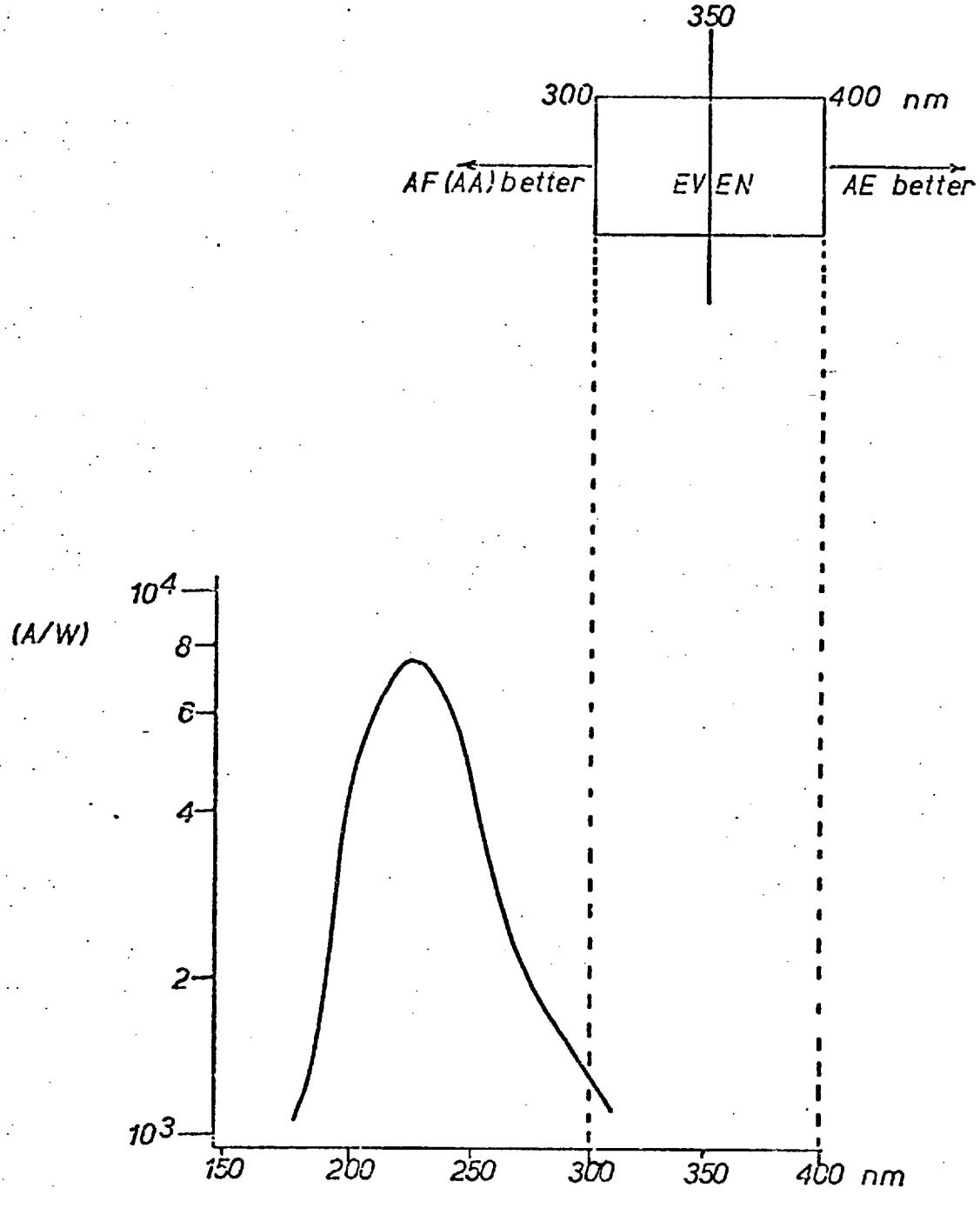

b) TYPICAL ANODE RADIANT SENSITIVITY CURVE FOR A Cs-Te PHOTOCATHODE

1.5.1. AA versus AF spectrometry.

Winefordner (34) has shown, utilising the ratio of absolute signals in AA and AF for sharp lines source and dilute atomic vapours that:-

$$\frac{\text{AA signal}}{\text{AF signal}} = \frac{(p\ \phi)^{-1}}{4\pi} \qquad \text{eqn.(35)}$$

where $\phi/4\pi$ is the fractional solid angle of radiation collected by the detector entrance optics. The value of p , the fluorescence yield, for a particular fluorescence transition, will depend on the type of fluorescence and on how much quenching of fluorescence occurs in the cell; resulting in values of p typically far below unity, eg 0.1. Also if a grating or prism monochromator is employed to select the wavelength of the fluorescence emission, $\phi/4\pi$ is often ca 0.01.

Thus under these conditions the ratio of AA signal/ AF signal may be ca 10^3. However, the AF signal strength may be increased considerably by using sources of high radiance (EDLs, lasers) and large aperture detectors (direct viewing by solar-blind photomultipliers, interference filter devices). Nevertheless, the absolute signal strength in AF rarely exceeds that obtained in AA.

In both techniques the detection limit depends primarily on the signal to noise ratio obtained and, that the sources used are of high radiance. Near the limit of detection, the ratio of AA noise /AF noise will exceed the ratio AA signal /AF signal. Source flicker and all background flicker noise are dominant in AA, and shot noise and cell background flicker noise are dominant in AF. Thus when usingeither flame or non-flame cells, the ratio AA noise /AF noise always exceeds unity, since source flicker always greatly exceeds all background flicker. In this case, AF will have superior detectability, particularly where the fluorescence emission can be collected over a large solid angle eg non-dispersive system.

In summary AF will yield superior limits of detection and greater range of linear response on the analytical growth curve at AA, and since the Cs-Te photocathode spectral response (fig. 3) shows maximun sensitivity at 250 nm,

it is therefore ideally suited for measurement in the appropriate spectral region.

1.6. Theoretical comparison of flame and non-flame cells.

The advantages of non-flame cells are :-

1.6.1. Increased atomic concentration.

The concentration of analyte atoms in a flame (atoms $cm.^{-3}$) is related to the concentration of analyte (moles. l^{-1}) in the solution nebulised into the flame (31,35,36) by

$$n = 1 \times 10^{19} F \varepsilon \beta C / Q e f \qquad \text{eqn.(36)}$$

where F denotes solution transport (flow) rate $cm^3.min.^{-1}$

ε is the efficiency of producing a gas of the analyte in the flame- the efficiency of nebulisation.

β is the efficiency of producing atoms from the gaseous analyte- the efficiency of atomisation.

ef is the flame gas expansion factor due to the increase in temperature of gas from room temperature and increase in number of moles of flame gas products.

Q is the flow rate of unburnt gases into the flame $cm.^3sec^{-1}$.

The atomisation efficiency, β, is the ratio of the concentration of free analyte atoms in the flame to the total concentration of analyte in all gageous forms (37). This factor accounts for incomplete dissociation of the analyte compound introduced into the flame, for the formation of compounds resulting from reaction between the analyte and flame gas molecules, and for ionisation of the analyte atoms in the flame gases.

The nebulisation efficiency ε is the ratio of the number of all gaseous analyte species produced in the flame per unit time to the number of analyte species nebulised per unit time (38). This factor accounts for volatilisation of the solid particles in the flame and also for the transfer efficiency (yield) of the nebulisation chambers and the associated tubes.

The peak atomic concentration n in atoms cm^{-3} of analyte in a non-flame cell is related to the analyte concentration C in moles.l^{-1} introduced into the cell by meams of a pipette, by the following equation:-

$$n = 6 \times 10^{20} \; VC \; \varepsilon \beta / Vc \qquad \text{eqn.(37)}$$

if the analyte vaporises instantly and then diffuses out of the cell slowly. The symbols are:-

V volume of analyte solution introduced into the cell cm^3

$\varepsilon\beta$ degrees of vaporisation and atomisation of the analyte within the cell.

Vc the inner volume of the cell.

Therefore, the ratio of atomic concentrations when the same concentration of analyte C is either introduced into the cell or nebulised into the flame is given by dividing equation 36 by 37 and so :-

$$Rn. = 60 \left[(V/Vc)(\varepsilon\beta)g \,/\, (F/Qef)(\varepsilon\beta)f \right] \qquad \text{eqn.(38)}$$

where all the terms have been defined above, subscripts g refer to non-flame and f to flame, and Rn is the ratio.

To compare the atom producing ability of the non-flame cell with the atom producing ability of a flame, several values for the parameters of equation 38 are typically $V = 0.01$ cm,^{3} $Vc = 0.5$ cm.^{3} $(\varepsilon\beta)g = 1$

$F = 2$ cm.^{3}min.$^{-1}$ $Q = 100$ cm.^{3}sec.$^{-1}$ $ef = 10$ $(\varepsilon\beta)f = 1$

For this particular case, $R_n = 600$, which shows that the non-flame cell produces atoms more efficiently than the flame cell. The reasons for this are twofold Firstly, the atomic vapour in the non-flame cell is contained in a smaller volume which is essentially a static system, whereas the flame is a dynamic system where the flame gases expand about tenfold in most analytical flames. The factor in equation 38 expressing the increased concentration is $(V/Vc)/(F/Qef)$ Secondly, for many analytes $(\varepsilon\beta)f$ will be considerably less than unity: particularly for analytes which do not undergo complete vaporisation within the flame gases and for analyte atoms that form stable monoxides, monohydroxides or other compounds with the species present in the flame gases. The factor in equation 38 expressing the efficiency of nebulisation - atomisation is $(\varepsilon\beta)g/(\varepsilon\beta)f$.

1.6.2. Decreased quenching of radiationally excited atoms.

The non-flame cell provides a less efficient quenching atmosphere (mainly inert monatomic gas molecules eg Ar) compared to analytical flames (mainly N_2, CO, CO_2 etc.) Therefore, due to the reduced quenching in a graphite cell, the signal level of an element in a non-flame cell will be increased with respect to the signal level in a flame-assuming all other factors being equal - by the ratio R_y given by:-

$$Ry = pg / pf \qquad \text{eqn.(39)}$$

where p is the quantum efficiency (yields)

The ratio R_y can be expressed in terms of pseudo-first order rate constants (16, 17, 18, 39-44) by :-

$$Ry = \left[Kf + \Sigma i(K_{Qi} n_{Qi})g\right] / \left[Kf + \Sigma i(K_{Qi} n_{Qi})f\right] \qquad \text{eqn.(40)}$$

Where Kf is the first order rate constant for radiational deactivation of the resonance level $sec.^{-1}$

K_{Qi} is the second order quenching rate constant for deactivation of the resonance level by collisions of the analyte element with a quencher, Q_i of concentration n_{Qi} $cm.^3 sec.^{-1}$

n_{Qi} is the concentration of quencher Q_i $cm.^3$

The summation is taken over all quenchers and subscripts g and f denotes the gaseous medium. Since non-flame cells should contain few quenchers.

$$Kf \gg \Sigma i(K_{Qi} n_{Qi})g$$

and so $$Ry = Kf / (Kf + (K_{Qi} n_{Qi})f \qquad \text{eqn.(41)}$$

In most common flames (16-18. 39-44) $Kf = 0.1 \Sigma i (K_{Qi}\, n_{Qi})\, f$

and so R_y should be of the order of ten, ie the atom emits its resonance line ten times more brightly in a non-flame cell than in a flame, if the same atomic concentration, in each, is radiationally excited.

Geometry factor.

The only real difference between the use of a non-flame cell and a flame in atomic spectrometry occurs in the measured area in AF. The geometry fator relating the signal in AFg to the signal in AFf assuming the previous factors Rn and Ry are unity is given by:-

$$Rg = \xi \eta \qquad \text{eqn.(42)}$$

where ξ is the ratio of fluorescence area in the flame to the area in the non-flame (area in direction of measurement system),

η is the fractional fluorescence from the non-flame cell measured by the detector.

The above expression is valid only if the fluorescence area in the non-flame cell and the flame exceed the dimensions of the entrance slit of the monochromator, thus for a non-dispersive system Rg has no significance.

1.6.3. Noise considerations.

The major sources of noise in AFf are flame flicker noise and phototube shot noise. Since measurements can sometimes be made in the non-luminous part of low-background hydrogen based flames (45,46) in AFf, then the flame flicker noise is then comparable to shot noise, and also source scatter noise in AFf can be made quite small compared to other noises. The major source of noise in AFg is shot noise.

1.6.4. Summary.

The non-flame cell offers greater advantage as an atom reservoir in AF over a flame, because there is a gain in signal by Rn Ry using a non-dispersive system. This gain in signal is ideal for trace analysis especially at low concentration of analytes. Theoretical considerations also show that AF is an ideal system for low concentrations therefore a combination of both would be extremely useful for trace analysis.

However it should be noted that the higher optical density causes curvature of the analytical growth curve at a lower concentration than expected in a flame, where the atomic vapour is more dilute. For trace analysis this is of little consequence.

1.7. General instrumentation.

The basic instrumental system required for measuring AF consists of a source, atom reservoir cell, and a detector arranged typically as shown in (fig. 2), where the detector views the absorption cell at right angles to the source cell axis. In the studies made in this thesis the normal rectangular arrangement was adopted for both a flame and a non-flame cell.

The arrangement using the non-flame cell, a hot-wire 'loop' (AFg system) can be seen in (fig. 4A and B). In this set-up a single quartz lens was used to focus the source immediately above the 'loop' atom reservoir cell, such that the image area covered the width of the cell and therefore the 'plume' of atoms produced by the cell. The area immediately above the 'loop' was viewed by the solar-blind photomultiplier tube (PMT), through a field stop made up of two

identically cut slits, separated by a small distance, and acting as a crude collimator.

In the second arrangement a flame atomiser cell was used (AFf) (fig. 5b.) This set up was essentially the same as shown in (fig. 4a) except the narrow line source was placed almost touching the argon sheath gas shield of the flame, and its radiant flux was allowed to fall directly onto the flame without focussing. A light shield (baffle) was placed, bisecting the angle subtended by the source, flame and detector such that the solar-blind PMT could not view the source directly. The PMT was restricted to viewing the width and height of the shielded (separated zone) part of the flame only by a field stop, which similarly to the source almost touched the outer argon shield of the flame.

1.7.1. The source.

The primary requirements for excitation sources for AF can be summed up as

1) high radiance over the absorption line of the analyte atoms ;
2) long (little drift) and short (little flicker) term stability ;
3) operation under either continuous or pulsed conditions ;
4) simple tuning and focussing ;
5) availability for all elements ;
6) long lifetime ;
7) safety of operation ;
8) low cost.

Electrodeless discharge lamps (EDL) are considered to have all these properties and are considered to be the brightest sources commonly available (32,33). They therefore have been the most used line source in atomic fluorescence. A more detailed study of the theory, preparation and operation of EDLs can be found in chapter 2.

fig.4

a) DIAGRAM OF THE NON-DISPERSIVE ATOMIC FLUORESCENCE SYSTEM (AFg)

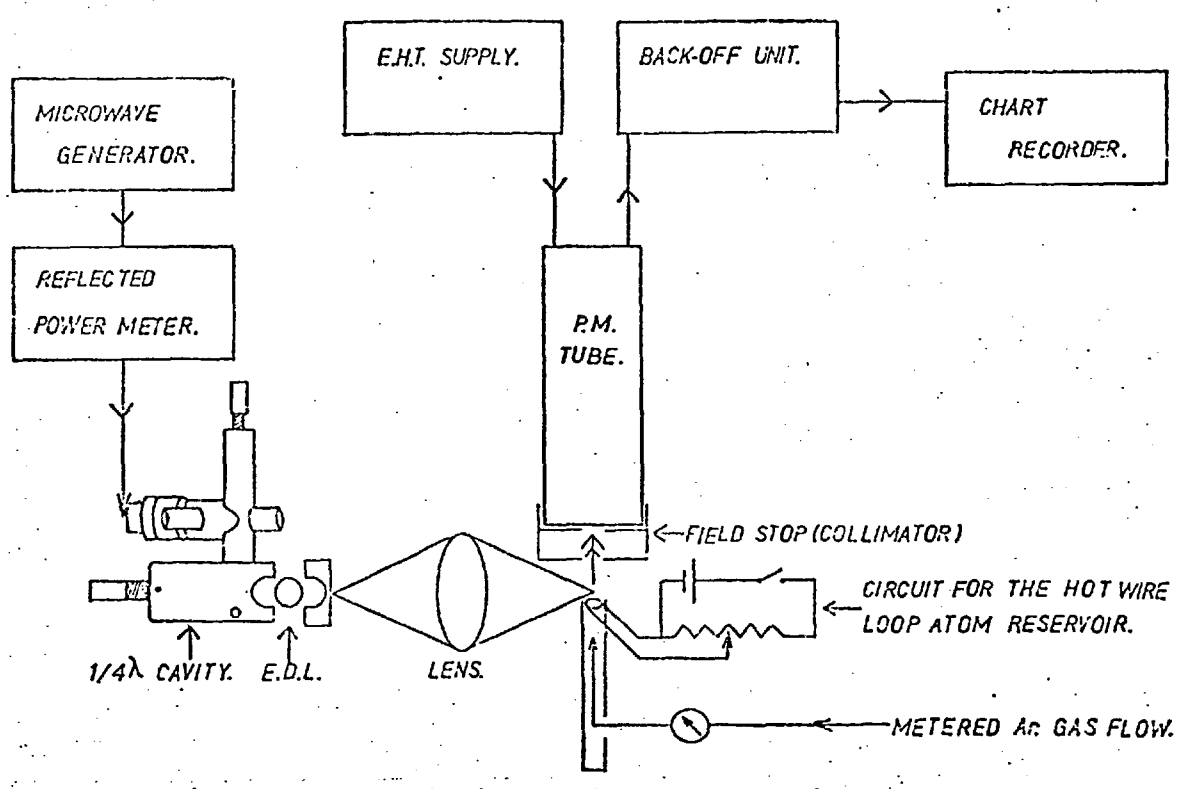

b) A SCHEMATIC VIEW OF THE NON-DISPERSIVE ATOMIC FLUORESCENCE SYSTEM (R431) (AFg)

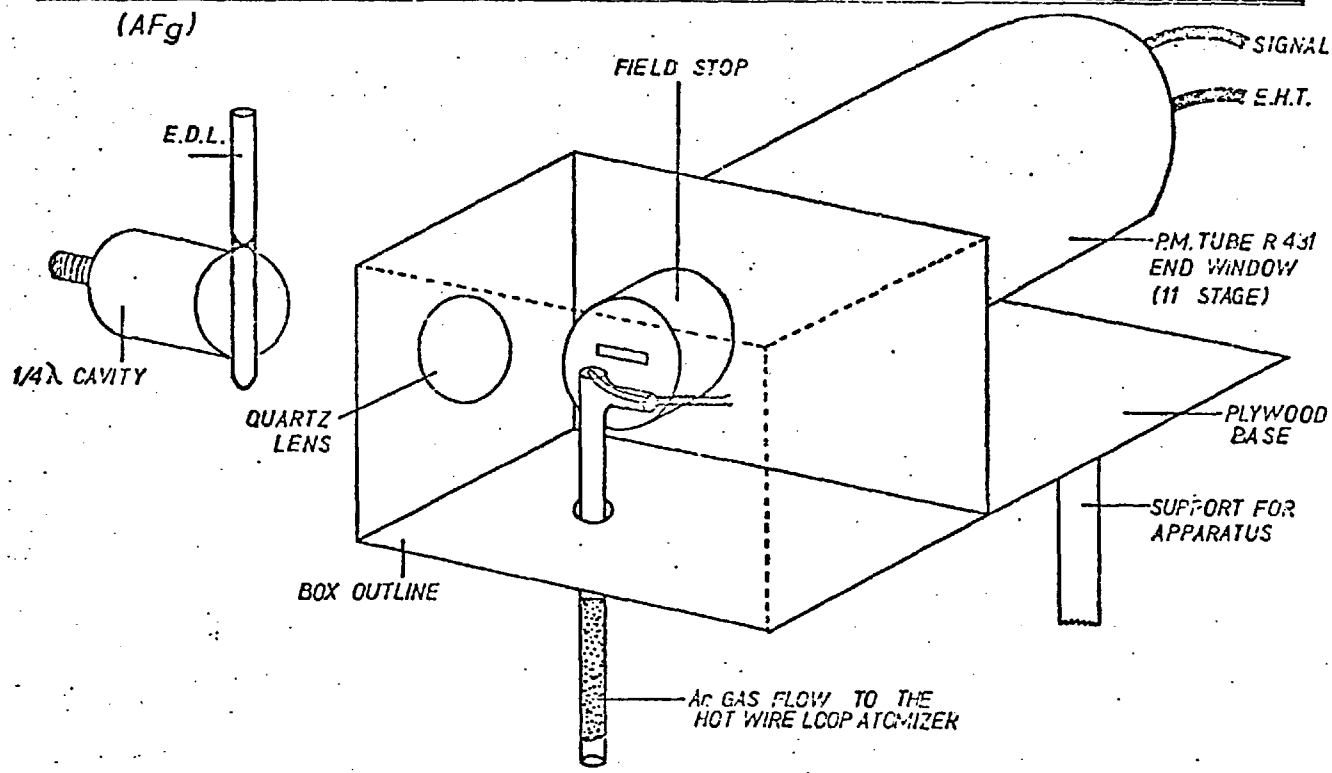

fig. 5

a) CIRCULAR CAPILLARY BURNER AND SEPARATOR

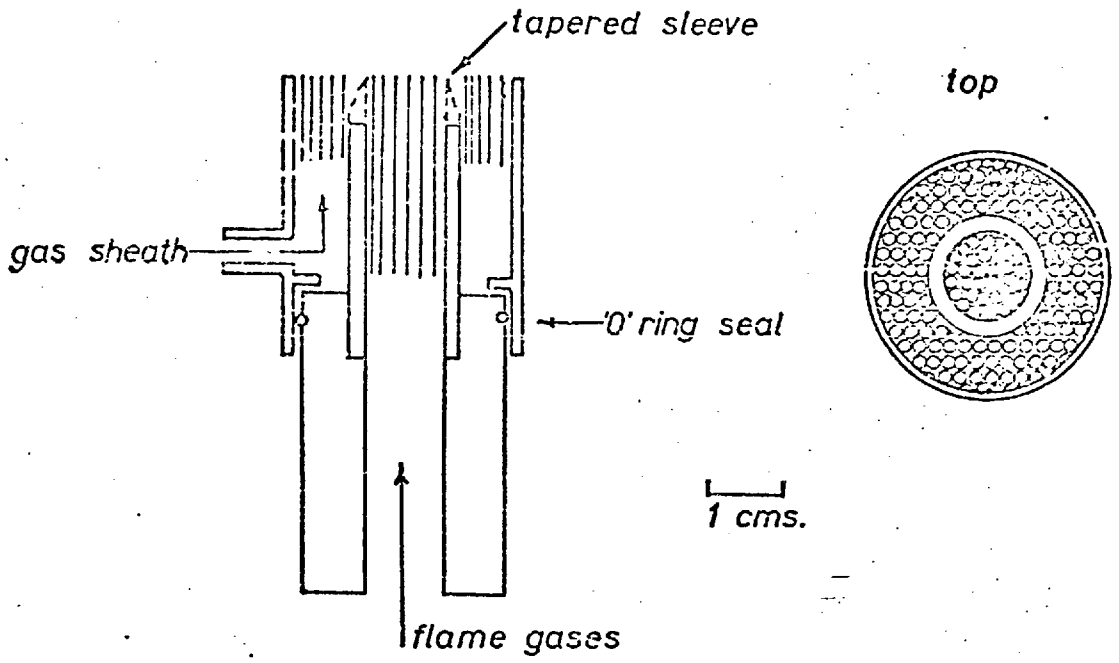

b) DIAGRAM OF THE NON-DISPERSIVE ATOMIC FLUORESCENCE SYSTEM (AF_f)

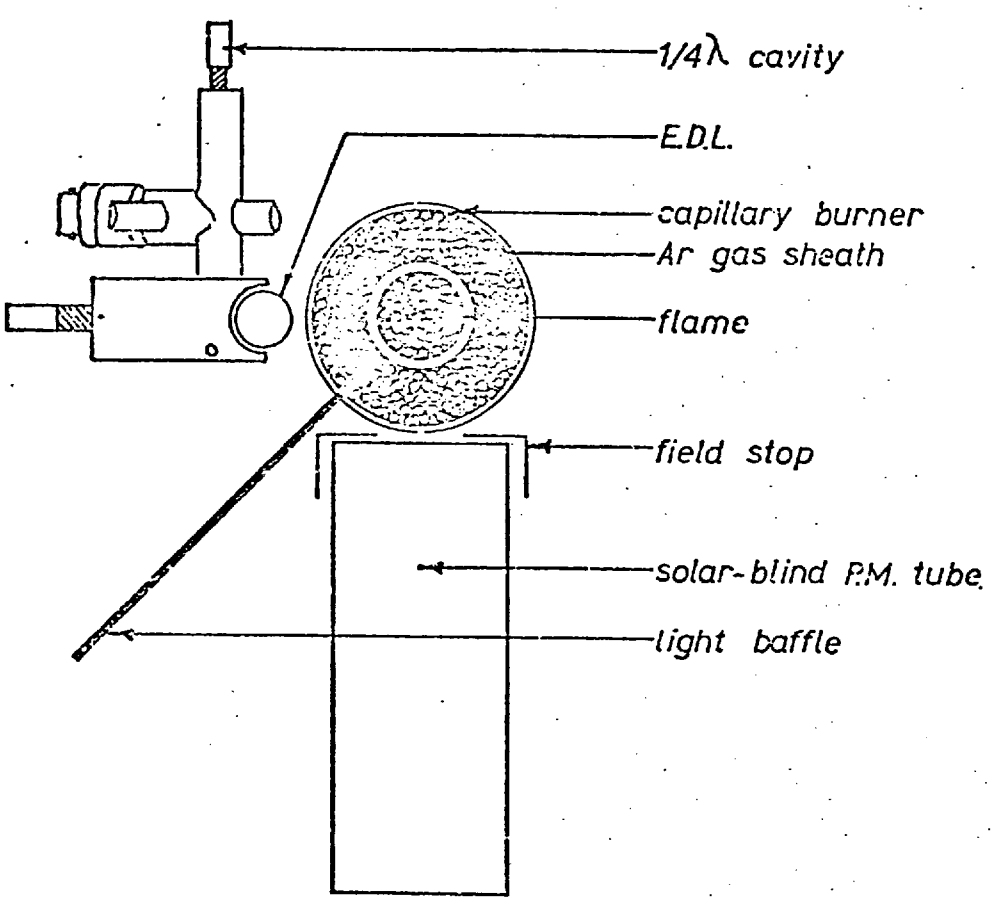

1.7.2. The detector.

In the past, various assemblies of mirrors and lenses have been described (33) which permit efficient collection of fluorescence over a large solid angle. Also to allow maximum radiant power to reach the PMT detector, the monochromators employed have been of high luminosity and have viewed the fluorescence with a large spectral band pass. This is permissible in AF rather than AA or AE because the atoms in the atom cell act as their own resonance monochromators ie unwanted radiation from the source at wavelengths close to that of the fluorescence emission is transmitted by the atom cell and therefore not detected.

However, the predicted increase in sensitivity (42,48,49,61) for AF spectrometry to be gained by non-dispersive systems is now begining to show results (50-63). Interference filter systems used with PMT have been used by several workers (53, 56, 59, 60) and the use of a photodiode by Boumans (57) has been reported. However, interference filters usually have poor transmission qualities and a significant proportion of the fluorescence brightness is lost. At present photocells do not have the sensitivity or gain of those PMTs employed at present.

All the completely non-dispersive systems reported to date have used solar-blind PMTs produced by the Hamamatsu T.V. Co. Ltd. Most commonly employed has been the nine stage side window R166 (Cs-Te photocathode) (50,51,52,54,55, 57,61,63,89,234-). The H.T.V. R431 end window eleven stage PMT has also been used (89). All the reported AF studies using a solar-blind PMT have been carried out in flames with the exception of Gough (57) who used a cathodic sputtering cell, Hargreaves(234) and King (235) who used a CFAR of the West design, and Mounce (89) who employed a hot-wire 'loop' cell.

Solar-blind PMTs have been available for some years and their characteristics have been discussed by Dunkelman (90,91,92). The work reported in this thesis has been confined to the use of a specific type of solar-blind PMT having a Cs-Te photocathode (H.T.V. Co. Ltd. R166 and R431) (see fig. 3B). Although the sensitivity of solar-blind PMT is considerably lower than other

other types of PMT (S5, S19) at wavelengths of 200 nm or greater, according to both Vickers (54) and Larkins (52), the noise in the same region is also correspondingly low and so the signal to noise ratio of the Cs-Te photocathode over much of its useful spectral range is in fact significantly higher than the S5 or S19. Also, broad band response detectors S5 S19 used in a non-dispersive mode with a bandpass filter would have the energy throughout of the system reduced, since peak transmittance of such filters is typically in the range of 5 to 25 % and a similar case can be made for loss of energy throughout for a monochromator.

The solar-blind PMT also has the advantage of collecting the fluorescence emission over a very wide solid angle. Furthermore their wide spectral band pass (160-320 nm) should result in an increase in the sensitivity of AF (see equation 28).

The advantages of a non-dispersive system can be summarised as:-

1) Greater energy throughout.

2) Simultaneous collection of a number of lines for elements with a complex fluorescence spectrum, which may result in increased sensitivity.

3) Wavelength stability.

4) Simplicity and ruggedness of instrumentation.

5) Convenience of rapid sequential multi-element analysis.

The disadvantages can also be summarised as:-

1) Since the system is relatively non-selective of wavelength, excitation sources must be free of other elements.

2) Overlapping resonance lines can cause spectral interference.

3) Where reflectory particles are present, the PMT will show a ratio of scatter to fluoresecence that is higher than when using a monochromator, since a number of lines from the source are scattered and detected, instead of the single monitored line.

4) A number of elements have their fluorescence lines outside the Cs-Te photocathode spectral range (Cu, Ag, Cr).

1.7.3. The flame atomiser.

Most analytical AF studies to date have been undertaken using a flame as the atom cell. The optimum flame for AF would have the following properties (33, 35):-

1) High atomisation efficiency for a wide range of elements.

2) Low radiative background and noise near to the analyte fluorescence wavelength.

3) Low partial pressures of flame species that have high quenching cross-section (to provide high p).

4) Long residence time of atoms in the optical path.

5) Safety and simplicity of operation.

6) Low cost of initial purchase and operation.

No single flame is known which shows all these properties for a wide range of elements. Most of these properties are shown by flames which are relatively cool, eg H_2 fuel (65-84) since these flames have a low, effective quenching cross-section, flame background intensity, and burning velocities (54). However, high atomisation efficiency can only be acheived with volatile analytes ie Bi, Pb and Sn, and often serious chemical inter-element interferences are found.

In the AFf arrangement a circular capillary burner head (fig. 6a) was used in conjunction with a standard Perkin Elmer variable spray chamber. The burner head was made in this Department and full details of its construction and performance have been described in (73). Two types of flame were used with this burner head, the hydrogen diffusion flame H_2/Ar (54,66,67,69,70,77,80,81) and the separated premixed laminar hydrogen-oxygen flame, $Ar/O_2/H_2$ (54,66,67,68,70 76,82,83,84). In the case of the hydrogen diffusion flame, argon was used as the support gas for the nebuliser. The primary flame front is at the outer mantle of the gas column with the inner region of the flame being highly reducing because of the absence of any oxidising species.

In the case of the premixed-laminar flame, argon was used as the support gas for the aersol/spray, hydrogen as the fuel gas, with the oxygen being supplied into the spray chamber via the auxiliary air inlet. The primary reaction zone of the flame was separated from the atmospheric oxygen by an inert gas sheath (73, 74, 76, 85, 86, 87). Thus the interconal area where most of the free atomic population exsists was studied without interference from the secondary combustion zone's radiation (54). Pure oxygen is used in preference to compressed air, as there is no introduction of diatomic nitrogen which quenches the fluorescence to a greater extent than argon. Also the introduction of argon into the flame gas mixture as a diluent, increases the fluorescence yield by lessening the quenching collisions between free atoms and polyatomic species in the flame, (H_2, O_2, OH etc).

Advantages of capillary burners.

These burner systems offer several advantages over the standard Meker or slot types;

a) The shape of the burner can be designed to suit the purpose for which it is required and to suit the fuel and oxidant flows of a particular nebuliser unit.

b) Because of the number of capillaries used, a very even flow pattern is established over the entire area of the head because each tube achieves a similar Poiseuille distribution of velocities. This leads to a very stable laminar flame not prone to disturbance by draughts.

c) By suitable choice of capillary diameter, all gas mixtures commonly used can be burned safely if the diameter chosen is less than the quenching diameter for the fuel/oxidant mixture; extinction will occur rather than flash back, if the burning velocity should exceed the supply velocity.

d) The burner may be made with only limited workshop facilities as the need for accurate machining of slots and hole patterns is not required, and facilities for a water cooled head were not necessary.

The laminar flow burner was also chosen in preference to the turbulent flow burner because in the latter the solution uptake rate is generally less and there is some evidence that some larger liquid droplets produced pass through the flame without being vaporised, (88). This may contribute to severe scatter signals in AF, and also chemical interferences, as a result of large sample droplets.

1.7.4. Hot-wire 'loop' atomiser.

Several successful non-flame cells have been reported for AF (32,33,34,102). The criteria for a successful non-flame cell are similar to those for a flame (1.7.3.). Non-flame cells were usually electrically heated. An argon atmosphere was necessary for all the non-flame cells by either passing a stream of argon through or around the cell. However, the graphite filament, metal filament tantalum strip (93-98) and hot-wire 'loop' (99-111) can be sheathed, in addition to an argon stream, by a hydrogen stream. The precision that can be obtained with non-flame cells is usually limited by the reproducbility with which the small sample can be transferred to the cell. It is frequently difficult to achieve better than ca 5 % reproducibility with microlitre (µl) liquid samples, but such precision is usually acceptable. Since the volumes involved are so small and the speed of measurement is rapid, pipetting errorscan be minimised by statistical treatment of 10-12 samples. In systems employing atomisers of this type, the detector-readout system must respond rapidly to the transient signal which results when the free atoms pass through the analytical detection zone.

The provision of optical screening around non-flame cells allows the AF signal to be measured against an almost negligible background, and with the small volume in which atomisation occurs, the attainnment of high population densities of the atomic species is possible.

The residence time of the atoms in the field of view is limited chiefly by condensation of the atoms in the 'cold' surroundings in which they find themselves immediately after generation (236).

One non-flame cell which has recently been used in a variety of combinations and modes is the hot-wire 'loop' (89,99-111) or metal strip (96-98).

In the studies described in this thesis, the hot-wire 'loop' (fig. 6) has been used as it possesses most of the advantages of other non-flame devices; ie . small sample size requirements, high atomisation efficiency, and yields a high atomic density. Other advantages include low cost, and elimination of elaborate power supply and water cooling of electrical terminals. This simplicity combined with its radial symmetry makes it an ideal atomiser to use in a non-dispersive spectrometer. Since there are no cumberous electrical leads to the cell, the endwindow of the PMT can be placed within 5 mm of the loop without any damage or obstructions. The high aperture of the system results in a high radiant flux throughout and the compactness facilitates flushing of the system for work in the lower U.V. region.

The hot-wire 'loop' atomiser can be made of any suitably inert metal wire (see table 1) eg platinum (99,101,100,104,106), tungsten (105-108), tantalum (89,96,94); other suggested materials include iridium and rhenium all between 0.1 and 0.25 mm in diameter. A short length of wire 1.0 to 1.5 cm was wound $1\frac{1}{2}$ times around a suitable mounted needle, in this case 0.8 mm diameter, and the equal length loose ends were spot welded to the shanks of the electrodes (fig. 6). These loops were of the open twist pattern (107) and were resistively heated throughout, as compared with previously used loops, which were partly heated by conduction (104, 105, 106).

The loop assembly was kept in a small vial until it was required, and then inserted into the non-flame cell, through a side arm at right angles to

fig. 6

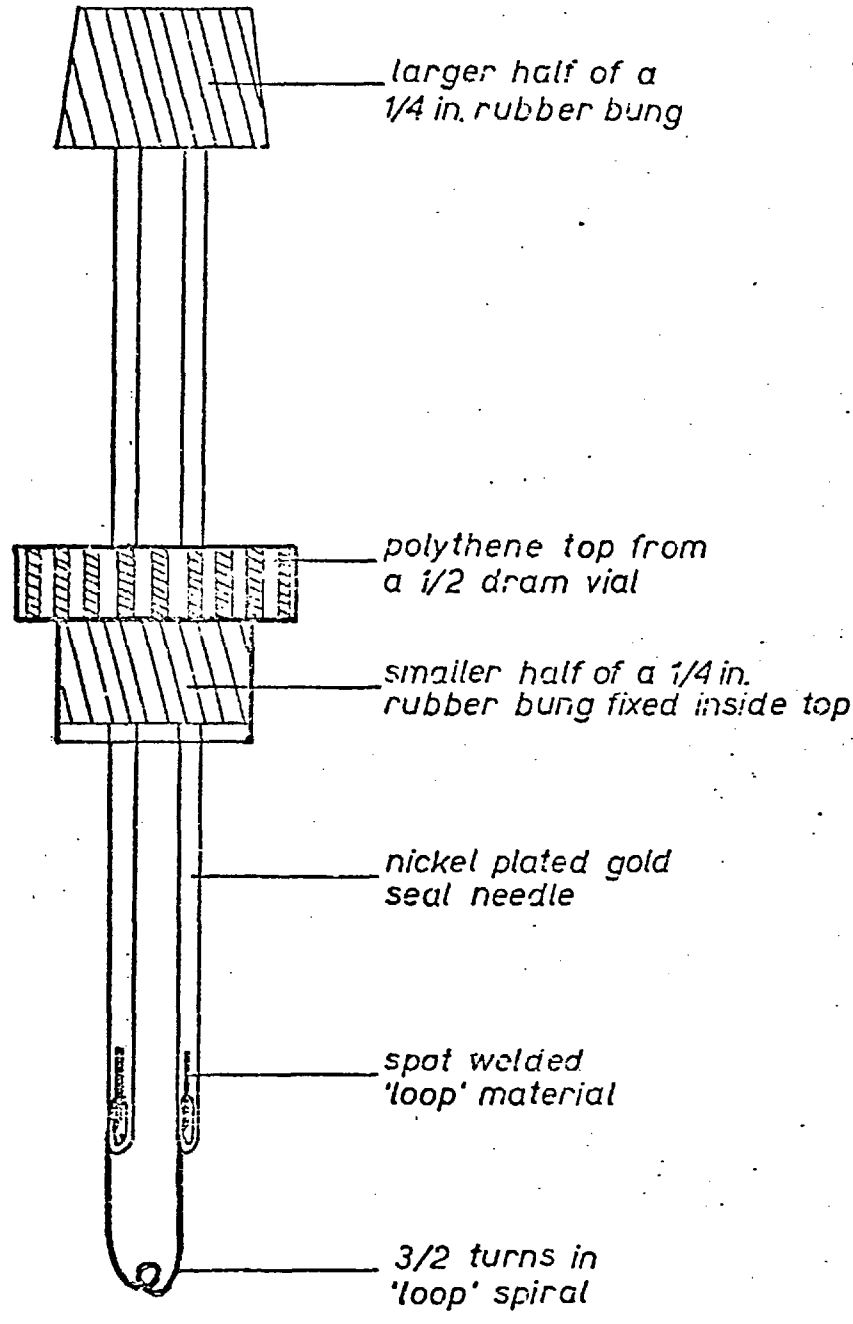

THE "HOT WIRE LOOP" ATOMISER ASSEMBLY

Table 1

Temperature Information

Suitable loop material	M.Pt. K	Analyte Elements	M.Pt. K	B.Pt. K	Matrix Elements	M.Pt. K	B.Pt. K
Platinum	2043	Arsenic	1090	885	Aluminium	933	2723
Rhenium	3453	Antimony	903	1653	Cobalt	1768	3173
Tantalum	3270	Bismuth	545	1833	Chromium	2148	2938
Tungsten	3683	Lead	600	1998	Iron	1812	3273
		Tin	505	2543	Nickel	1728	3003
					Titanium	1941	3533
					Molybdenum	2890	5833

Hwang (94) has successfully recorded atomic absorption from an electrically heated tantalum strip at a temperature for the following

elements:-	Temperature K
As	2670
Bi	2470
Pb	1670
Sb	2670
Sn	2670

the vertical flow of argon (see fig. 5b.). The wire loop was just proud of the top of the quartz tube (i.d. 8 mm o.d. 10 mm). The loop electrodes were connected to a power circuit as shown in (fig. 5a), which comprised a variable resistance and 6 volt, 4 amp. supply from a mains transformer.

The 0.8 mm diameter spiral was chosen as it provided adequate retention of a 5 µl water or methyl-isobutyl-ketone (MIBK) drop from a Marburg piston type pipette.

The loop was operated in a timed sequence, first the liquid of the 5 µl drop was evaporated at a low temperature, it was allowed to cool for a fixed time and then the material on the loop was 'atomised' at a chosen higher temperature. During this cycle, the argon flow rate remained constant and the temperatures were selected by changing the variable resistance.

Argon was chosen as the support gas. This was predicted from theory and has been verified by a number of authors (34, 89,103-109). Argon possesses near ideal properties of low thermal conductivity, low specific heat and high atomic weight so minimised the cooling rate of the loop. Argon prevents oxidation of the metal surface of the loop, therefore increasing the useful lifetime of the loop. With much use the loop begins to lose material and become thinner and more crystalline thus altering the heating characteristics. This usually occurred only after many hundreds of shots in normal use.

1.8. Scope of this thesis.

An attempt has been made to find a relatively direct method by which the determination of five trace elements could be achieved. These analyte elements arsenic, bismuth, lead, antimony and tin are present in very low levels in a matrix where large excesses of other metals are present, (table 2).

Theoretical and practical considerations have gone into the design and development of the systems used, with particular emphasis placed on reaching sufficient sensitivity (x10 lower than the amount to be detected) for each analyte, before using separation, extraction and preconcentration techniques in dealing with the analysis of the samples.

To achieve the required sensitivity for these analytes AF was chosen in preference to AA and AE because lower limits of detection are obtainable. This thesis describes the development of a non-dispersive AF method capable of high sensitivity for the required elements.

Table 2

COMPOSITION OF THE STANDARD METAL ALLOY SAMPLES
Dissolution of samples: 0.5g. in 50ml. soln.

		Trace Elements					Matrix Elements						
Sample		Bi	Sn	Pb	Sb	As	Ni	Cr	Co	Mo	Ti	Al	Fe
R3385	wt.% in soln	0.0002	0.0II	0.0002	0.0006	0.0I	60	I5	I5	5	2.5	2.5	-
	ppm	0.02	I.I	0.02	0.06	I.0	6000	I500	I500	500	250	250	-
	amt. in 5 µl	0.Ing	5.5ng	0.Ing	0.3ng	5.0ng	30µg	7.5	7.5	2.5	I.25	I.25µg	-
R3386	wt. % in soln	0.0003	0.0056	0.0003	0.00II	0.005I	"	"	"	"	"	"	-
	ppm	0.03	0.56	0.03	0.II	0.5I	"	"	"	"	"	"	-
	amt in 5µl	0.I5ng	I.8ng	0.I5ng	0.55ng	2.55ng	"	"	"	"	"	"	-
R3387	wt. % in soln	0.00I2	0.00I5	0.00I2	0.0056	0.00I6	"	"	"	"	"	"	-
	ppm	0.I2	0.I5	0.I2	0.56	0.I6	"	"	"	"	"	"	-
	amt. in 5µl	0.6ng	0.75ng	0.6ng	2.8ng	0.8ng	"	"	"	"	"	"	-
R3388	wt. % in soln	0.0006	0.0025	0.0006	0.0022	0.0023	"	"	"	"	"	"	-
	ppm	0.06	0.25	0.06	0.22	0.23	"	"	"	"	"	"	-
	amt. in 5µl	0.3ng	I.25ng	0.3ng	I.Ing	I.I5ng	"	"	"	"	"	"	-
Iron Base A	wt.ppm in soln	20	20	-	40-49	20-32	-	-	-	-	-	-	balance
	ppm	0.2	0.2	-	0.4	0.2	-	-	-	-	-	-	I0,000
	amt. in 5µl	I.0ng	I.0ng	-	2.0ng	I.0ng	-	-	-	-	-	-	50µg
B	wt.ppm in soln	I0	I0	-	80-89	I0-22	-	-	-	-	-	-	"
	ppm	0.I	0.I	-	0.8	0.I	-	-	-	-	-	-	"
	amt. in 5µl	0.5ng	0.5ng	-	4.0ng	0.5ng	-	-	-	-	-	-	"
C	wt.ppm in soln	40	40	-	20-26	40-50	-	-	-	-	-	-	"
	ppm	0.4	0.4	-	0.2	0.4	-	-	-	-	-	-	"
	amt. in 5µl	2.0ng	2.0ng	-	I.0ng	8.0ng	-	-	-	-	-	-	"
D	wt.ppm in soln	80	80	-	I0-I6	80-96	-	-	-	-	-	-	"
	ppm	0.8	0.8	-	0.I	0.8	-	-	-	-	-	-	"
	amt.in 5µl	4.0ng	4.0ng	-	0.5ng	4.0ng	-	-	-	-	-	-	"

CHAPTER 2

2.1. History of Electrodeless Discharge Lamps.

The high frequency electrodeless dicharge was discovered by Hittorf (114) in 1884. This was followed in 1891 when Thomson (115) published two papers on 'the discharge of electricity through exhausted tubes without electrodes'. The spectra of many species were observed using a Wimshurst machine coupled to a coil of copper wire surrounding an evacuated glass vessel. Jackson, (116) in 1928, used an EDL operated from a 10MHz oscillator to obtain the spectrum of Caesium in order to study its hyperfine structure. Meggers et al (117,118,119) in 1948-50, described the preparation of an EDL of mercury 198 and proposed it as a secondary standard, as there is no hyperfine structure owing to the absence of nuclear spin and isotopic shifts. The wave-lengths of the lines were quoted to 10^{-5} nm. More recently these lamps have been used to study the spectra of the lanthanides and the actinides and their isotopes, (120-124). Tompkins and Fred (122) have shown that as little as 0.1 μg of a given element was sufficient to produce strong emission in an EDL. It can be seen that for radioactive elements and isotopes (120-125), these sealed sources are much safer and more economical than the commonly employed DC arc. The advent of the laser caused a great deal of interest in EDLs for optical pumping studies. (126).

Radio frequency EDLs have been used as spectral sources for alkali metals (127) and for excitation of atomic resonance fluorescence of alkali metals (128,129). Ham and Walsh (130) describe 2450 MHz powered sodium and mercury sources for use in 'Raman' work. Microwave excited EDLs have been used to obtain continuous sources in the vacuum UV using argon, hydrogen, krypton and xenon filler gases (131-6). A microwave discharge can easily be operated at low temperatures.

Vaughan (137) used a helium discharge cooled by liquid helium to obtain spectral lines with an effective Doppler temperature of 10K.

The preparation of metal EDLs has been described in many publications (117-25, 127-30, 138, 139), but these sources were prepared primarily for spectral elucidation studies. Certain EDLs have also been prepared as spectroscopic standards where absolute cleanliness of prepation was essential, (117-9, 140). However, until 1966, there had been little work on the production of EDLs, solely for use as sources in AA and AF. Ivanov et al (141) report the use of lamps with high frequency excitation for use as a source in AA, and Goodfellow (142) has made some AF measurements using a continuous flow microwave system. This type of continuous flow system has also been proposed as a spectroscopic source by Richards (143). Winefordner (21,24) has used some commercially available EDLs (Opthos Instrument Co. Rockville Ma. USA) for AF studies, with rather poor results mainly because of the EDL design. These sources were not of high intensity or stability since they were marketed primarily for use in interferometry and wavelength calibration studies. The real potential of EDLs as sources for AF and AA was realised by Dagnall, Thompson and West (145) and they described the preparation of EDLs for several elements. (see table 3).

2.2. Basic principles of microwave discharge.

The excitation of a discharge by radio and microwave fields is very efficient as these fields accelerate electrons over a confined region, thus maintaining an emitting plasma without internal electrodes within the plasma. The discharge is equivalent to a cold plasma because of its non-isothermal nature (210). This means that in the neutral gas the effective temperature of the atoms and the molecules (700K) is much less than that of the electrons (2×10^4K) at 10 torr pressure (219,220).

The ratio of the electric force to the charge on a particle is the electric field strength. Thus, an electron in the path of an electromagnetic wave is subjected to an oscillating electric field, the frequency of which is very important. Energy can be transferred effectively from the electric

Table 3.

An indication of the range of elements available and compounds used for EDLs.

Element	Constituents (Alternative)	Element	Constituents (Alternative)
Al	Al + I_2	Pb	Pb + I_2
Sb	Sb + I_2	Mg	Mg X93 glass
As	As + I_2	Hg	Hg
Ba	$BaCl_2$	Mo	Mo + Cl_2
Be	Be + I_2	Ni	$NiCl_2$
Bi	Bi + I_2	Nb	Nb + I_2
B	B + Cl_2	Pd	Pd + Cl_2($PdCl_2$)
Br	Br_2	Pt	Pt + Cl_2
Cd	Cd	K	K X93 glass
Cs	Cs pyrex	P	P
Ca	$CaCl_2$	Pr	$PrCl_3$
Cl	Cl_2	Rh	Rh + Cl_2
Cr	Cr + Cl_2 ($CrCl_3$)	Rb	Rb pyrex
Co	Co + I_2 ($CoCl_2$)	Se	Se
Cu	Cu + I_2 ($CuCl_2$)	Si	Si + I_2
Ga	Ga + I_2	Ag	AgCl
Ge	Ge + I_2	Na	Na X93 glass
Au	Au + Cl_2	Sr	$SrCl_2$
Hf	Hf + Cl_2 (HfI_4)	S	S
In	In + I_2	Ta	Ta + I_2
I	I_2	TE	Te + I_2
Ir	Ir + Cl_2	Tl	Tl + I_2 (Tl Cl)
Fe	Fe + I_2 ($FeCl_2$)	Th	Th + I_2
La	La + Cl_2 ($LaCl_3$)	Sn	Sn + I_2
V	VCl_3 (V + I_2)	Ti	Ti + I_2
Zn	Zn ($ZnCl_2$)	W	W + Cl_2
Zr	Zr + I_2	U	U + I_2

field to the gas for all frequencies up to about 10,000 MHz. (Radio frequency 2×10^5 to 10^9 - microwaves 10^9 to 10^{12} Hz). The microwave unit is somewhat simpler than either the rf or the dc unit to operate.

Microwaves can be generated in the laboratory using commercially available electronic valves, such as magnetrons or klystrons. They can generate energy either in pulses or continuously. The magnetron valves radiate energy from their anodes in all directions. The energy is contained and transmitted over a distance by wave guides, the use of which is limited to the microwave region. Thus with a magnetron placed at one end of a closed wave guide, electro-magnetic waves are formed and microwave energy is transmitted to the gases, through a quartz tube situated at the other end of the wave guide.

Rose and Brown (215) have given the following picture of the physical mechanism in a steady state microwave discharge "Electrons gain energy from the field, and lose energy by elastic and inelastic collisions. Ionisation of gas molecules provides a source of new electrons, and flow to the tube walls in the presence of density and space potential gradients provides the sink". In order to produce free radicals or excited atoms at relatively low temperatures, the ratio of the electron temperature to the gas temperature must be at least 10:1. Many people have shown (216) that there is an approximately linear relationship between this ratio and the electric field strength to gas pressure ratio.

The maximum electric field strength available in an empty wave guide is proportional to the square root of the input power. Thus as the power level is increased, the field strength will also increase until at some particular value it will be strong enough to initiate breakdown of the gas contained, in this instance, in a quartz bulb that passes through the wave guide. To assist this process a source of external electrons can be introduced into the field by a tesla sparking coil applied to the quartz surface containing the (argon) gas. A discharge is then initiated.

The physical mechanism by which a stable discharge is formed is as follows. Under the action of the electric field an electron is accelerated by the field until it collides with a gas molecule. The direction of motion is then reorientated almost randomly. Most of the kinetic energy gained during the acceleration period is kept during the scattering process, since the mass of the molecule is large compared with that of the electron. After collision the electron is either accelerated or decelerated by the field, depending on the direction of the electron velocity relative to the field. The kinetic energy of the electron is built up through successive accelerations, until finally an inelastic collision is possible resulting in ionisation, free radical formation, or excitation.

Additional electrons are formed from ionising inelastic collisions; these electrons gain energy from the field while undergoing elastic collisions with gas molecules. Similarly, in attempting to restore the ordered oscillatory motion, the field does net work on the electrons and thereby increases their energy.

This lowers the gas impedance which causes the field strength to fall. The lower the field strength produces fewer electrons, and therefore the impedance and the field strength finally reach an asymptotic balance. Maximum power transferance is achieved when the gas impedance matches the characteristic impedance of the wave guide termination. This termination may take the form of an antenna or resonant cavity, the purpose of which is to transfer power from the microwave source to the gas in an efficient manner. If the cavity is designed so that its impedance can be adjusted even when a discharge is present, highly efficient energy transfer to the gas can be achieved.

The relationship between the electric field strength, pressure and electron concentration of a microwave discharge has been theoretically predicted by Brown (217) and experimentally verified by Lathrop (218). The average power transferred to a unit volume of gas in a microwave discharge is given by:-

$$p = \frac{e^2 \varepsilon^2 n \quad \nu c}{2m \quad \nu_c^2 \quad \omega^2} \qquad \text{eqn.(43)}$$

where ε is the max. field strength

$\varepsilon = E_0$ is the amplitude of high frequency field

n is the electron concentration (density)

m is the electron mass

ν_c is the elastic-collision frequency

ω is the frequency of the applied field

The value ν_c usually lies between 10^9 and 10^{11} collisions/sec.

As the specific power level is reduced, a value is reached at which electrons are lost to the tube walls at a rate greater than that at which they are being produced by the field. The discharge is then extinguished.

Optical plasma diagnostics.

In the sealed quartz bulb, there is the inert gas argon and the metal or metal halide vapour. These various constituents of the plasma emit line spectra as a result of excitation by electron collision. At low pressures these lines are broadened by the thermal motion of the emitting particle (Doppler) and by random electric field fluctuations (Stark) due to the fluctuating charge density around the emitting particle.

In the presence of a large neutral particle concentration in the plasma, the condition of local thermodynamic equilibrium is difficult to achieve.

2.3. Preparation of EDLs.

2.3.1. Apparatus.

1) Vacuum system. The vacuum system used in these studies consisted of a two stage rotary pump, a means of introducing argon (or other gases) and two B10 outlets on the manifold (see fig. 7). This particular system was essentially the same as the system first reported by Dagnall et al (147,145), and Aldous et al (148), but has had the number of outlets and taps reduced and also the overall dead space reduced. These reductions were made to speed up the process of flushing and evacuating and also to make the whole line easily dismountable for regular cleaning. Other authors have described elaborate

vacuum systems, these being primarily for ultra-purity spectral lamps used as spectroscopic standards (117-9, 221). A three step oil diffusion pump and a fore pump (5×10^{-7} torr) has been used by Gleason and Pertel (221). Mansfield et al (112) used a kinetic type system (10^{-6} torr) and an oil manometer instead of a mercury gauge, which precludes any mercury vapour being sealed into the lamp. Other workers in this department are now using continuous reading, non-mercury, vacuum gauges supplied by Edwards High Vacuum Ltd. (212).

2.. General procedure.

The lamp blank was connected to a B10 cone with PVC medium pressure tubing, (Apiezon M grease was used for all ground glass joints and taps), and the whole was attached to one of the outlets on the vacuum line. The mercury gauge was similary attached to the other outlet. The system was pumped down to about 0.1 torr. Argon (B.O.C. compressed gas) was introduced into the system and again repumped to 0.1 torr. The lamp bulb and seal area were baked out at a temperature just below its softening point (using an oxy-propane hand torch) for a few minutes, during which time argon was flushed through the system to remove any released gases. The lamp neck constriction was further reduced at this time, ready for rapid sealing at a later stage. The lamp blank was then allowed to cool with a high partial pressure of argon filling the vacuum line.

The degree to which the inner quartz surfacesare degassed (122,138,222) is thought to play a part in the spectral purity of the output and also the lamps useful lifetime. However, the above procedure was found to be adequate for degassing the quartz (81,153,147).

Other authors have paid more attention to the degassing of lamp blanks. Dagnall et al (150) heated the blanks up to 1000K for a period of 12 hours and purified them further by applying an intense microwave excited argon discharge in the EDL blank for 30 mins. This resulted in a decrease of wall-darkening (clean up), an increase of average life and decrease in drift.

fig. 7

a) VACUUM LINE FOR PREPARATION OF EDL's

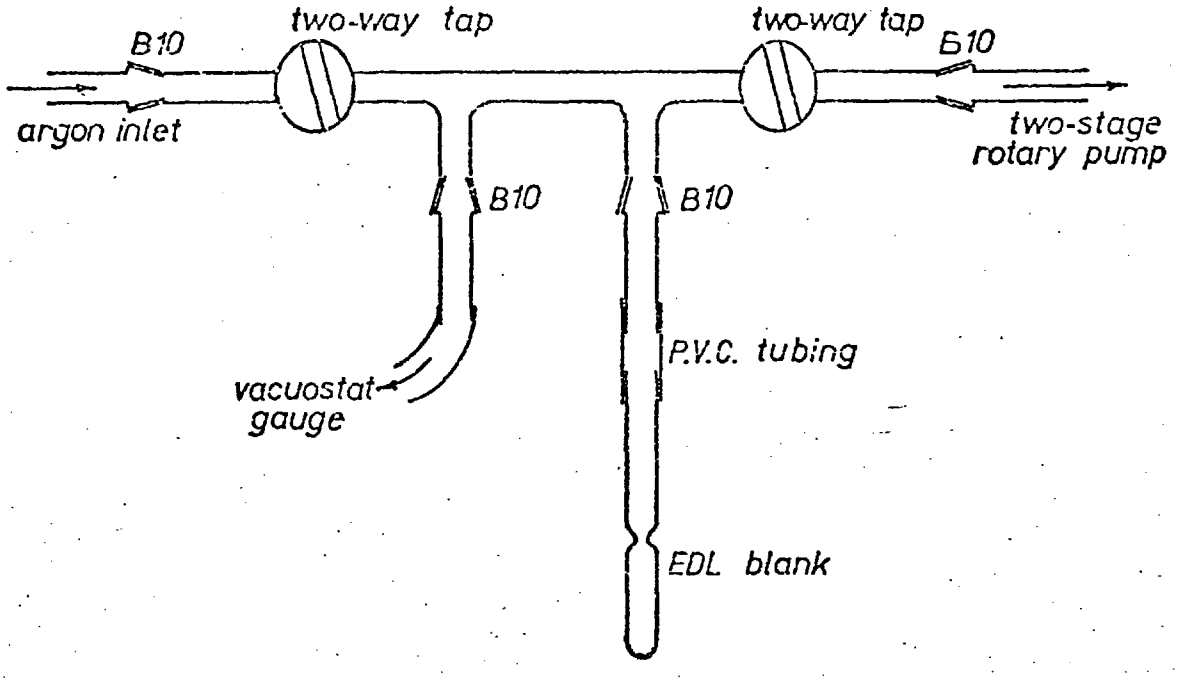

b) ELECTRODELESS DISCHARGE LAMP BLANK

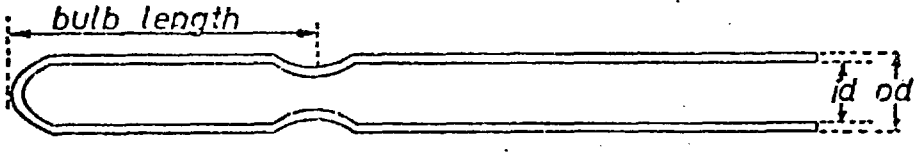

Others have used a microwave discharge for cleaning (221,222). An argon discharge was initiated in the EDL blank, and the colour of the discharge was used as an indication of the presence of gases other than argon. The quartz was then heated to near its melting point and water vapour and oxygen are released. To avoid decompositon the quartz should be heated only once. For the same reason, too high a temperature should be avoided when sealing off the lamps. Tompkins (122) degassed by heating for at least two hours in an electric furnace with the EDL blank under high vacuum.

Once the lamp was cool, it was removed from the vacuum line. A minute amount of the required element was introduced into the lamp blank, at the neck of the constriction by a micro-spatula and then tapped so that it passed through into the bulb. The lamp blank was then reconnected to the system, and evacuated as before, flushed out with argon and re-evacuated to a pressure of about 0.1 torr. Gentle heat from a micro-burner, depending on the volatility of the material, was applied to the base of the bulb intermittently to drive off any moisture or occluded gas in the charge used. During this procedure the vacuum system was flushed several times with argon and often the material was distilled or sublimated up on the wall of the EDL blank for some distance (127,169,174,230,83). Some authors have degassed the blank and the material at the same time (121,123,168). When the material was very volatile, no heat was applied directly, but the lamp blank was immersed in warm water and the system was only flushed with argon gas, eg iodine.

Depending on the nature of the charge and the final composition to be sealed in the bulb, several different procedures were followed. If the material was a pure metal or stable metal halide, it was heated until it vaporised and condensed as a thin film around the cooler top of the bulb. The total amount of the metal or metal halide introduced to the bulb initially was then carefully reduced by the use of the micro-burner. A portion passes out of the bulb and the other portion condenses back at the bottom of the bulb, which is

partially submerged in cold water. The whole bulb was then filled with argon, partially evacuated and left to cool.

If the material to be sealed in the bulb was to be a metal halide formed in situ or metal in an excess of metal halide, the metal was first introduced into the lamp blank as in the process above. The lamp blank with metal was then removed from the line and a small amount of iodine or metal halide was introduced into the bulb. When a metal chloride was to be formed in situ, the chlorine gas was introduced by a fine capillary as a purge. The metal was then reacted with the chlorine by gently heating the lamp bulb. In the case of the metal halide or, the iodine, the occluded moisture or gas in the solid was removed, when reconnected to the line, in a manner similar to the initial charge. The mass of the new charge was reduced as before, except no direct heat was applied in the case of iodine owing to its volatility. The bulb was then filled with argon and partially evacuated and left to cool.

In all cases, the bulb was sealed by placing two thirds of the bulb in cold distilled water. This kept the material cool and at the base of the bulb, whilst an oxy-propane torch was used to melt the quartz and rapidly seal the bulb at the prepared constricted region.

Prior to the bulb being sealed, a known pressure of argon was introduced into the vacuum line. This was achieved by evacuating the whole line to 0.1 torr. Argon gas at a slight positive pressure was allowed to fill the line. The argon was then evacuated for a set period of time. The tap between the line and pump was then closed. The pressure of the trapped argon in the line was measured, prior to the seal.

Other methods of introducing material into the lamp blank have been reported. The procedure was more complicated when the metal or the compound had to be prepared in situ. Alkali metals have been prepared by heating the chloride with excess of calcium (194). Iodides of lanthanides and actinides were prepared by heating the appropriate oxide with AlI_3 (123). If the quartz wall was attacked during the preparation or if a residue remained, the

preparation could not be done in the EDL blank; so a side tube was used, from which the material was sublimed from the side arm into the blank (112, 122,123,162,168,224,).

In the preparation of mercury isotope EDLs, mercury was sublimed from a platinum foil (222) or a gold wire (221), the mercury being deposited electrolytically on these metals beforehand. Cunningham (162) carefully controlled the amount of iodine introduced into the bulb, by controlling the vapour pressure of the iodine in a side arm by a temperature bath. Cooke et al (160) deposited known amounts of material into the lamp blanks in aqueous solution ($CdCl_2$ and $ZnCl_2$). The water was driven off carefully under vacuum, leaving behind the solid which was treated as reported befcre. This technique has been extended to organic solvents as well and will be described later for solvent systems CCl_4/I_2, $PbCl_2$/HCl, diethyl ether/SnI_4 and acetone/SbI_3.

2.3.2. Lamp dimensions.

The lamp blanks were made from transparent quartz tubing (Quartz Fused Products or Thermal Syndicate), nominally 1 mm wall thickness (see fig. 7b). About 25 cm length of this tubing was taken and thoroughly washed with Decon solution, distilled water and finally acetone to remove any loose particulate matter and grease. Other cleaning procedures have been reported: Gleason and Pertel (221) used 50 % HNO_3 and 50 % H_2SO_4; other investigators used 50 % HNO_3, 10 % HF, water and acetone (157) or chromic acid and water (118). The clean, dry tube was formed into two lamp blanks using an oxy-coal gas Scorah burner. After marking the centre of the length of tubing with a slight constriction, two constrictions were made (2 mm internal diameter id), a measured distance either side of the centre mark. The tubing was then allowed to seal at the centre mark and whilst still molten the two halves were drawn apart. The final rounding off of the individual lamp bases could then be performed.

This procedure was found to be the most economical and rapid way to fabricate the lamp blanks. Because of the intense emission from the quartz at its softening temperature protective goggles should always be worn and the whole operation performed in a fume cupboard, to prevent the inhalation of vaporised silica. Surface etching of the quartz tubing was removed by heating the lamp blank to just below its softening point in the oxy-coal gas flame.

Instead of quartz sometimes glass (198), pyrex (121,127), or vycor (118, 154) were used. Borosilicate presents difficulties of implosion at higher working temperature (154). Aldous et al (223) used borate quartz with boric acid, which forms a protective layer of borate glass. They also washed the quartz with hydrofluoric acid, resulting in a higher BO-concentration at the inner wall. Two-ply sodium vapour resistant glass has also been used. These methods were used in the preparation of EDLs of alkalis and alkaline earths, because of the rapid and irreversible attack of these elements on the quartz or pyrex glass walls. Dagnall and West (147) de-activated quartz with boric acid and baked it for some time at 400C.

2.3.2.1. Diameter of tube.

The majority of lamps used in these studies were made from 8 mm internal diameter and 10 mm outer diameter tubing, as this has been widely reported to yield optimum intensities, low noise and increased lifetime (112,113,145). Similar findings have been reported by Mansfield et al (112), that fluorescence intensities tended to drop off rapidly when inside diameters (id) of 9 or 10 mm were exceeded, with exception of some mercury-metal amalgam lamps. Lamps of smaller diameter ($\leqslant$5 mm) tended to be characterised by excessive noise and short lifetimes, but high intensity. Lamps containing charges which yielded high vapour pressures, eg mercury and iodine, were made with tubing of smaller diameter (6 mm) but much longer bulb length.

2.3.2.2. Bulb length (volume).

In these studies all lamps were made of uniform bore tubing, and so all conclusions for lengths also apply for lamp volume. Manfield et al (112) have reported that there is a definite relation between the fluorescence

intensity and length, and the limit for lamp length was determined in most cases by an increase in noise. This point was reached when the plasma no longer completely filled the lamp and fluctuations of intensity occured. Silvester (113) states that this effect was probably due to simple increase in total emission from the lamp due to increased source area. Many authors have reported optimum lengths for the bulb in EDLs, and it is generally agreed that 2.5 - 2.5 cm is the best length for operation with a $\frac{1}{4}$ wave resonant cavity 214L and 3.5 - 5.0 cm with a $\frac{3}{4}$ wave resonant cavity and the A type antenna. The bulbs were then completely filled by the plasma, at normal operating powers in the respective microwave cavities.

Most authors also report that the lamp's length should be slightly larger than the norm for charges with high vapour pressure eg 6-10 cm for mercury and iodine (71,72), 5-6 cm for tin iodide and antimony iodide. Similarly the length of the bulb should be reduced in cases of charges with low vapour pressure, to prevent movement of material from the hotter parts at the centre of the cavity field, condensing out in cooler parts at the base and top of the bulb. Movement of the charge causes instability in the lamp emission.

2.3.3. Filler gas.

2.3.3.1. Type of gas.

Previous workers (113,157,177,213) have noted that helium at pressures between 1 and 20 torr produced optimum spectral radiant out-put. However, helium was not the prefered fill gas, as the helium was found to diffuse through the lamp wall, when hot, causing lamp failure after approximately 150 hrs. (177). Consequently, argon was the filler gas choice, as indefinite lifetime has been achieved with a minimum sacrifice in emission intensity. A wide range of gases has been investigated, including He, Ar, Ne, Xe, Air, O_2, N_2, (113,157,213) but all authors are in agreement that helium and argon, a narrow second, were the best gases to use.

2.3.3. 2. Fill Pressure.

The most recently published work on optimum fill pressure of argon gas

was made by Browner (177), who recommended 0.5 torr. This was the fill pressure that was adopted for all lamps made in this thesis. Silvester et al (113,157) made a thorough study of fill pressure for He and Ar and reported much lower fill pressures as being optimum. Browner (117) reported that a discharge could not be maintained at these pressures. The majority of published work from this Department has reported 1 torr of argon for a $\frac{1}{4}$ wave (214L) and 3-4 torr for $\frac{3}{4}$ wave (210L) resonance cavities (144-153,164-171). Other workers, have reported 1 torr of argon as being the optimum gas pressure (162,112).

2.3.4. Material.

2.3.4.1. Type of material.

Generally a number of types of EDLs may be distinguished depending on the material introduced.

1) Element.

2) Metal halide.

3) Amalgam or metal halide with mercury.

4) Other compounds.

The element as such was only used when it provided sufficient vapour pressure in the tube. For metals this was often a problem. Corliss (121) and Dagnall (147) stated that a vapour pressure of 1 torr at the operating temperature was required. Well known examples are Hg, Zn, Cd. However, Browner (177) stated that most lamps showed peak radiance at a vapour pressure, of the lamp material, of 5×10^{-3} torr when run in a carefully controlled thermal environment.

If the volatility was insufficient, metal halides were used, generally iodides or chlorides. Metal halides were used also, when the reaction of the metal with the quartz was too fast, (112). If for some reason (volatitity, decomposition) the metal halide could not be introduced into the EDL blank directly, it was prepared in situ. In order to prevent a halogen spectrum, excess metal was added to the lamp (153,159,168,169,83). Sometimes the metal-

halogen ratio was critical, eg for tin with iodine (83). A halogen spectrum may be produced if part of the metal reacts with the lamp material.

Often it was not clear which gave the best results. An appreciable vapour pressure at the working temperature was necessary, but other factors also play a role such as volatility, reversibility of the dissociation of the compound, attack of the quartz wall, clean up, band spectra and temperature. Generally, however these factors have not been mentioned by authors describing the preparation of EDLs. For Cr, Mn, Fe, Co, Ni, and Cu, some authors (83, 147, 168) used chlorides, others iodides (112, 159). For EDLs of lanthanides, the preparation of iodides in situ was somewhat cleaner than the chlorides, and yielded EDLs with a longer life (123). The use of bromides has been mentioned only for the preparation of Be (121) and Mo (159) EDLs. This could be accounted for because Br_2 can rarely be obtained pure, and was more difficult to handle.

EDLs have been described containing amalgam or metal halide with mercury, which decreased the reactivity of the metal with the quartz (147, 198). It is possible that the mercury substitutes the noble gas. Mansfield et al (112) have prepared amalgam EDLs for a number of elements with reasonable resonance line intensity. (Silver-amalgam gave the best lamp). At lower microwave powers, however, they produced only a mercury discharge and at high power, the atomic fluorescence intensity was very noisy. The advantage of higher lamp-intensity was offset by the increased noise.

Other compouds have also been used for the preparation of the EDLs because less reaction with the quartz wall occured. Of the compounds used (phosphates, silicates and tetraborates of Li, Na, K, and Mg,) phosphates gave the best results (154). Phosphorus and sulphur EDLs (224) have to be handled carefully, because a high microwave power may result in thermal decomposition of the compounds.

Veillon (225) used oxides of stable isotopes of Hg, In, Zn, and Cu and reduced the oxides in the blank with hydrogen.

2.3.4. 2. The amount of material.

The amount of material introduced depends on the element and the operating conditions. It was difficult to give a general conclusion on the amount of material needed, as it was rarely reported in detail. It has been my pratical experience (as a rule of thumb), that if the amount can be seen, then too much material has been introduced. Meggers (118) described the amount used as 'an invisible quantity of mercury'. However with the advent of thermally controlled environment for EDLs (174-7) the amount of charge in the blank become less important. The teperature controls the vapour pressure of the material, and therefore the amount of material in the plasma; 5×10^{-3} torr has been found to be an optimum.

Early workers reported that in general the amount used was in the milligram range. This is generally much more than can be evaporated in the lamp. Mansfield et al (112) proved statistically that lamp intensity was independent of the amount introduced for Cd. This seems to contradict the results of Worden et al (123). They found that quantities of 1 milligram or more gave rise to self-reversal.

In the first years, West et al, used milligram amounts and this gave excellent EDLs. Later, however, they emphasised the necessity of a small quantity, such that all the material introduced was in the vapour phase at the operating temperature (148). Cooke et al (160) found that small quantities of metals or metal halides were most successful, eg for a zinc EDL, 20 µg of zinc chloride sufficed. The advantage of small amounts is explained by the prevention of the occurrence of moving solid particles. The decrease of the signal in AF with increase of material in the EDL was attributed to the increasing pressure, giving self-reversal and line broadening. Similar results were obtained by Hollander.

Tomkins et al (122) used a 0.1 μg amount, as also did Budick (126), for the rare earths in EDLs. Worden et al (123) also used microgram (0.1 - 100 μg) quantities of metal iodide, which was very similar to the quantitive result reported by Cooke (160) 20 μg. These reports are all in line with the conclusion drawn from recent work (174-7) in which optimum temperatures and vapour pressures (5×10^{-3} torr) are used.

2.4. Operation of Electrodeless Discharge Lamps.

2.4.1. Frequency.

In general microwave energy is used (10^9 to 10^{12} Hz) for the excitation of EDLs. The most frequently used microwave generator has been the Microtron 200 (Electro-Medical Supplies, Wantage UK). The frequency is 2450 MHz and the maximum power varies from 0-200 watts. Brandenberger (186) described a modification of the generator resulting in better short term stability and an improvement of several orders of magnitude.

At an earlier stage of the development of EDLs, excitation was often performed with radio waves (2×10^5 - 10^9 Hz). Thus Bell (127) used 100 MHz for alkali metal EDLs. Brewer (195) used 20 MHz for Rb EDLs. This author observed that the lamp intensity remained constant for many hundreds of hours. Meggers (118) compared radio frequency excited EDLs (30-370 MHz) and found clean-up decreased at higher frequencies. This is in agreement with Jacobson et al (192) who found for mercury tubes that 300 Hz gave a much better lamp intensity, efficiency and ease of operation than the 150 MHz discharge.

For the coupling of the microwave energy to EDLs, cavities and antennas are used. If the coupling is inadequate, the energy transfer is inefficient and the coaxial transmission line will dissipate some of the energy as heat and some energy will be reflected back to the generator with possible damage to the valve. Schrenk (232) described the design considerations, construction details and operation of an independent means for minimising the reflected power. The assembly has a tunable double stub impedance-matching transformer. A similar design has been reported elsewhere (148).

2.4.2. Type of cavity.

The most popular cavities are those of the $\frac{1}{4}$ wave-type (EMS 214L Evenson) and the $\frac{3}{4}$ wave-type (EMS 210L Broida) (see fig. 8). These two cavities have been compared in the literature (147,161,168,197). In the threequarter wave cavity the position of the EDL is not critical, but for lack of tuning possibilities, the coupling is less efficient and relatively high reflected power results. The closed shape gives good thermal stability to the EDL and makes it more suitable for the less volatile compounds. The $\frac{1}{4}$ wave cavity on the contrary gives, after critical tuning with a reflected power meter, very efficient coupling. But the open shape can result in thermal instability of the EDL. Considerable stray light and possible interference with the amplifiers can be caused by the pick up of stray microwave radiation from the cavity. If this is a problem, aluminium foil shielding will act as a screen. This cavity is more suitable for volatile components as the lamp is not enclosed by the cavity.

Modifications have been described for the $\frac{3}{4}$ wave cavity (147,156,160). In special cases there were some advantages but generally the modifications did not give much improvement. Cooke et al(156)noted intheir studies of cavities that it was often preferable to use a less efficient cavity than to cool it, and that rhodium was probably a better surface material than silver. The possible oxidation and sulphide formation with silver results in a less efficient cavity (cavity deterioration). Other important conclusions were reached by Fehsenfeld et al (161). They investigated six types of cavity of which the foreshortened $\frac{3}{4}$ wave co-axial (2a) was the forerunner to the Broida cavity as was the foreshortened $\frac{1}{4}$ wave co-axial (5) to the Evenson cavity. The cavity 2a was reported to operate most efficiently when the gas pressure was above 1 torr, which confirms the numerous reports that recommend 3 torr as a fill pressure for the EDL. Similarly when they reported their designs, cavity 5 showed the widest pressure range in operation and was nearly 100 % efficient over the entire range, particularly at low pressure.

fig. 8

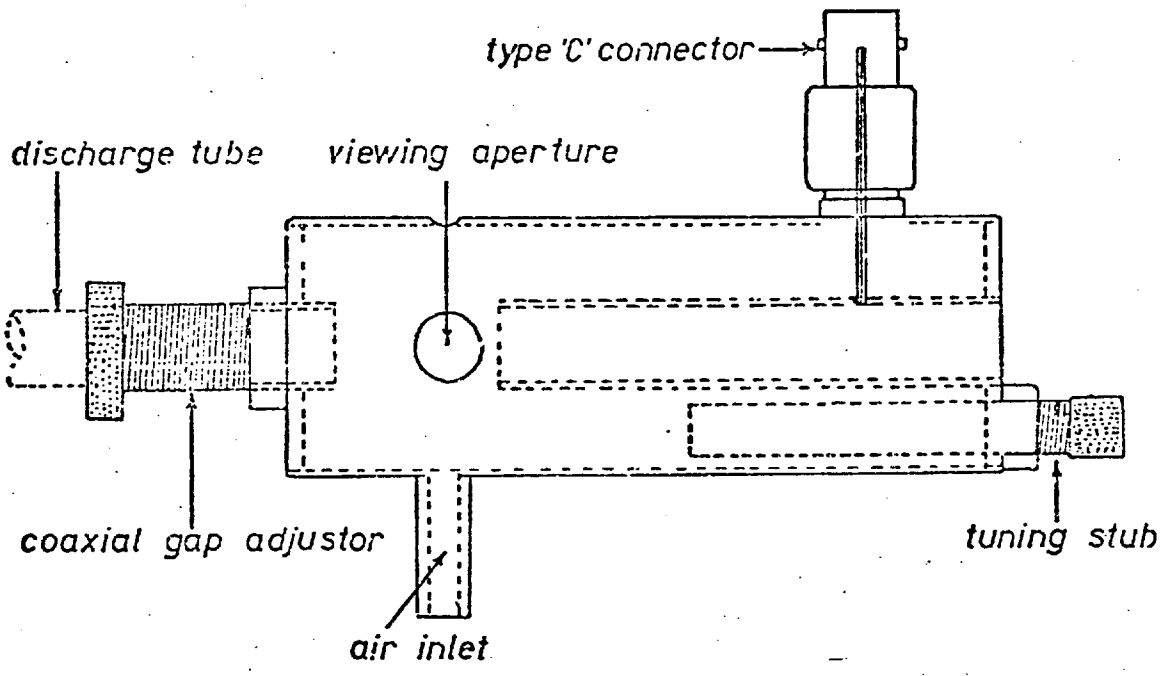

b) A 3/4 λ Broida type cavity No. 210 L

a) A 1/4 λ Evenson type cavity No. 214 L

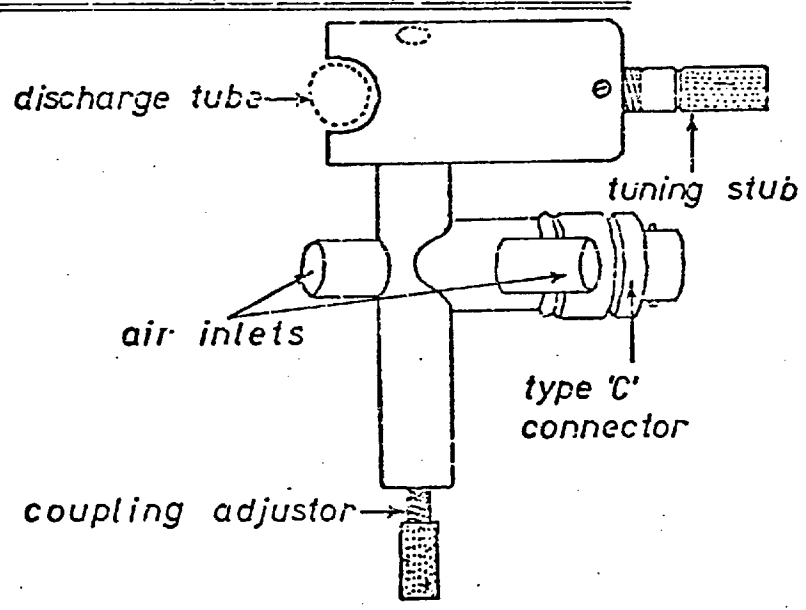

Often microwave antennas have been used instead of cavities (112,113,157, 159). Manfield et al (112) have used in AF Raytheron antennas of the A and C type as well as cavities. The A antenna was found tc be of most use for AF measurements. The advantages, over resonant cavities, were that they did not run hot, and hence did not require strong air-cooling, and that there were no tuning facilities. The A antenna focussed more microwave energy at the lamp than the C antenna. One of the disadvantages of antennas is that a fair amount of microwave power is scattered with possible harmful effects to the operator.

2.4.3. Power.

The optimal operation conditions with a cavity can be achieved best by correctly adjusting the microwave power supplied to the cavity and lamp; a change of 5-10 watts can result in a change of up to 90 % in the atomic fluorescence signal. However, optimum conditions ascertained for operation of a lamp in one type of microwave cavity will by no means be optimal for operation in another one. Likewise the optimal type of cavity and power for one lamp will not necessarily be the same for all lamps of that element, each individual lamp has its own operating power in a particular cavity. This also holds true for antenna operation.

However, with the advent of stable thermal environments, the lamp reaches a threshold power at the optimal working temperature and the AF signal varies little with any further increase of power. Hence, power supplied to the cavity becomes less critical, as does the type of cavity used. The uniformity of the electric field created around the lamp may well be more important, and the $\frac{3}{4}$ wave cavity may show an advantage over the $\frac{1}{4}$ wave cavity and the directional antenna with future work.

2.4.4. Modulation.

Electronic modulation of EDLs in AF studies has been used, as the distance between the EDL and the atom reservoir is shorter than with the mechanical chopping arrangement. Also a chopper can cause disturbance of a flame, resulting in instability. Dagnall (150) investigated seven wave forms and found that the 'square wave' gave the best light intensity of the EDL. The optimum modulation frequency was about 20,000 Hz. The electronically modulated EDLs also gave an improved lamp noise and drift. If the modulation depth of the microwave amplitude was 50 % or less, noise decreased below 1 %. The mean microwave power was always less than with unmodulated lamps.

Alger (233) used a switched resistor modulator which was both simpler and cheaper to construct and more versatile in operation. Wildy (197) found modulation sucessful for more than 30 elements. In most cases the stability was not changed by modulation. For iodine it was not possible to maintain a modulated lamp that was stable enough. When modulated, the lamp intensity proved to be more sensitive to variation of power, position in the cavity and cooling. Larger amounts of material in the lamps made successful modulation difficult. According to Browner (153), 50 Hz modulation improved the lamp stability and inhibited the migration of material, which is probably the main cause of drift in non-modulated lamps.

2.4.5. Thermally stable environments.

Some investigators apply cooling to an EDL, others do not. The material introduced and the microwave power applied largely determine the necessity and magnitude of cooling. Cooke et al (156) have stated that greater lamp stability was obtained by isolation from draught, especially in the case of the open $\frac{1}{4}$ wave cavity. This gave better stability in AF measurements. The cooling air stream has to be carefully adjusted, otherwise the air stream itself causes lamp instability. If the vapour pressure in the EDL is too high, the discharge may be limited (constricted) or even extinguished completely, or cause line broadening and self-reversal. This may often be prevented by

using smaller amounts or a less volatile compound. If this is impossible, air cooling has to be applied.

Forrester (155) stated that with air cooling sharper lines were observed but with a sacrifice of intensity. Other authors have also used air cooling especially for iodine and arsenic iodide EDLs (71,72,146,151,214). Aldous (168) observed that cooling of a platinum EDL resulted in a decreasing lamp intensity and an increasing background emission. According to Aldous the vapour pressure in the lamp has to be regulated by means of cooling especially when very volatile compounds or elements are used. Browner (71) did not need air cooling for thorium EDLs but it was applied for mercury EDLs. Brewer (195) has pointed out that accidental cooling, eg by draught, may cause serious lamp instability. Cooling has also been applied in order to prevent the buring of a hole or deep dent in the lamp or formation of cristoballite, which can result in rupture of the EDL (123). This is especially common when high microwave powers are used.

Water cooling has also been applied. Several techniques have been described in which a thin stream of water flowed over the EDL (225,192) - EDLs have also been placed in a jacket in which water at room temperature circulated (221).

Another technique applied to place EDLs in a stable thermal environment has been described by Mansfield (112) and Zacha (159). These workers found that there was inadequate thermal support provided from the A type antenna. They overcame this by the use of either an open quartz insulation jacket with or without quartz wool around the EDL, or a quartz vacuum jacket surrounding the lamp and attached to a vacuum pump capable of producing a pressure of 1 torr or less. A similar approach was made by Aldous (148) and also by Cresser (226). Aldous says that the use of vacuum jacketed EDLs provides a source of increased stability and allows the use of less volatile charges as an increased operating temperature results. An added advantage gained by surrounding EDLs with permanently attached low pressure envelopes was that it did not necessitate the permanent use of a vacuum pump.

Other workers have found it necessary to heat up the EDL to obtain the best emission intensity from the lamp. Zacha (159) and Cunningham (162) both used simple nichrome heaters, where the lamps slipped smoothly into a piece of wider quartz wrapped uniformly with nichrome wire. Cunningham fitted the lamp and heater inside another outer quartz jacket, to reduce convection currents and improve heating efficiency. Many earlier workers, mainly using alkali metal lamps, have heated one end of the lamp bulb directly with nichrome wire to obtain a sufficient vapour pressure inside the lamp (127-9,194,195). Another approach, whereby part of the lamp bulb was contained in an oven or furnace, has been used to obtain temperatures of up to 800C (120,122,123,126, 138,200).

Recently a series of papers has been published (174-7) in which more sophisticated systems of temperature control are used. Air from a small fan was heated by passing it over a nichrome heater coil, and then over the EDL, which was contained in a quartz outer jacket. The temperature was controlled by a thermocouple feed-back. This simple apparatus provided a stable thermal environment for the EDL over a wide range of temperature, from a cooling effect of air at room temperature up to a temperature of over 500 C.

This work in many ways was a fundamental breakthrough. The thermally stable environment offers the advantage of operating the lamp at its optimum emission intensity, often showing many orders of magnitude improvement. This is of vital importance, as AF studies have often been held back for the lack of sufficiently intense sources. Also many of the lamp's parameters previously discussed become far less critical; this is especially so for the amount of material introduced, as the amount in the vapour phase and therefore in the plasma is controlled by the environmental temperature. Large microwave powers are no longer required to provide the thermal energy to vaporise the charge. A further important consequence is that the stability of the microwave energy output is not so critical, since on reaching a threshold power, the emission intensity of the lamp varies very little with further microwave power supplied. Lamp stability and reproducibility are greatly improved by temperature control,

and far less operator skills are necessary to obtain optimum performance from these sources.

Browner (176,177) noted that the slopes for Zn and Cd were almost identical with plots of partial pressures of Zn and Cd metals respectively vs. temperature. It was also stated that at their respective optimum operating temperatures, the lamps prepared from pure elements (Hg, Zn and Cd) contained the same partial pressure of the elements (approximately 5×10^{-3} torr). In table 4, all the information from various papers where optimum working temperatures are reported, together with the vapour pressure of the respective elements at that temperature are given. All show a similar vapour pressure, approximately the same as given by Browner, contrary to previous reports of 1 torr (121,147).

Since the EDL bulbs are made from uniform bore tubing, the volume of a bulb can be calculated eg r = 4 mm id., L = 40 mm length so using $\pi r^2 L = V$, the volume is 2 ml. Assuming that the vapour pressure of the charge in the EDL has an optimal value of 5×10^{-3} torr and behaves as an ideal gas, it is possible to calculate the minimum amount of material needed in an EDL.

These calculations have been made from the scant information in previous reports using the following equations:-

General gas law for fixed volumes gives

$$P_1/T_1 = P_2/T_2 \qquad \text{eqn. (44)}$$

where $V_1 = V_2 = 2$ ml

P_1 is 5×10^{-3} torr at optimum working temperature T_1K

P_2 is the corrected vap. pressure at standard temperature 273K and

1 g mol. occupies 22.4 l at S.T.P. equ. (45)

therefore

$$\frac{2}{22.4 \times 1000} \times \frac{P_2}{760} \times \text{1 g mol. occupies 2 ml at 273K and at pressure } P_2 \text{ torr.}$$

This calculated amount of material in the vapour phase in the EDL bulb can then be compared to the optimum weight found empirically, (see Table 4a).

Table 4

List of calculated vapour pressures from reported temperatures.

Ref.	Author	Element	Optimum Temp. C	Vapour Pressure torr
129	Burling	Cs.	110	8×10^{-4}
		Na.	210	2×10^{-4}
127	Bell	Rb.	120	1.5×10^{-3}
128	Atkinson	K.	180	2.6×10^{-3}
		Rb.	130	1.2×10^{-3}
194	Gerrard	Cs.	185	2×10^{-2}
		Rb.	205	2×10^{-2}
195	Brewer	Rb.	180	1.5×10^{-2}
176	Browner	Hg.	50	5×10^{-3}
		Cd.	250	5×10^{-3}
		Zn.	310	5×10^{-3}

Table 4a

A comparison of reported and calculated amounts of material needed in an EDL at optimum temperature.

Compound	Ref.	Author	Optimum temp.C.	Ref.	Author	Optmum wt.μg	Calc. wt. μg
$ZnCl_2$	174	Patel	310	160	Cooke	10	0.09
$CdCl_2$	174	Patel	260	160	Cooke	5	0.12
GdI_3	126	Budick	500	126	Budick	0.1	0.11
NdI_3	122	Tomkins	750	122	Tomkins	0.1	0.08
SbI_3	Unpublished		75	Unpublished		5	0.24

It can be clearly seen, that few authors who have made careful note of the optimum weight or the minimal weight needed to obtain a useful spectral output from the EDL have come very close to the calculated weights (cf 5-10 mg in references 147, 148).

Because of the many advantages gained by running EDLs in a stable thermal environment, a similar system to that reported by Browner (176), has been constructed. The heater system was designed and made in this College. The furnace was made from stainless steel, and has a large central metal core which has a nichrome wire coil surrounding it suitably insulated. The length and gauge of nichrome wire were chosen to develop a temperature of 850C from a maximum current of 2 amps. at 90 volts from a mains variable transformer (see fig. 9,10).

The compressed air supply delivered air at 15 psi. pressure through a ballast-stabiliser tank. The air then passed into a control valve and flow meter tube before entering the furnace as a tangential flow. This was to obtain maximum residence time over the heating element. Also the gas was forced to pass over the nichrome wire between the narrow gap of the outer case and the large central core, allowing maximum contact of the cool air with the heater. The core also acted as a heat-sink reservoir so stabilising the temperature.

The temperature of the gas was controlled by varying the current supplied to the nichrome coil from the transformer (see fig. 11). Fine control of the temperature of the air was obtained by varying the gas flow at a fixed setting (see fig 12) of the power supply.

The hot air was then passed through a quartz outer tube 13 mm id 15 mm od which just fitted into the $\frac{1}{4}$ wave cavity. The EDL was then held centrally inside the quartz outer tubing, by a brass collar which had slots cut into it, to vent the hot air. The EDL was adjusted so that the bulb was fully in the microwave field (see fig. 9).

The $\frac{1}{4}$ wave cavity was tuned, with the EDL alight at optimum working temperature, to give a minimum reflected power. The result of matching the

E.D.L. temperature control assembly

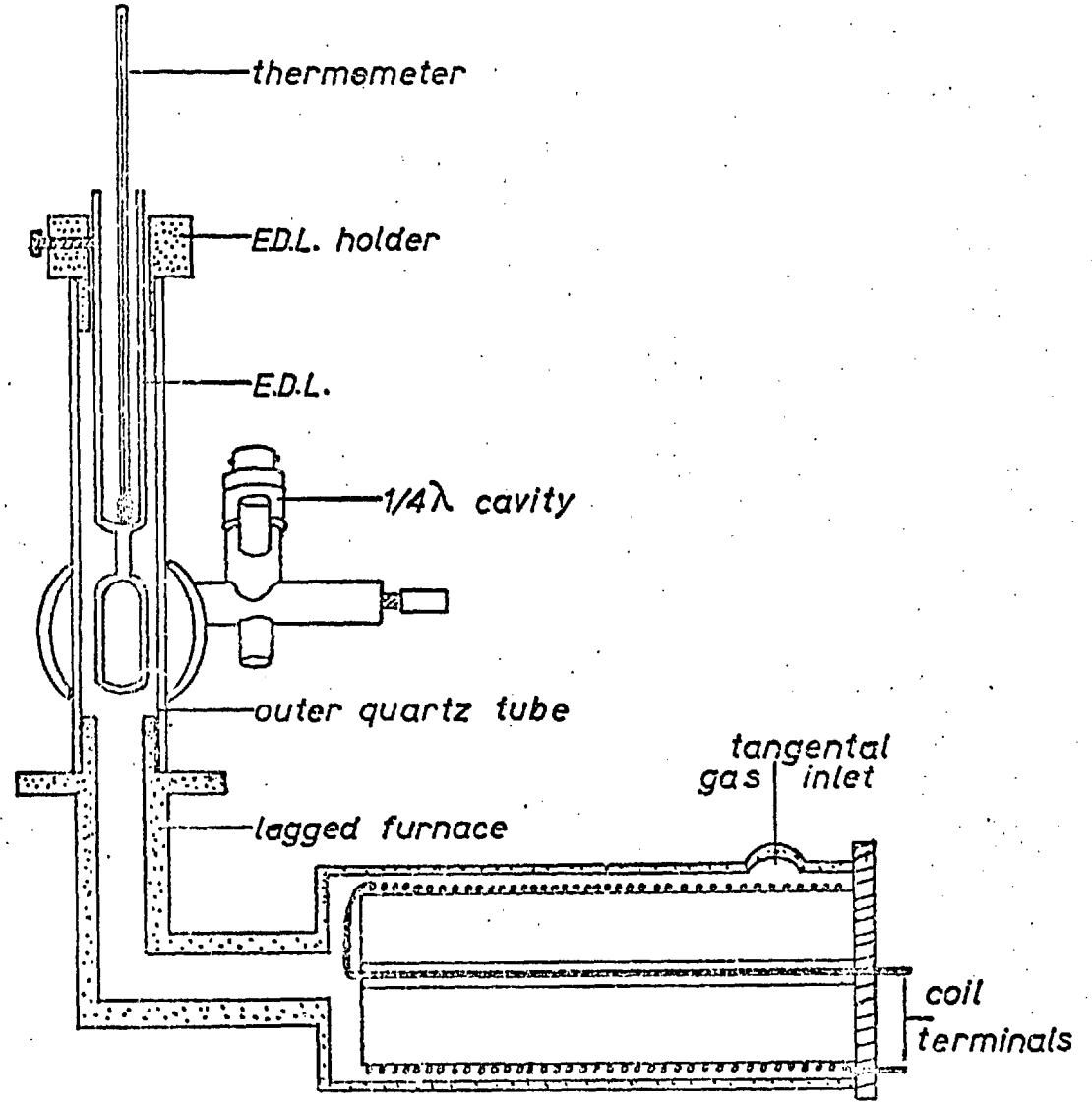

fig. 9

fig.10

DETAILED CONSTRUCTION OF THE FURNACE.

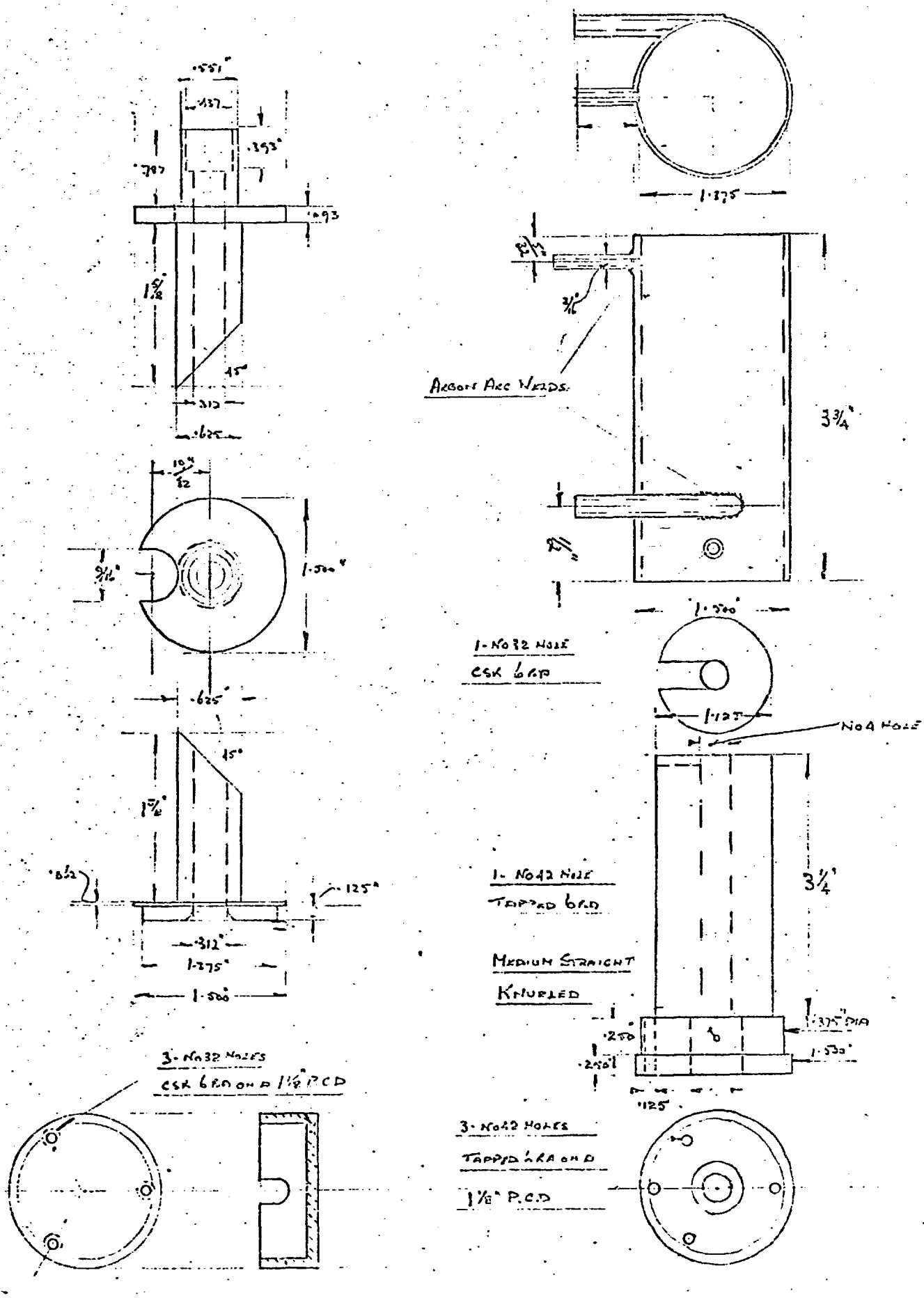

cavity's impedance was to obtain maximum transfer efficiency from the microwave energy source to the gas discharge.

2.4.6. Multielement Lamps.

Multielement EDLs have been developed as a convenient means of carrying out multielement AF analysis. For Li, Na and K, Woodward (154) developed a lamp in which he introduced the elements as silicates and tetraborates. He found that the amount of material was more critical than in single element lamps but the lamp stability and power applied were equal. Fulton (152) developed an As-Sb EDL; here again stability was comparable with that of single element lamps. But from the higher detection limits in AF with this dual element EDL, they supposed that the microwave energy is divided between the metals involved.

Norris (230,231), however, found no difference for Cr-Mn and Co-Ni dual element EDLs over single element lamps. Marshall (173) has prepared Bi-Hg-Se-Te, Cd-Zn and Ga-Zn multielement lamps. These authors noted no inter-element interferences were evident in the lamps.

Because multielement EDLs require a very careful choice of fill material in order to maintain an adequate vapour pressure for each component under operating conditions, Patel et al (174) investigated temperature controlled multielement EDLs. They found that two modes of operation were possible, either the optimum temperature for each element present could be selected sequentially, or alternatively, a comprise temperature could be selected for all elements present, but with some less spectral radiant output for some elements.

Instead of multielement EDLs, dual element EDLs with each element contained in a separate concentric outer and inner compartment of the lamp have been described (226).

fig.11

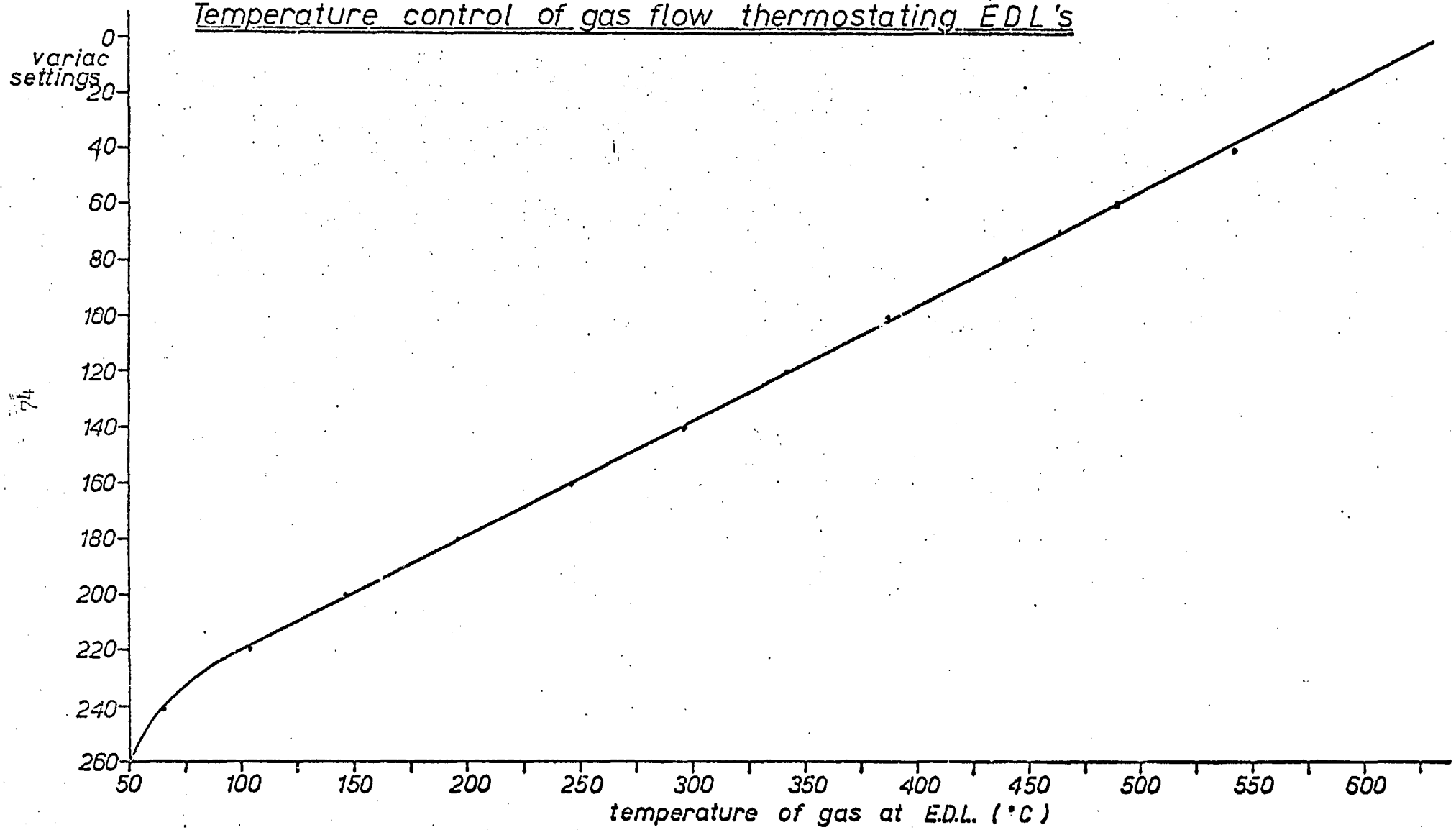
Temperature control of gas flow thermostating E D L 's
variac settings
0
20
40
60
80
100
120
140
160
180
200
220
240
260
50
100
150
200
250
300
350
400
450
500
550
600
temperature of gas at E.D.L. (°C)

fig. 12

Temperature control by gas flow regulation

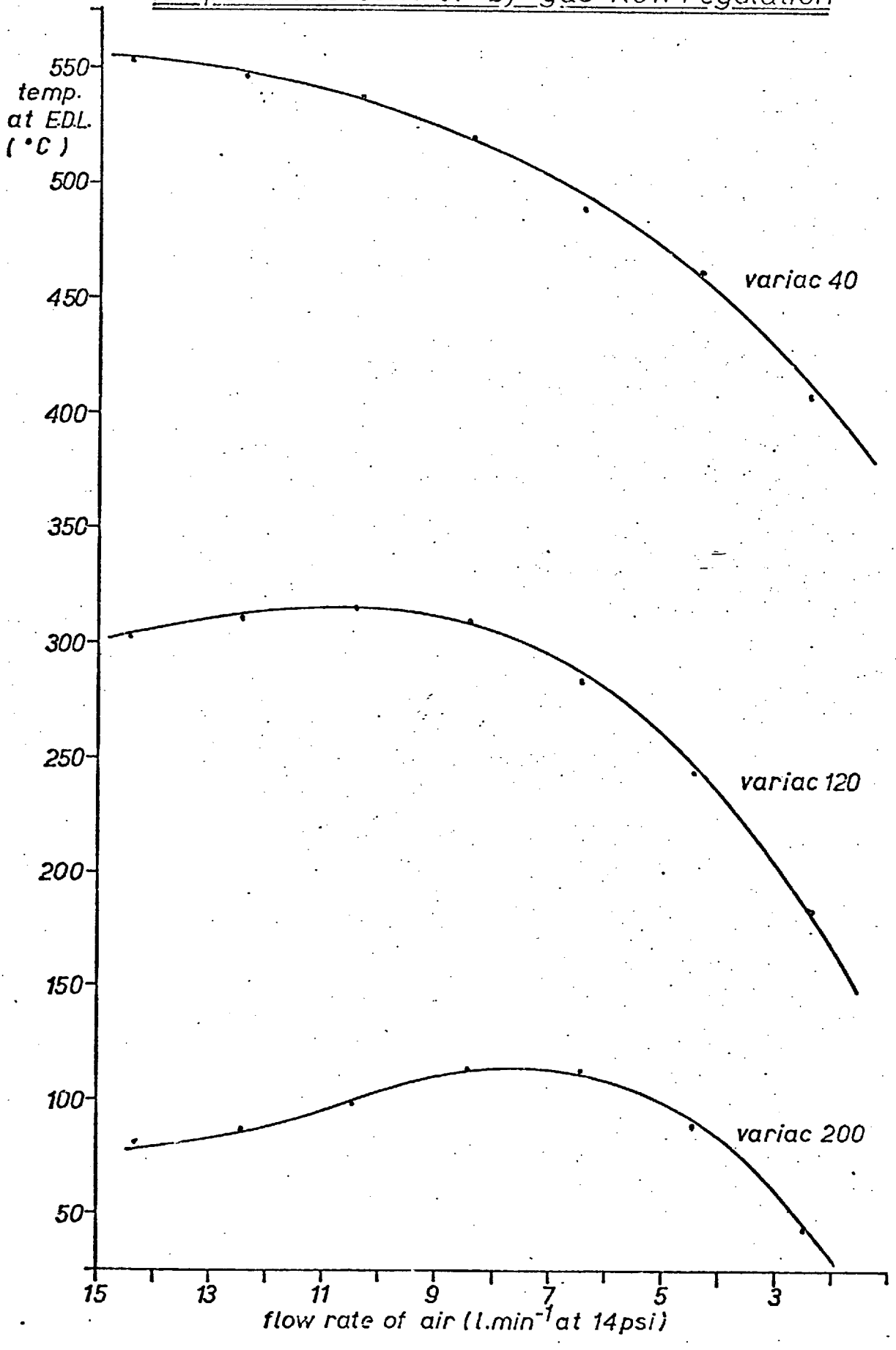

2.4.7. Miscellaneous.

Run-in period. During the first hours of operation, the characteristics of an EDL may change considerably. Therefore the EDL is conditioned for some time, by starting a discharge results in stable lamp intensity after that period. Usually the run-in period took a few hours at low power (50 watts) (154,223). In other cases the run-in-period was shorter, but the power to be applied was higher (159). An alternative method is to warm the lamp bulb gently in a Bunsen burner flame until all the material introduced is in the vapour phase. This allows any reaction between chemical components of the charge to reach completion and complete homogenous mixing. If the lamp base is then cooled in distilled water, all the material collects at the base of the bulb. The lamp can then be used immediately for analytical determinations.

Lifetime/Clean up. If EDLs are used for sometime there is an observed colour change of the walls. This phenomenon is called 'clean up' and the mechanism undoubtedly involves a series of complicated reaction or group of reactions. Mansfield (112) states that the main cause is the collision of charged species with the wall causing reduction of the silica and metal diffusion into the wall. The lifetime of the EDL is shortened by this phenomenon. The frequency of the atom-wall collisions are determined to a large extent by the diminsions of the lamp, hence the limited lifetime of tubes of ≤ 5 mm id (2.3.2.1.).

Williams (107) when investiating Hg EDLs (vycor tubes) observed that an excitation frequency over 100 MHz and a fill gas pressure over 5 torr resulted in the clean up proceeding more slowly.

Always the clean up was located on the walls near the high frequency terminals, which resulted in black bands on the inner side of the lamp. If the black parts were heated to redness the black colour disappeared and the lamp gave the original Hg emission again. Gleason (221) applied moderate heating whereas Silvester (157) heated to bright redness in a H_2/O_2 flame., Al-Ani (198) reported the inclusion of mercury when making metal halogen EDLs to eliminate metal wall reactions.

Gas fill pressure also affects wall-darkening, and was found to be much stronger at low pressure (112,113,160). It is reported that the processes at high pressure are different from those at low pressure. This also conveniently fitted the fact that the lifetime of an EDL was generally longer, at relatively high pressures (1-50 torr). Dagnall (150) has reported that modulation prolonged lifetime because the attack on the quartz wall was decreased.

Intensity-stability. The EDL has often been compared with other light sources (81,112,147,159,237,238) with special attention being paid to intensity, stability and life. The general conclusion were that the resonance line intensity of the EDL is high and self-reversal is small, and therefore it is the preferred source for AF.

Browner (153) compared EDLs with hollow cathode lamps HCLs and found that the intensity of the EDLs was 60 to 1250 times greater, depending on the element. Moreover, the background was much smaller for EDLs. Dagnall (229) found for a Si lamp, an intensity ratio of HCL to EDL of 6.4 to 100 (251.6 nm), and a line-to-background intensity ratio of 44 to 1 for HCLs and 130 to 1 for the EDLs. Dagnall (81) also gives the lamp intensity ratios between EDLs and HCLs for Sb, As and Se; values between 110 and 800 were obtained. Fleet (169) compared a Co high intensity hollow cathode lamp HIL and an EDL, the lamp intensity ratio was 20 to 1, the EDL also showed less background and a narrower line profile; furthermore no drift was observed over a one hour period.

2.5. Spectral characteristics of electrodeless discharge lamps.

By using a monochromator it was possible to measure the integrated line intensity from the source (EDL). But this does not give any indication of self-reversal at the line centre, also the PMT sensitivity varies over the spectral region, as does the energy throughout of the monochromator. This then, only gives a measure of relative intensities between lines, and shows the lines present, allowing the detection of lines from other elements (Hg, I_2) present in addition to those lines from the element required. The spectral range investigated was that of the response of the solar-blind PMT (190-320 nm) (see fig. 3b).

Browner (176, 177) stated in his reports that the optimum working temperature of the EDL, obtained from integrated line measurements, was often 10-20C higher than that found necessary to produce the maximum fluorescence signal. But because monitoring the integrated line intensity was more convenient and rapid, a preliminary study was carried out by this means. But the trueness of measurement of the source line intensity variation with temperature can only be gained by observing the fluorescence signal. These results can be found in the relevant chapters of the determination of specific elements.

Spectral scans were made with the use of a monochromator with a conventional end-window wide-response PMT. The DC signal thus developed was displayed on a 'Servoscribe' chart recorder, which had a variable range. The scanning speed of the monochromator was 5 nm/min., representing 1 nm / mm on the chart paper. When comparisons were made between two different conditions, the position of the EDL and the monochromator settings were held constant and only the thermal environment or microwave power was altered. A number of EDLs were made for each element and the best were selected for use in the determination of that element. The lamps were made following the procedure set out in section 2.3.1., unless specifically reported to the contrary.

2.5.1. Mercury.

Many authors have reported successful mercury EDLs made from the element (23,68,117,118,147,163,164,173,174,177,180,192,197,202,217). The EDL used in these studies was made from mercury metal with a fill pressure of 0.5 torr argon, and of tube dimensions 6 cm length, 6 mm id.

The lamp gave the maximum signal at the 253.652 nm intercombination line, when operated in a stable thermal environment of 60C at 20 watts power. When the power was increased to 50 watts the integrated line intensity of the 253.652 nm line showed an improvement of 3.3 %, but the S/N ratio decreased by 33 %.

All the lines present in the Grotrian diagram of mercury for the spectral region scanned (fig. 13a) were present, with the exception of the 275.278 nm line. The principal ground resonance line, being at 184.96 nm was outside the spectral range scanned. The lamp showed less than ± 0.5 % variation for short term stability (flicker noise) and long term stability (drift) of 1 % per hour.

2.5.2. Iodine.

Many authors have reported successful iodine EDLs made from the elemental iodine (72,151,152,159,173,185,214), but these lamps have always been used with strong air cooling to minimise the high vapour pressure of the iodine in the bulb. To overcome this problem, EDLs were made by introducing known amounts of iodine in carbon tetra-chloride solution. The most successful lamp made for iodine was achieved using this method (1 µg). Unfortuneatly, no importance can be attached to this weight since to remove all traces of CCl_4 from the lamp, the lamp blank was left under vacuum for an appreciable period of time. During this time iodine was also lost *via* the vapour phase. It was important to remove all traces of CCl_4, otherwise Cl_2 and C_2 emission (lines and continuum) was obtained.

The EDL used in these studies was made from elemental iodine, introduced as a CCl_4 solution, with a fill pressure of 0.5 torr argon and bulb dimensions of 6 cm length and 6 mm id.

The lamp showed a very simple spectrum consisting of two lines (fig. 13b), the iodine line at 206.163 nm and the mercury line at 253.652 nm. The mercury vapour sealed into the lamp came from the vacuum gauge.

The only iodine line observed was an extremely intense one resulting from the non-ground state transition at 206.163 nm. The remainder of the spectrum was a broad low intensity continuum. This iodine line at 206.163 nm coincides with the bismuth ground resonance line at 206.170 nm first reported by Thompson (72).

fig.13

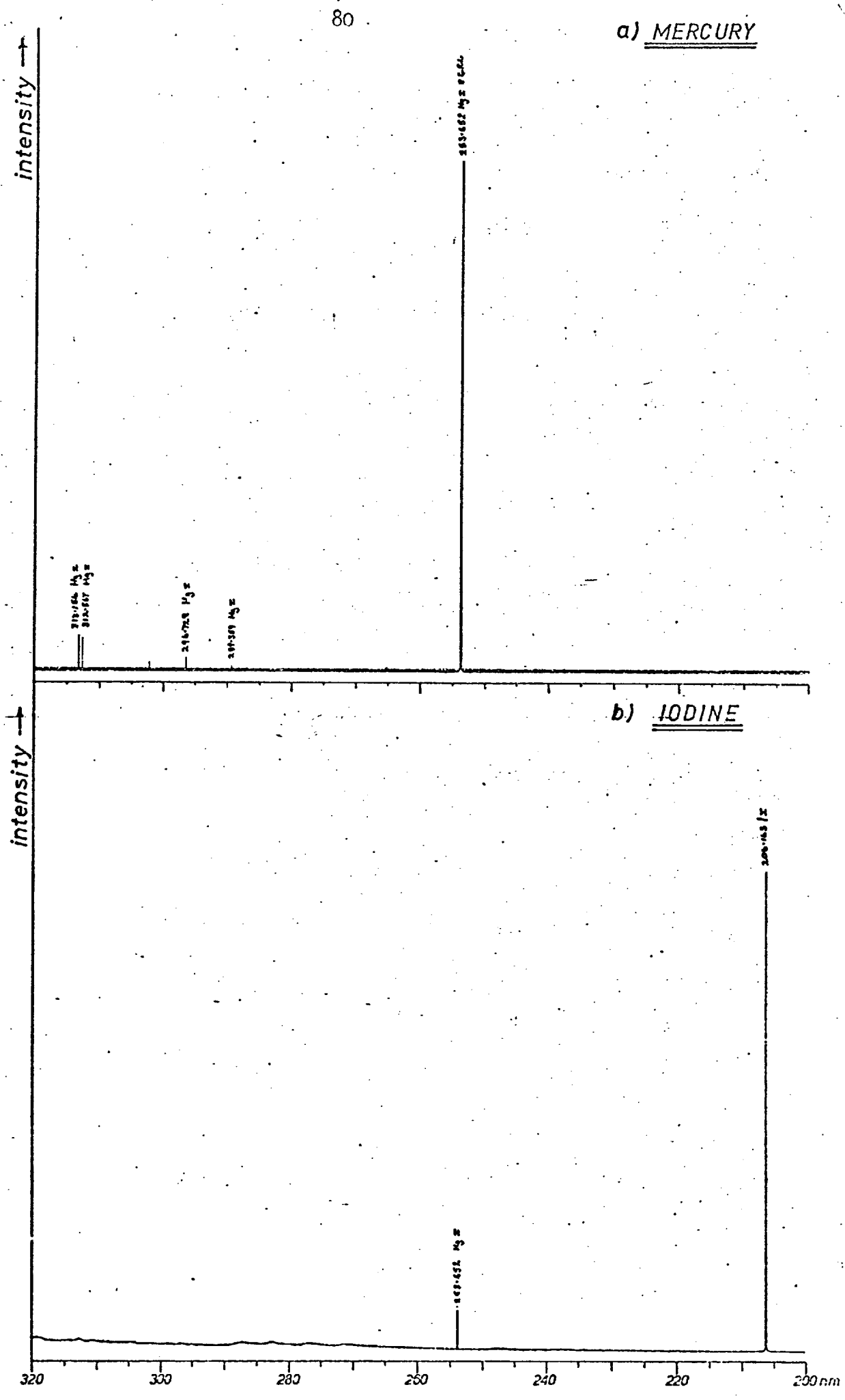
a) MERCURY
intensity →
b) IODINE
intensity →
320
300
280
260
240
220
200 nm

The lamp was operated, with air cooling, at minimum power to give the maximum S/N ratio. The integrated line intensity was increased by 33 % by supplying 50 watts power, but this resulted in a decrease on the S/N ratio by 85 %. The lamp showed a drift of 1 % per hour with flicker noise of less than ± 0.25 %.

2.5.3. Bismuth.

All bismuth lamps reported (72,122,141,159,181,161,197,202,214) have used bismuth iodine, this being formed in situ. An attempt was made to use only bismuth metal, but the maximum operating temperature of the furnace gave insufficient vapour. The best lamp was achieved by sealing a minute quantity of commercially available bismuth oxy-iodide into the lamp bulb, which had previously contained elemental bismuth. The lamp bulb dimensions were 3.5 cm and 8 mm id and the lamp was sealed at 0.5 torr pressure or argon.

The bismuth lamp discharge showed a colour change as the temperature increased; this was also matched by an intensity increase. The discharge started as a red-pink argon colour and changed to an 'arctic' blue colour at 150C, finally reaching a very bright 'electric' blue colour at 180C. The optimal working temperature was found to be 190C giving maximum intensities for the ground resonance lines at 306.772 and 223.061 nm (see fig. 14a nd b).

The majority of the lines present in the Grotrian diagram of bismuth were found to be present in the spectrum of the heated EDL (fig. 14b).

There was also present, the ground resonance line 222.725 nm, which was accounted for by Brode (240). This line can be predicted from the energy difference between the $^4S_{1\frac{1}{2}}$ and $^4P_{1\frac{1}{2}}$ states. It has been used elsewhere for AA of bismuth (241). The 223.061 nm ground resonance line is the most strongly absorbed of these lines. Bismuth has nine ground resonance lines of which four (211.206, 202.121, 195.948, and 195.389) were never detected, and the other five were present (306.772, 227.658, 223.061, 222.725, 206.170) (See fig 14b). There was an improvement in the integrated line intensity for each of the lines present (x50) when a change from30C to 190C was made to the thermal

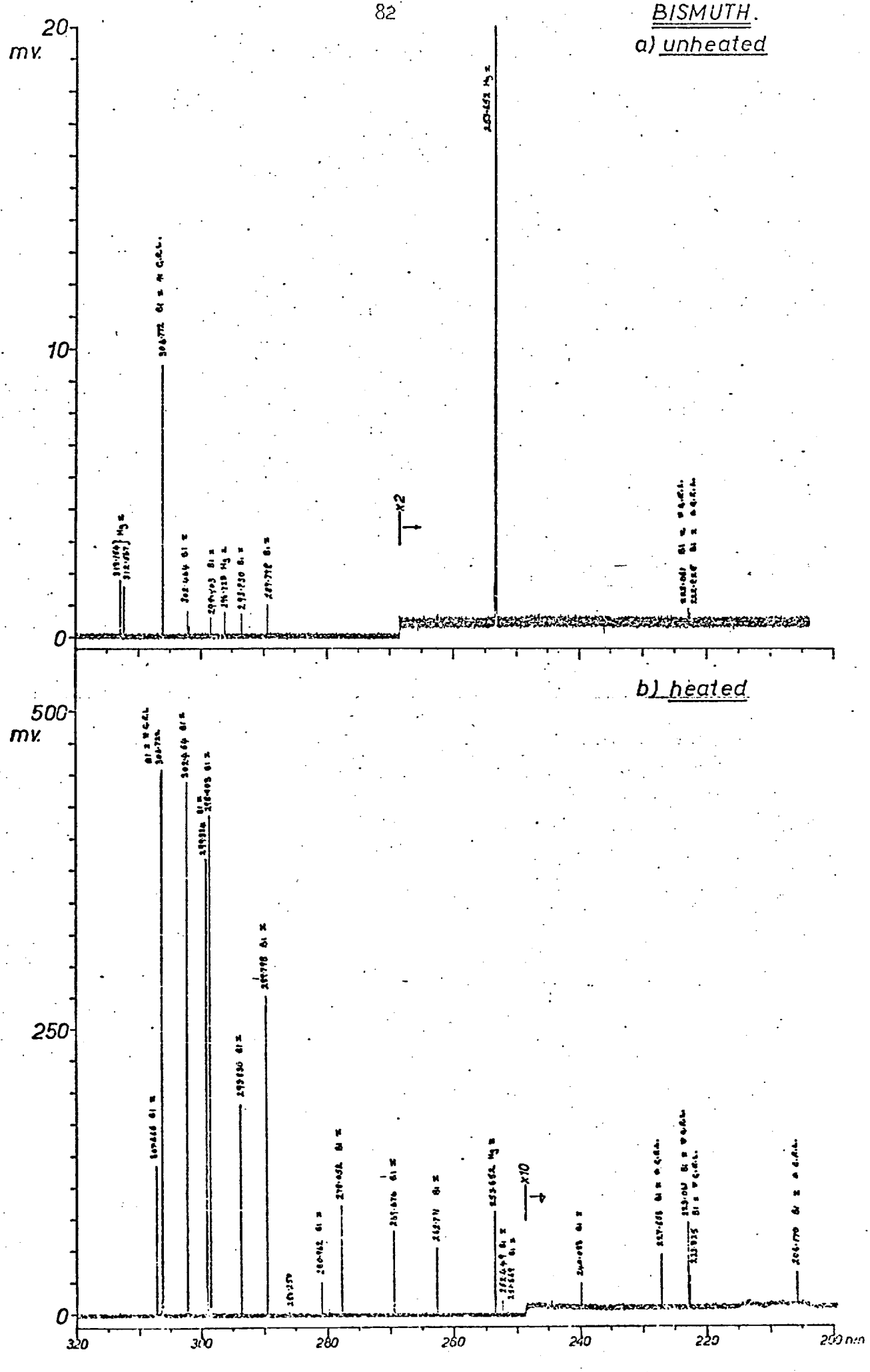
BISMUTH.
a) unheated
20
mv.
10
0
x2
b) heated
500
mv.
250
0
x10
320
300
280
260
240
220
200 nm

environment of the lamp at a constant power of 40 watts. (see fig. 14a & b).

The lamp showed little change in intensity of the ground resonance lines when the power was increased above a threshold value of 30 watts, provided that the optimum working temperature was maintained. However the S/N ratic for the ground resonance line at 306.772 nm decreased above 50 watts. Hence the lamp was operated at 40 watts.

2.5.4. Lead.

Many authors have reported successful lead EDLs made from lead iodide (65,84,122,141,153,159,161,174,177,181,188,202,217). As an alternative material for the EDL, lead chloride and lead phosphate (153-4) have been used. An attempt to make a lamp only using elemental lead failed, as the furnace did not produce a sufficiently high temperature to maintain an adequate vapour pressure. Lead chloride could be quantitatively deposited in the lamps from a concentrated hydrochloric acid solution. But lamps containing lead chloride suffered from chlorine continuum, resulting in a poorer S/N ratio, when compared with lead iodide lamps.

In lead iodide lamps it was very important to have excess lead present, otherwise iodine tended to dominate the discharge. Also after a period of operation with lamps made from lead iodide only, there was a loss of intensity for lead line, because of clean-up whereby lead was lost to the wall of the lamp. On the other hand, too much free lead in the lamp resulted in the metal plating out on the wall which caused a loss in transmission and stability. Hence a very fine balance between lead and lead iodide introduced into the bulb was necessary (cf the critical ratio of Sn/I_2 in tin lamps)(83). The lamp used in these studies was made from lead iodide, with excess lead. and a fill pressure of 0.5 torr argon and bulb dimensions of 3.5 cm length and 8 mm id.

By monitoring the ground resonance line, 283.306 nm, a maximum integrated line intensity was observed at constant power, when the lamp was operating at a temperature of 325C. The line intensity at the optimal working temperature

varied little with change in microwave power after a threshold value of 30 watts. With increasing power, the noise also increased, resulting in a poorer S/N ratio above 60 watts, hence the lamp was operated at 50 watts.

Most of the lines present in the Grotrian diagram of lead were found to be present in the spectrum of the heated EDL (fig. 15b). Lead has three ground resonance lines of which the 202.202 nm line was never detected, but the other two, 283.306 nm and 216.990 nm, were present (see fig. 15). The line at 216.990 nm is the most strongly absorbed of the two, but that at 283.306 nm showed the greater intensity. There was an improvement in the integrated line intensity for both of these ground resonance lines (X20) when a temperature change of 60C to 325C was made to the thermal environment of the lamp at a constant power 50 watts (see fig. 15 a & b). When the lamp was operated at its optimum working temperature, the mercury and iodine lines were not so prominent in the spectrum.

2.5.5. Tin.

A number of authors have made successful lamps for tin, from tin iodide (81,83,117,145,149,150,181,184,188), formed in situ. One set of authors has laid particular emphasis on the Sn/I_2 ratio (83). It was particularly difficult to make a very intense source for this element, because stannic iodide has a very high vapour pressure. This usually resulted in iodine dominating the discharge, or too much material causing a 'pinched' discharge. This problem was partially overcome by introducing a minute amount of elemental tin into the lamp blank with a small amount of stannic iodide in an ethereal solution. More control of the amount introduced into the lamp blank can be achieved in this way. Again this suffered from the same problem as the CCl_4/I_2 solution. The yellow-orange stannic iodide, once sealed into the bulb with excess tin, on heating reacted to form a white compound, possibly stannous iodide. The lamp used in these studies was made from stannic iodide, with excess tin, with a fill pressure of 0.5 torr argon and tube dimensions of 3.5 cm length and 8 mm id.

Fig.

LEAD

a) unheated

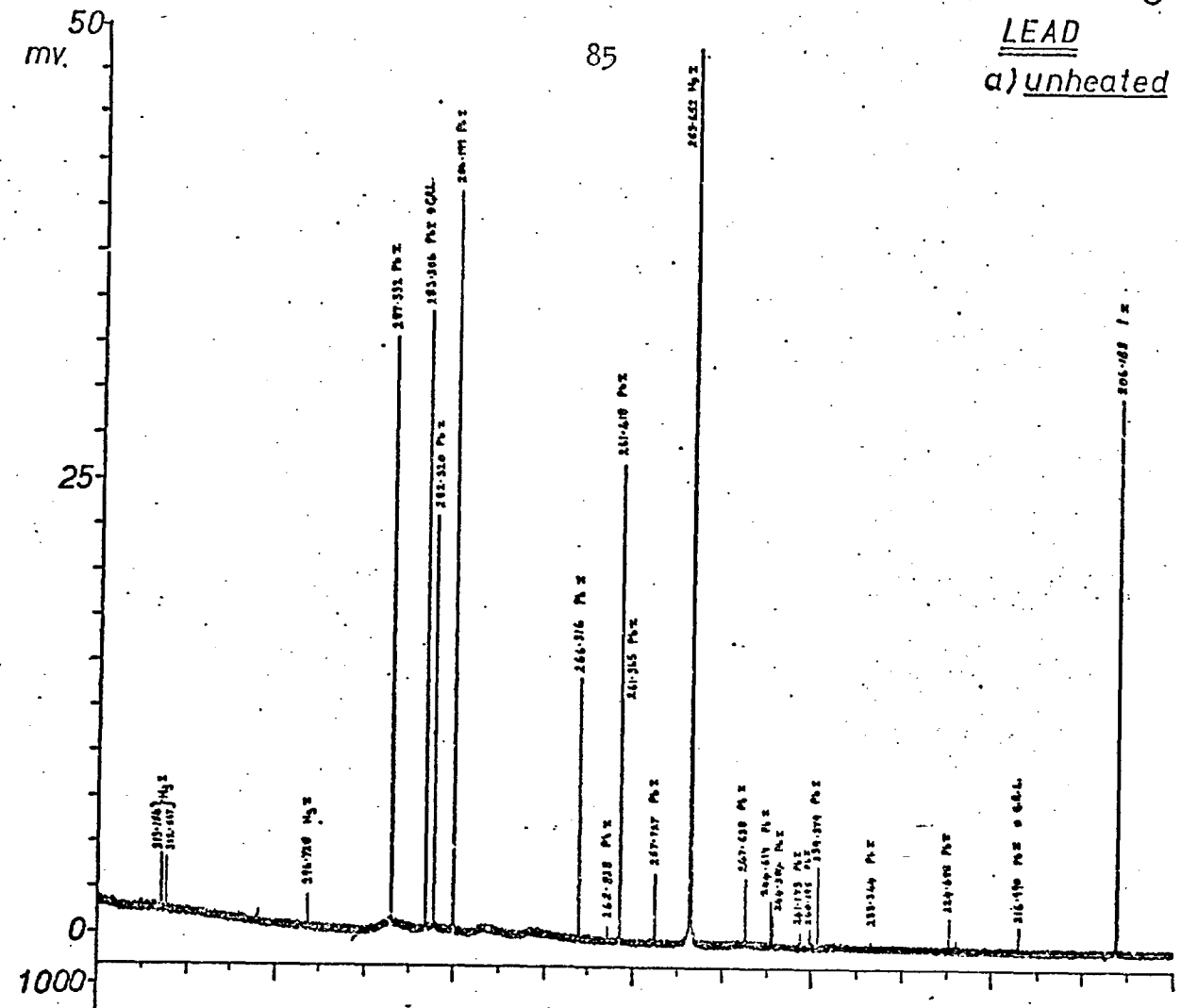

b) heated

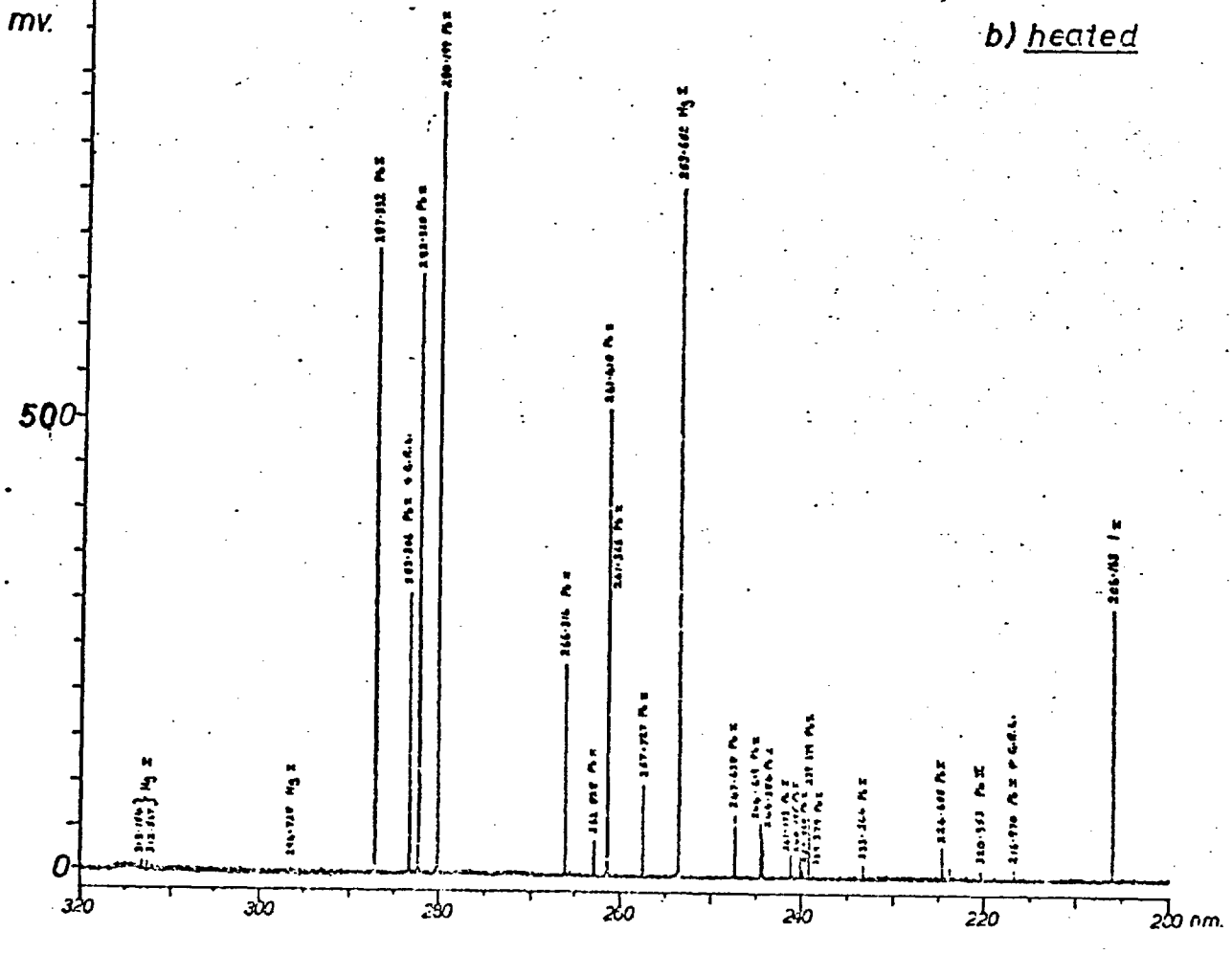

By monitoring the ground resonance line, 286.333 nm, a maximum integrated line intensity was obtained by operating the lamp at 40C at a fixed microwave power. The line intensity at the optimal working temperature showed some variability with change in microwave power. An optimal power of 60 watts gave the best integrated line intensity and also the best signal to noise ratio.

The majority of the lines present in the Grotrian diagram of tin were found to be present in the spectrum of the heated EDL (see fig. 16b). Tin has four ground resonance lines and all four were detected. The 286.333 nm line was the most intense of these lines, and 224.605 nm is the most strongly absorbed of the four. The line at 207.308 nm is not shown on the Grotrian diagram but is accounted for by Brode (240). There was a 10 fold improvement in the integrated line intensities of all the ground resonance lines when operated at 40C when compared to the lamp operated with air cooling (see fig. 16a & b).

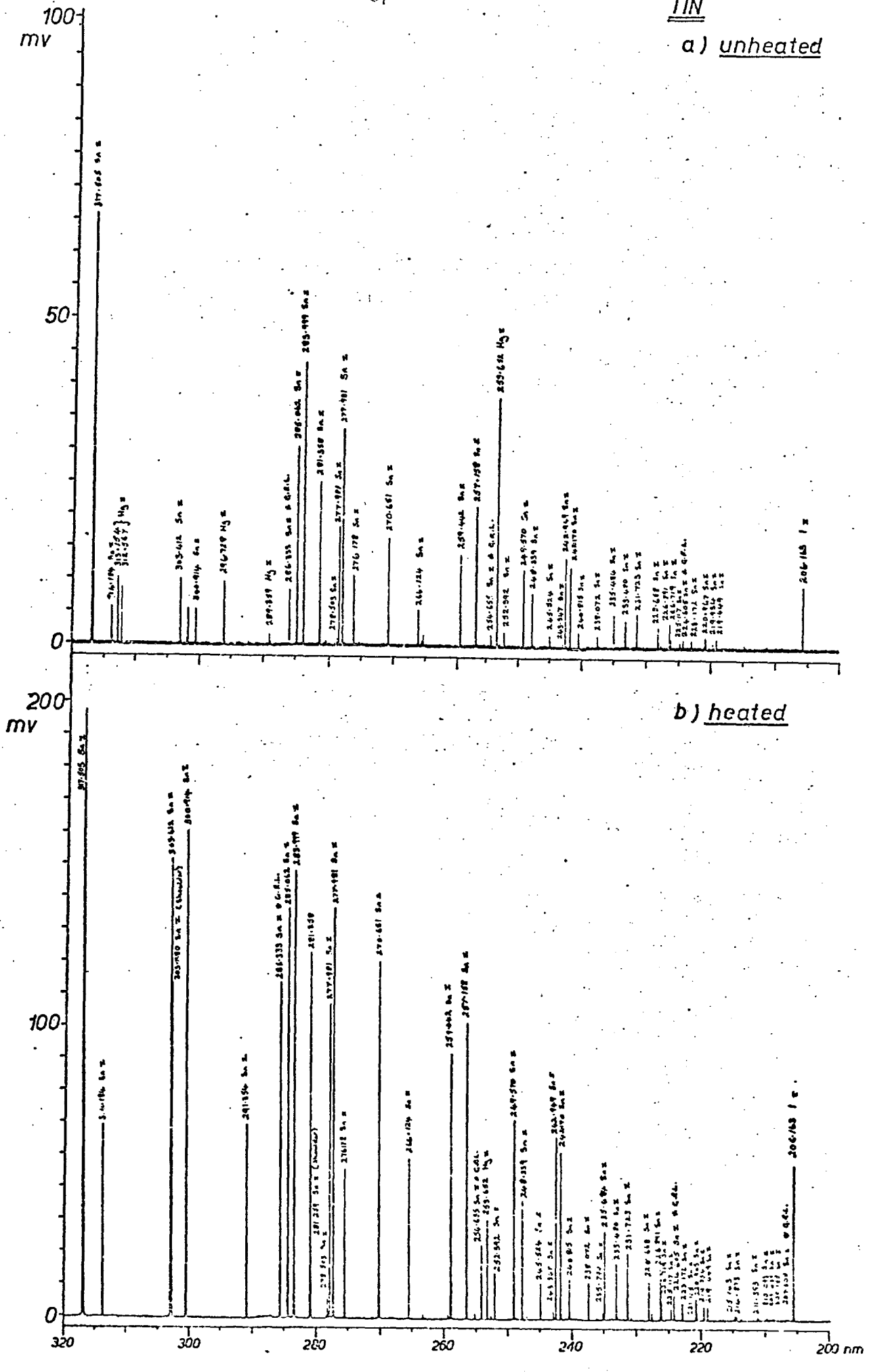
TIN
a) unheated
100
mv
50
0
b) heated
200
mv
100
0
320
300
280
260
240
220
200 nm

Chapter 3

Mercury

3.1. Introduction.

Several authors have determined mercury using non-dispersive optics and a flame atomiser. Vickers et al (54), using a solar-blind PMT R166 with a chlorine filter, have reported mercury AF determinations. They used H_2/air and premixed H_2/O_2/Ar flames as their atom reservoirs and reported a detection limit of 1 μg/ml. Larkins reported a detection limit of 0.07 μg/ml from a separated air/acetylene flame. The best results obtained were those quoted by Warr (53). He has determined mercury at a level of 0.00025 μg/ml in an air/town gas flame using an R166 PMT.

Other workers in this Department have reported the determination of mercury from a non-flame cell (CFAR) in the non-dispersive mode. King (235) reported a detection limit of 2×10^{-11}g., Sanz-Medel (235) reported 1×10^{-11}g. and Hargreaves (234) 5×10^{-11}g.

Previous to these workers, the best AF results for mercury using a monochromator (253.7 nm line), were obtained by Browner (164) from a premixed H_2/air flame. He reported a detection limit of 0.08 μg/ml.

The only reported mercury AF determination from a loop atomiser was that made by Bratzel (105). A monochromator (253.7 nm line) was used and the platinum loop was sheated with Argon. The detection limit obtained was 2×10^{-10}g. (0.01 μg/ml).

The work described in this chapter is a detailed investigation into the atomic fluorescence characteristics of mercury, measured in the non-dispersive mode. Both a flame and non-flame atomiser were investigated, and from this, optimum conditions for the determination of mercury were established.

3.2. Fluorescence characteristics.

The only fluorescence signal obtained was that due to resonance fluorescence at the 253.652 nm intercombination line. The principal resonance line at 184.96 nm is in the vacuum ultraviolet region of the spectrum and outside the spectral range of the PMT.

3.3. Experimental.

3.3.1. Apparatus.

The apparatus has been previously described (see chapter 1.7). Both the flame system AFf and the loop system AFg used the same instrumental units. These were shown in the block diagram Fig. 4a. The signal produced by the PMT was displayed on a Servoscribe potentiometric chart recorder. This instrument had a response of one second and scale ranges of 2 mV to 20 V for full scale deflection. When faster response times were required a storage oscilloscope was employed.

3.3.2. Reagents.

A stock solution (1000µg /ml) of mercury (II) was prepared by dissolving mercuric chloride in 0.01 M hydrochloric acid.

3.4. Atomic fluorescence measurements.

3.4.1. Optimisation of AFf parameters.

3.4.1.1. Source.

The tube parameters, preparation and the spectral characteristics of the mercury EDL have been reported in section 2.5.1. The optimum operating conditions of the EDL, after critical tuning of the $\frac{1}{4}$ wave cavity, were 20 watts of microwave power and a thermal environment of 60C (see Fig. 19). These conditions, obtained from fluorescence measurements, closely followed those obtained from integrated line measurements made in section 2.5.1.

3.4.1.2. Flame atomiser.

Because the flame background emission adversely affects the signal-to-noise ratio (S/N) of the fluorescence measurements, it is of considerable importance to choose the optimum flame type. The principal element in the flame background was OH emission at 280-320 nm which was just within the spectral response range of the detector (180-320 nm).

fig. 19

a)

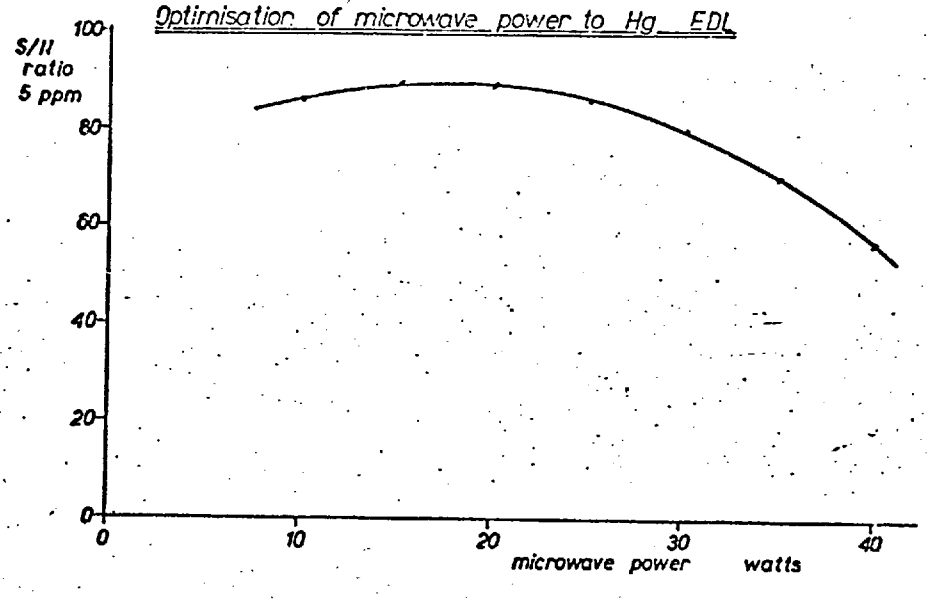
Optimisation of microwave power to Hg EDL
S/N ratio 5 ppm
100
80
60
40
20
0
0
10
20
30
40
microwave power watts

b)

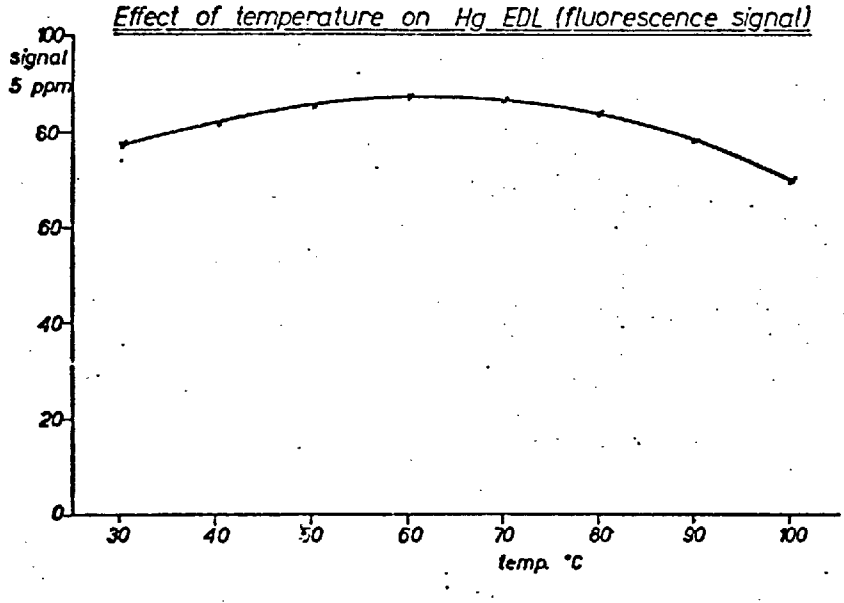
Effect of temperature on Hg EDL (fluorescence signal)
100
signal 5 ppm
80
60
40
20
0
30
40
50
60
70
80
90
100
temp. °C

Spectral studies were therefore made, under identical conditions, to compare the various flame background emissions (see Fig. 20,21). The separated premixed $H_2/O_2/Ar$ flame (Fig. 20a) showed the smallest background emission and this was further reduced (Fig. 21a) by the use of a chlorine cut-off filter (54), the transmission characteristics of which are recorded (Fig. 22) with a Unicam Sp.800. The only features that remained in the spectrum were weak OH bands with heads at 260.85 and 267.78 nm. However, the filter also caused a loss of transmission of the fluorescence signal, and better results were obtained using the separated $H_2/O_2/Ar$ flame, without inclusion of the filter.

Optimum flame conditions for mercury measurement were investigated and these are shown in Table 5. The Perkin-Elmer nebulising chamber had a variable uptake rate. This was optimised with respect to the fluorescence signal (Fig. 23a). This was also the optimum setting for all the other studies made.

TABLE 5

Mercury AFf flame conditions.

Premixed	Gas pressure	Flow rate
	Hydrogen 15 psi	2.5 1/m.
	Oxygen 5 psi	1.0 1/m.
Support	Argon 30 psi	7.7 1/m.
sheath	Argon 15 psi	7.5 1/m.
Diffusion	Hydrogen 15 psi	6.7 1/m.
	Argon 30 psi	7.7 1/m.

fig. 20

Spectral scans of a premixed $H_2/O_2/Ar$ flame recorded under identical conditions.

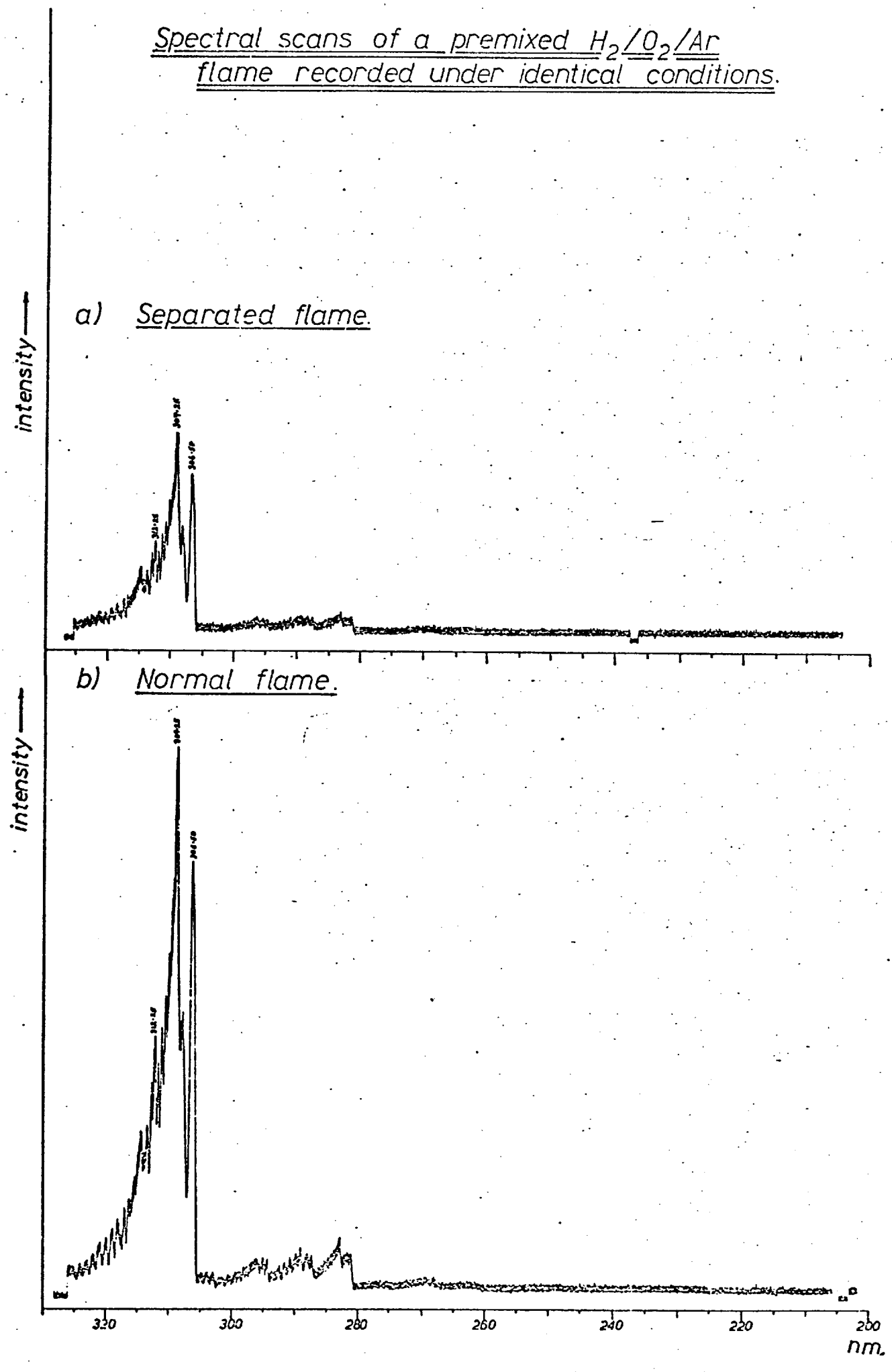

fig. 21

Spectral scans of an Ar/H_2 diffusion flame recorded under identical conditions.

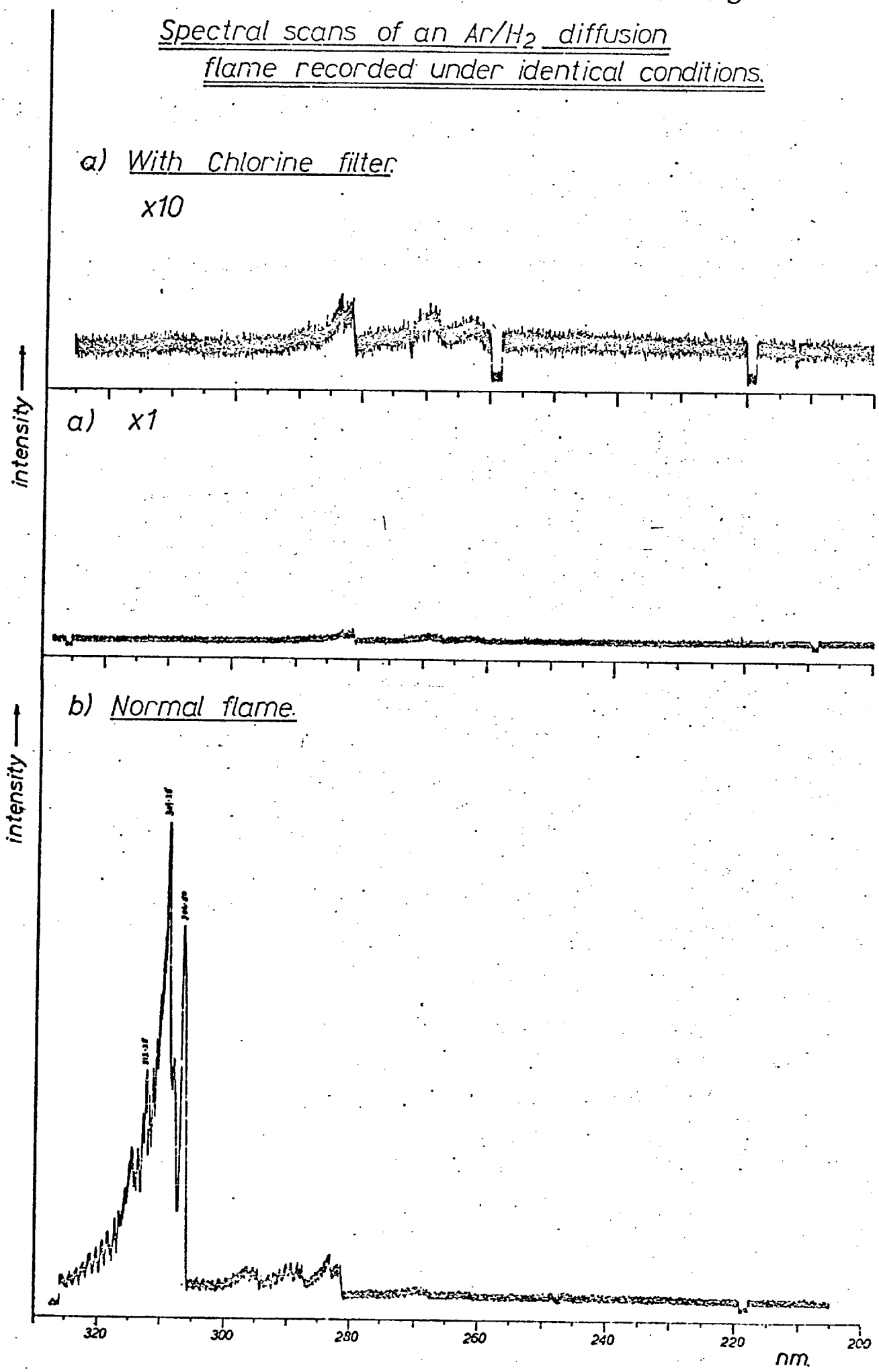

fig. 22

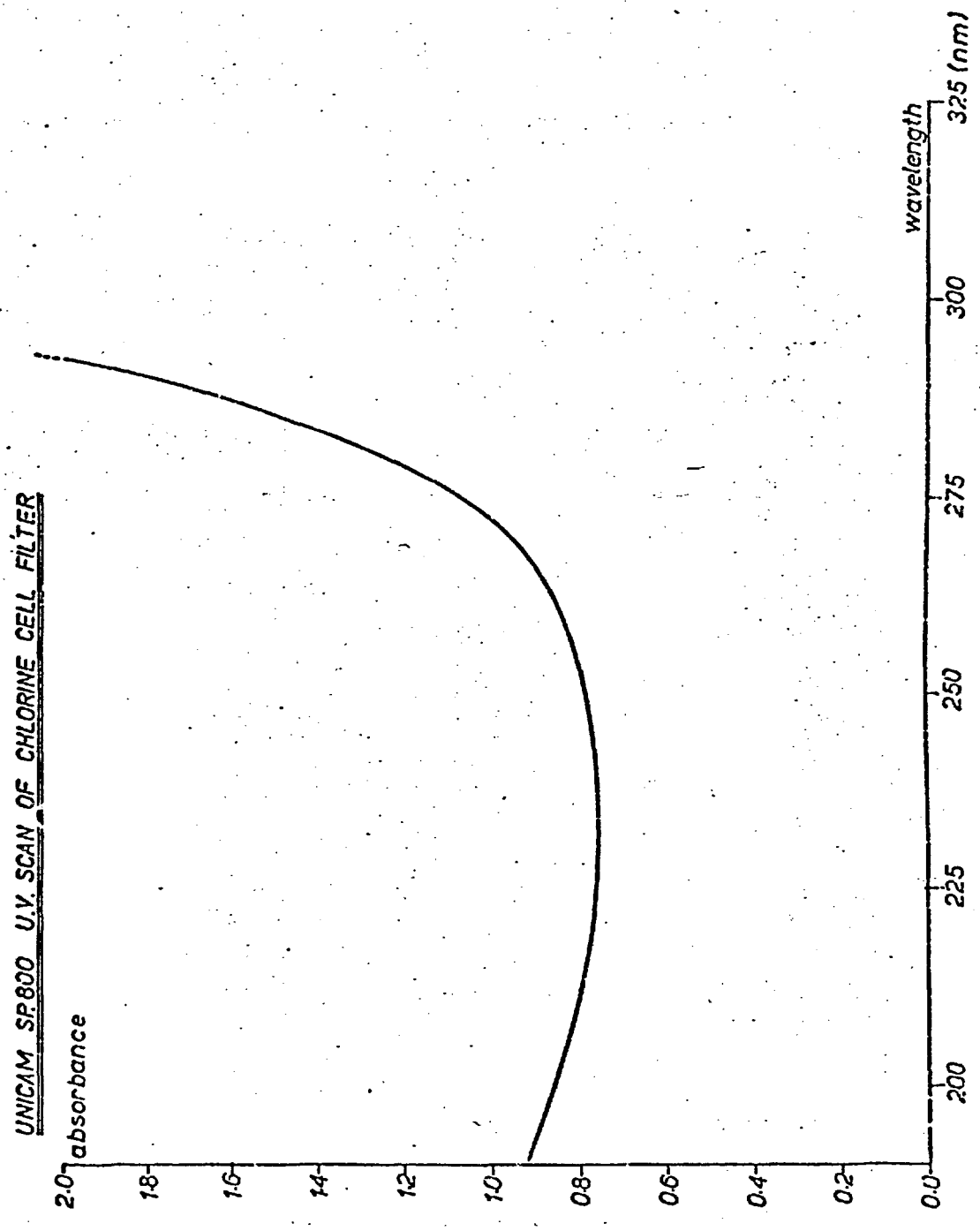
UNICAM SP.800 U.V. SCAN OF CHLORINE CELL FILTER
absorbance
2.0
1.8
1.6
1.4
1.2
1.0
0.8
0.6
0.4
0.2
0.0
wavelength
200
225
250
275
300
325 (nm)

3.4.1.3. Instrumental.

In the AFf system no focussing optics were used for the source, or the detector. The optimum position for both source and detector (PMT viewing entrance) was found to be as close as possible to the argon gas sheath, ie 0.5 cm from the burner circumference (see Fig. 23b). The mercury fluorescence signal showed little variation with height when viewed in the separated region of the flame. The PMT slit was fixed nominally at 1.5 cm above the burner head.

3.4.1.4. Detector.

Both the end window R431, and the side window R166 PMTs were used for the measurements of mercury fluorescence. The EHT settings that gave the best signal to noise ratios were found to be 900 V for the R166 and 1050 V for the R431. However, the R166 PMT was found to be less sensitive to the flame background emission and was therefore used exclusively in the AFf system.

A backing-off unit (see Fig. 4a) provided a range of four time constants for 'damping' and smoothing the noise and the signal variations at or near the detection limit.

3.4.2. Calibration studies AFf.

The stock solution of mercury(II)was diluted to provide a range of concentrations and these solutions were used to construct an analytical curve. A linear growth curve was obtained from 0.1 to 100 µg/ml. At higher concentrations of mercury, curvature towards the concentration axis occurred. Little or no difference was found when solutions of mercury (I) were used. (Fig. 24).

The limit of detection was calculated to be 0.2 µg/ml at a S/N = 2, and the precision (% SD) was 7.2% (10 readings) at a concentration of 0.25 µg/ml.

3.4.3. Optimisation of AFg parameters.

3.4.3.1. Source.

The optimum conditions of source operation were identical to those reported for the AFf system in section 3.4.1.1.

fig. 23

a) b)

Optimisation of nebulising uptake rate & position of PMT & EDL from flame

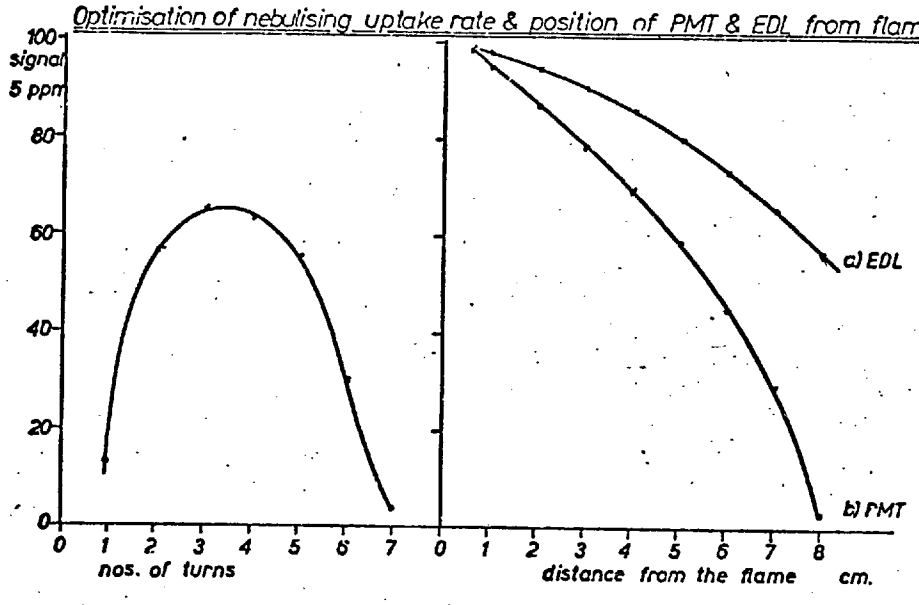

c)

Optimisation of EHT to R166 & R431 PMTs for Mercury fluorescence AF(r)

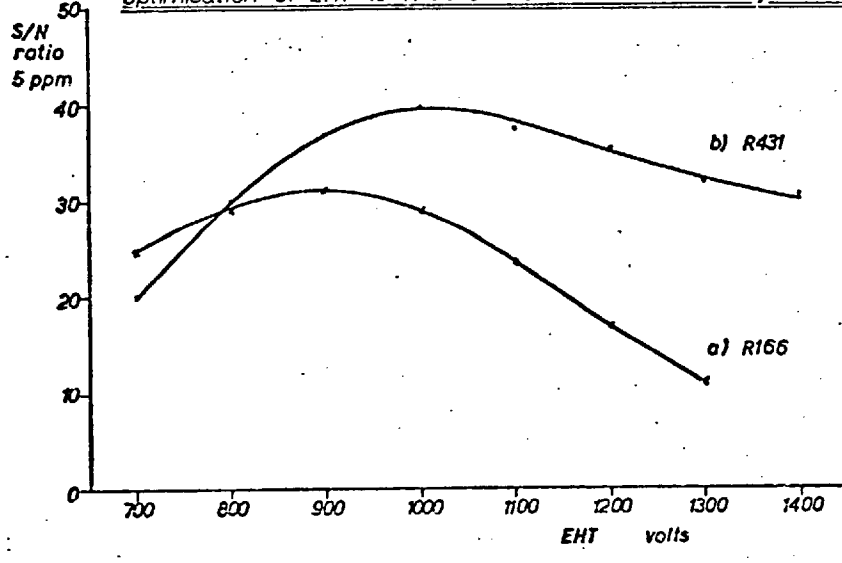

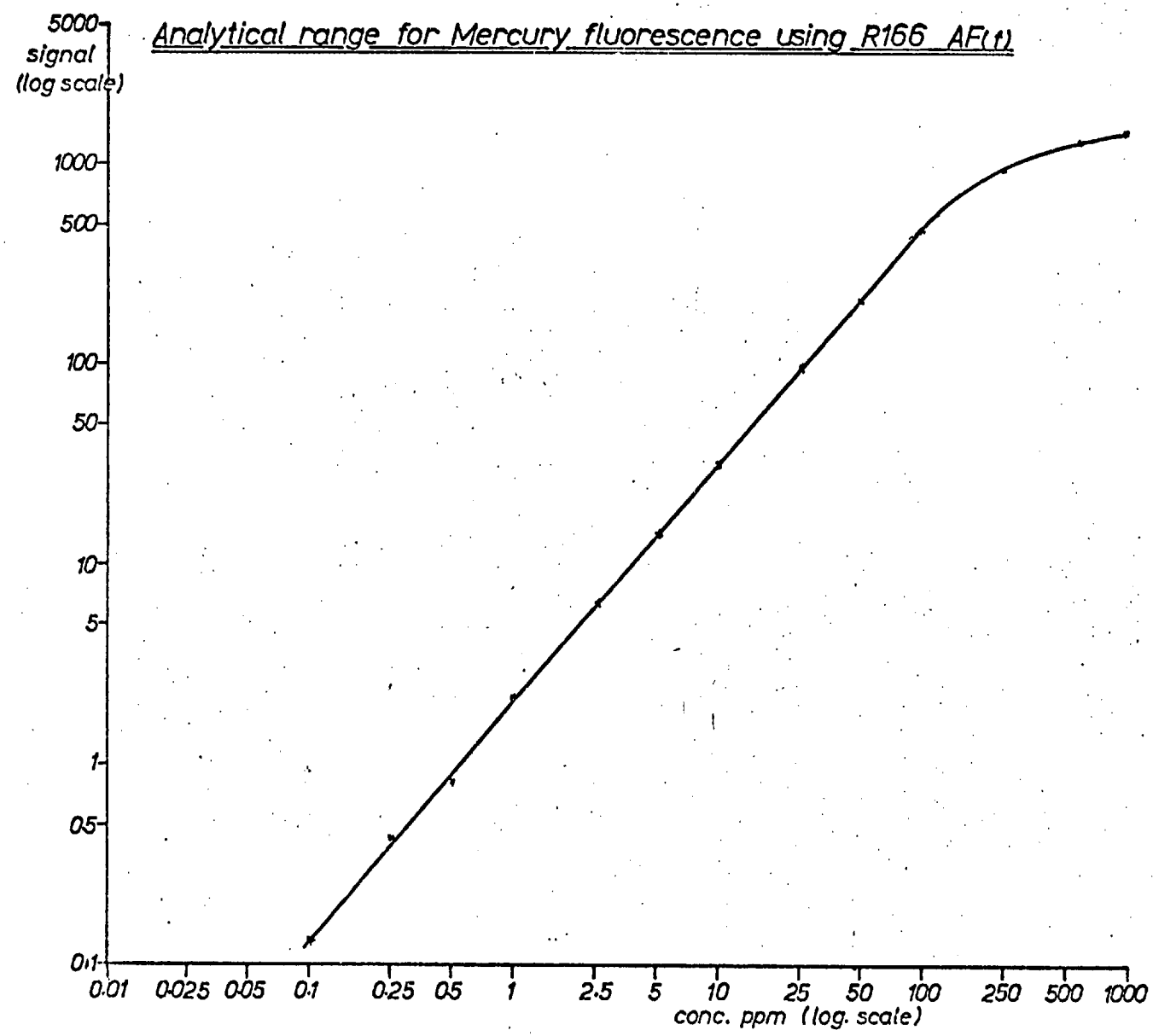
Analytical range for Mercury fluorescence using R166 AF(1)
5000
signal
(log scale)
1000
500
100
50
10
5
1
05
0.1
0.01
0.025
0.05
0.1
0.25
0.5
1
2.5
5
10
25
50
100
250
500
1000
conc. ppm (log. scale)

fig. 24

3.4.3.2. Loop atomiser.

The normal cycle of operation for the loop has been discussed previously in section 1.7.4. However, for mercury, a modified form was used as some mercury was lost during the drying sequence. When the events of the cycle were followed using an oscilloscope, a smaller signal preceded the main signal. The sum of these two signals was constant, but the main signal showed a larger variation than expected because of the loss of mercury during the drying period. This problem was overcome by drying for 15 sec. at low temperature, and then flashing the loop whilst a small amount of solution remained. This procedure resulted in reproducible peak heights. The burn temperature was estimated to be 900C.

The maximum fluorescence signal from the loop was obtained with an argon flow rate of 2.5 1/min. Similar curves to those of bismuth Fig. 29 and lead Fig. 33 were obtained. When a higher temperature 'burn' was used, some emission glow from the loop atomiser was recorded.

3.4.3.3. Instrumental.

The position of the loop in relation to the slit collimator (see Fig.4b) was found to be critical for obtaining the best S/N ratio. Fortunately the optimum position was the same for all the elements determined by this technique AFg.

The collimator slit (6 mm width x 2 mm height) was placed 3-4 mm from the nearest edge of the loop and the top of the loop was just level with the bottom opening of the slit. Typical optimisation results are shown for lead (in Fig. 34a,b).

The source was focussed by a single quartz lens. The maximum fluorescence signal was obtained when the source formed an image 1-2 mm behind the loop. The source image just grazed the top of the loop and covered an area, at the loop centre, greater than the width of the loop. The height of this image was also greater than that of the PMT collimator slit.

3.4.3.4. Detector.

The R431 end window PMT was the preferred choice for the AFg system as this was more sensitive to the transient fluorescence signals (see Fig. 30). The background emission of the loop was minimal and normally occurred after the signal had finished (Fig. 36), therefore the side window R166 had no advantage over the R431. The R431 was operated at 1050 V as before (see Fig. 35).

3.4.4. Calibration studies AFg.

The stock solution of mercury (II) was suitable diluted to provide a range of concentrations. These solutions were transferred to the loop in 5 µl aliquots by a micropipette, and were determined in the AFg system. A linear growth curve was obtained from 0.001 to 100 µg/ml. Higher concentrations of mercury resulted in a curvature towards the concentration axis. As before no difference was found when solutions of mercury (I) were used. The limit of detection was calculated to be (0.00025 µg/ml) 1.25×10^{-12}g. (S/N=2). The precision was found to be 13.3% for a concentration of 0.0025 µg/ml (10 readings).

3.5. Summary.

From the preliminary studies, it can be clearly seen that a solar-blind PMT can replace the monochromator in a conventional AF system. Moreover this replacement is found to be more than adequately suitable for both the atom reservoirs employed.

Similar sensitivities for the flame cell to those reported using a monochromator are obtained in the mercury AF determination. These results also compare favourably with those from other non-dispersive systems reported.

The non-flame cell provides far better sensitivities for the mercury AF determination than those reported using a monochromator. This was in accordance with the theoretical predictions made in Chapter 1.

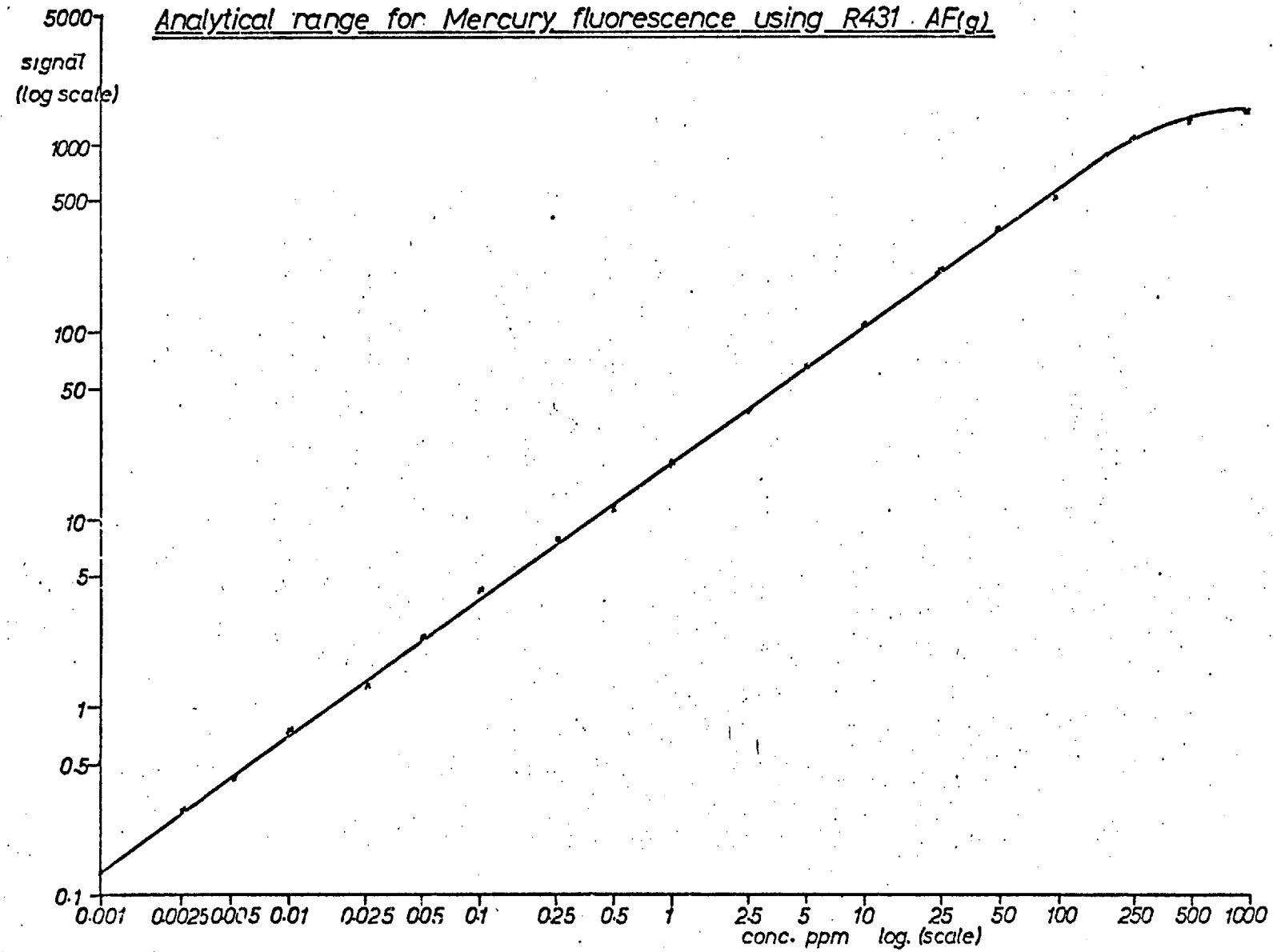
Analytical range for Mercury fluorescence using R431 AF(g)
5000
signal
(log scale)
1000
500
100
50
10
5
1
0.5
0.1
0.001
0.0025
0.005
0.01
0.025
0.05
0.1
0.25
0.5
1
2.5
5
10
25
50
100
250
500
1000
conc. ppm log. (scale)

fig. 25

Chapter 4.

Bismuth

4.1. Introduction.

There has been only one published report for the determination of bismuth using a non-dispersive technique. Larkins (50) has obtained a detection limit of 0.25 μg/ml from a separated air/acetylene flame using the R166 PMT. Another worker in this Department has reported the determination of bismuth from a non-flame cell. (CFAR) in the non-dispersive mode. King (235) reported a detection limit of 10^{-10}g.

The best AF results for bismuth using a flame were obtained by Dagnall et al (146) and Hobbs et al (214). Dagnall reported a detection limit of 0.05 μg/ml at the 302.5 nm line. The excitation of the bismuth fluorescence was achieved by the iodine non-resonance line 206.2 nm, in an H_2/Ar diffusion flame. Hobbs reported a detection limit of 0.04 μg/ml at the 306.77 nm line. Excitation of the bismuth fluorescence was achieved by the use of a bismuth EDL focussed into a separated air/acetylene flame.

The only reported bismuth AF determination from a loop made by Bratzel (105). A monochromator (306.77 nm line) was used and the tungsten loop was sheathed with argon. The detection limit obtained was 4×10^{-11} g. (0.02 μg/ml).

The work described in this chapter is a detailed investigation into the atomic fluorescence characteristics of bismuth measured in the non-dispersive mode. Both a flame and non-flame atomiser were used. From this, optimum conditions for the determination of bismuth by the technique have been established, and the method is shown to be a viable technique for the analysis of real samples.

4.2. Fluorescence characteristics.

The fluorescence spectrum of bismuth was complex, and possessed many lines. A comprehensive study has been reported by Dagnall et al (146) of the fluorescence emission from an Ar/H_2 diffusion flame excited by an iodine lamp. Hobbs et al (214) have also reported the fluorescence emission from a separated

air/acetylene flame excited by a bismuth lamp. The most intense fluorescence signals obtained were as follows:-

Line nm	Relative fluorescence signal		Iodine excited
	Ar/H_2 (146)	A/A (214)	
206.17	12	9.9	
269.70	6	7.7	
302.46	100	100	
306.77	54	71	
			Bismuth excited
206.17	-	1	
223.06	-	1	
227.66	-	1	
306.77	-	130	

In addition to the more intense fluorescence signals, many unexpected and much weaker signals were recorded by Dagnall (146). The 195.4, 195.9, 252.4 and 281.0 nm lines could not be detected. No fluorescence signal was observed from the 202.1 nm line, as this has a low transition probability.

4.2.1. Mechanism.

As expected, the ground state bismuth atom absorbed energy from the iodine non-resonance line at 206.17 nm to be excited to the $^4P_{2\frac{1}{2}}$ state from the overlap (146). Three fluorescence signals were obtained from the $^4P_{2\frac{1}{2}}$ state, 206.2 nm resonance fluorescence and direct line fluorescence at 269.7 and 302.5 nm, the additional signal at 306.8 nm, multiple stepwise fluorescence, must be due to the deactivation of the excited $^4P_{2\frac{1}{2}}$ state atom by readiationless transitions to the $^4P_{\frac{1}{2}}$ excited state. The high intensity from the emission at 306.8 nm arises becauses the $^4P_{\frac{1}{2}}$ is the lowest lying excited state and it

may be populated by radiationless transfers from other excited states. Moreover, it is the only line other than the 472.2 nm which can be emitted from this state.

Of the weaker fluorescence lines, the emissions at 262.8 and 293.8 nm which orginate from the $^2P_{1\frac{1}{2}}$ state are examples of thermally-assisted direct line fluorescence. The others may be attributed to stepwise and/or direct line fluorescence.

When a bismuth source was used for excitation the most intense emission line was the 306.8 nm line, as a result of resonance fluorescence. This was expected since the most intense ground resonance line of the bismuth lamp was at 306.8 nm (see Fig. 14b). The emission lines 227.66, 223.06 and 206.17 nm were all as a result of resonance fluorescence.

4.3. Experimental.

4.3.1. Apparatus.

The apparatus has been previously described in section 3.3.1.

4.3.2. Reagents.

A stock solution (1000µg /ml) of bismuth was prepared by dissolving 1g. of bismuth metal in 20 ml. of concentrated nitric acid, and was then diluted to 1 litre. Stock solutions (1000 µg/ml) of the elements Ni, Co, Cr, Mo, Ti, Al, Fe, to be used for interference studies were prepared from their chlorides or nitrates, together with the minimum amount of the appropriate acid necessary to prevent hydrolysis.

Potassium iodide solution (60 % w/v) was made up in distilled water. Methyl-isobutyl ketone (MIBK). Impurities were found to be present in the solvent. So the MIBK was purified by washing twice with saturated aqueous ethylenediaminetetra-acetic acid, followed by washing with distilled water. Fractional distillation followed in which only the 113-116C boiling range fraction was collected. Saturated citric acid solution: Analar grade citric acid was dissolved in distilled water till a small amount of solid remained

4.4. Atomic fluorescence measurements.

4.4.1. Optimisation of AFf parameters.

4.4.1.1. Source.

The tube parameters, preparation and the spectral characteristics of the bismuth EDL have been reported in section 2.5.3. and the iodine source in section 2.5.2.

The optimum operating conditions of the iodine EDL, after critical tuning of the $\frac{1}{4}$ wave cavity, were found to be forced air cooling at minimum microwave power, to obtain the best S/N ratio (see Fig. 27a) from the fluorescence signal.

The optimum operating conditions of the Bi/I_2 EDL, after critical tuning of the $\frac{1}{4}$ wave cavity, were 40 watts of microwave power and a thermal environment of 180C (see Fig. 26 a,b). The optimum conditions that gave the best S/N ratio, obtained from fluorescence measurements, closely followed those recorded from the integrated line intensities (section 2.5.3.).

4.4.1.2. Flame atomiser.

Optimum flame conditions for bismuth measurements were investigated and found to be as shown in Table 6. The optimum uptake rate of the nebuliser chamber was the same as that reported for mercury (Fig. 23a). The brightness of the bismuth fluorescence varied greatly with the alteration of the hydrogen flow (see Fig. 27b).

fig. 26

a) SIGNAL V. INTENSITY OF EDL.(Bi/i_2) FLUORESCENCE SIGNAL

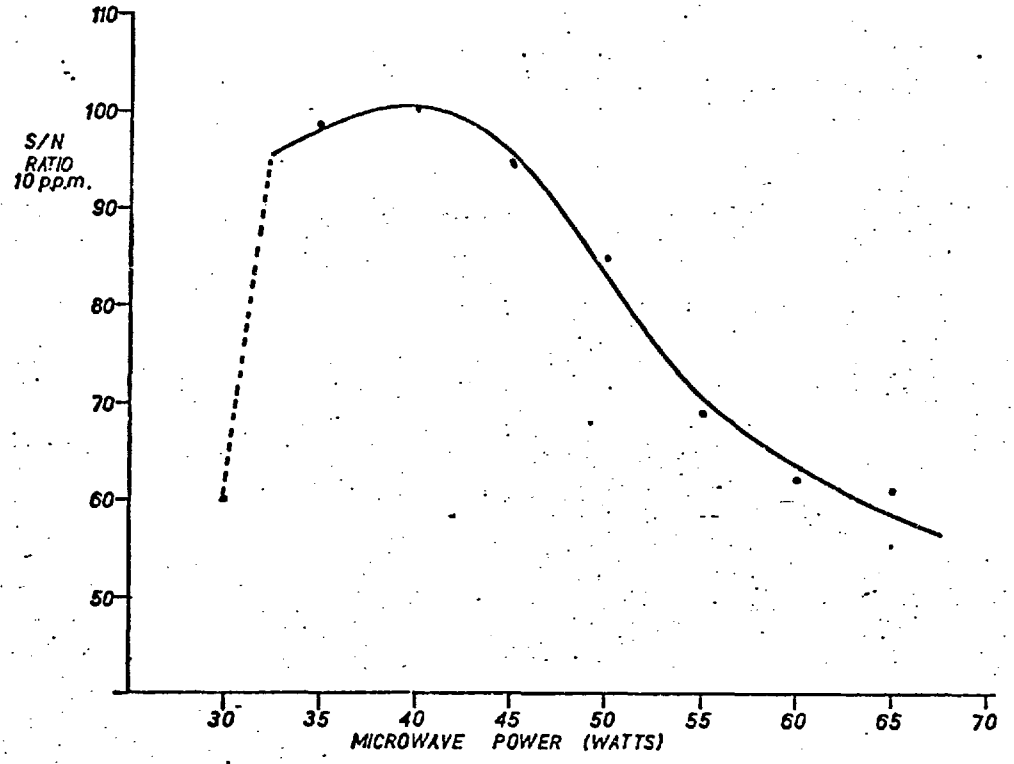

b) Effect of temperature on Bi/I_2 EDL (fluorescence signal)

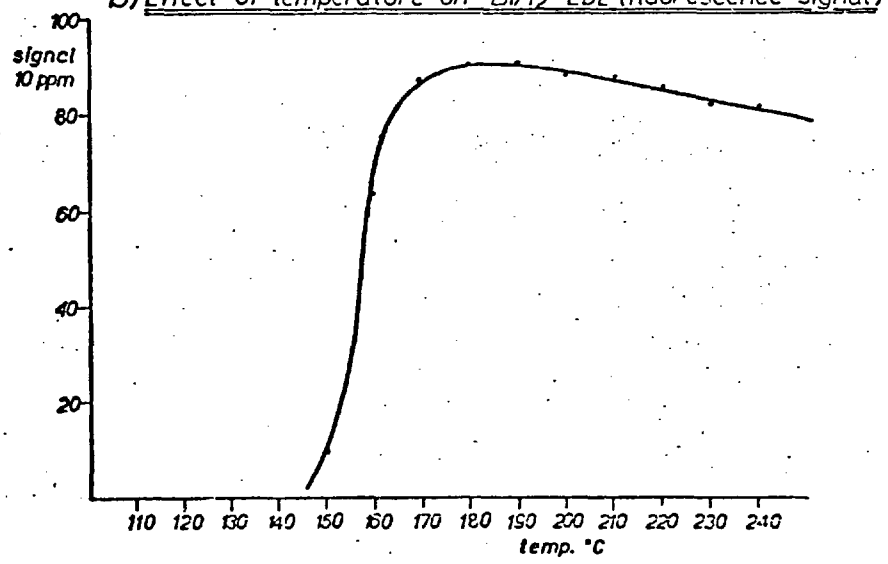

fig. 27

a)

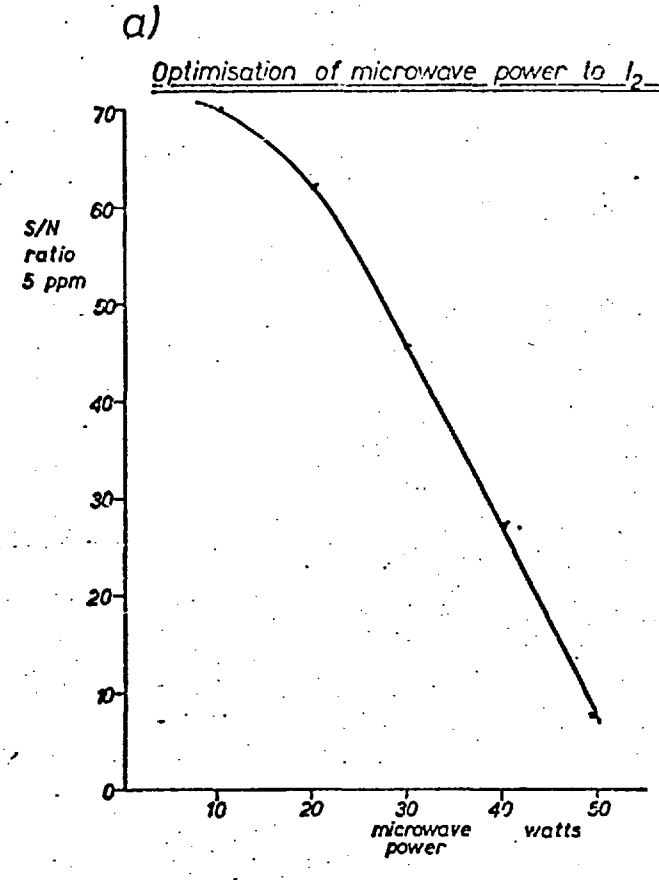
Optimisation of microwave power to I_2 EDL
S/N ratio 5 ppm
70
60
50
40
30
20
10
0
10
20
30
40
50
microwave power
watts

b) c)

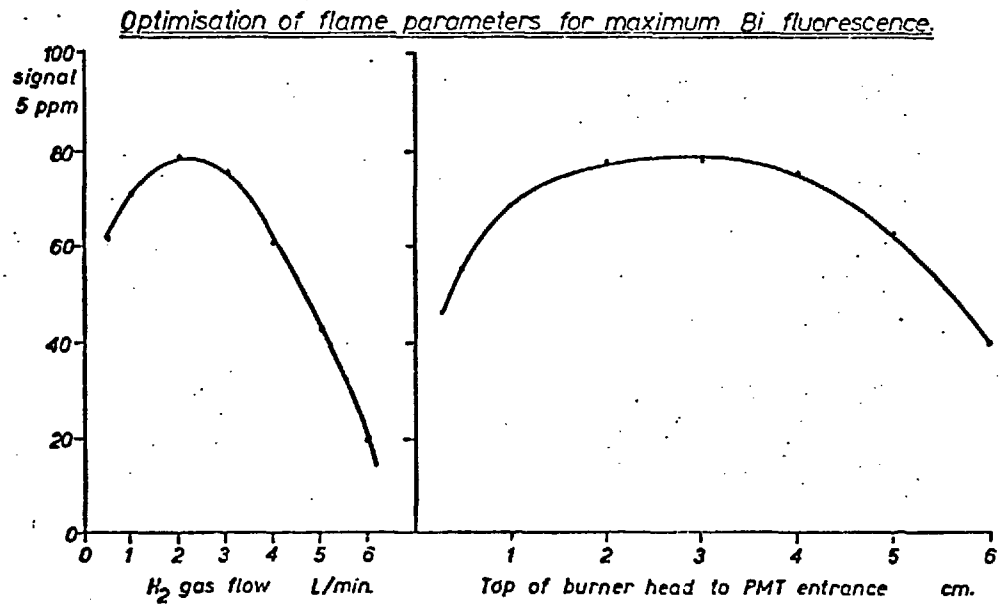
Optimisation of flame parameters for maximum Bi fluorescence.
100 signal 5 ppm
80
60
40
20
0
0 1 2 3 4 5 6
H_2 gas flow L/min.
1 2 3 4 5 6
Top of burner head to PMT entrance cm.

Table 6.

Bismuth AFf flame conditions.

		Gas pressure		Flow rate
Premixed		Argon	30 psi	7.7 1/m
		Hydrogen	15 psi	2.5 1/m
		Oxygen	5 psi	0.7 1/m
	Sheath	Argon	15 psi	7.5 1/m
Diffusion		Hydrogen	15 psi	3.4 1/m
		Argon	30 psi	6.8 1/m

4.4.1.3. Instrumental.

The optimum positions were the same as those reported for mercury in section 3.4.1.3. However, the bismuth fluorescence signal showed considerable variation with height in the separated region of the flame. The best signal was obtained when the PMT viewed the flame 3 cm above the burner head.

4.4.1.4. Detector.

The R1666 PMT was operated at 900 V to give the best S/N ratio; this was the same setting found to be the optimum for mercury.

4.4.2. Calibration studies AFf.

The stock solution of bismuth was suitably diluted to provide a range of concentrations and these solutions were used to construct an anlytical curve (see Fig. 28). The results obtained are summarised in Table 7.

Table 7.

PMT	Source	Linear range µg/ml	Detection limit µg/ml	Precision µg/ml	Precision %
R166	Bi/I_2	1-250	0.2	2.5	7
R166	I2	2.5-500	0.5	5	8.3

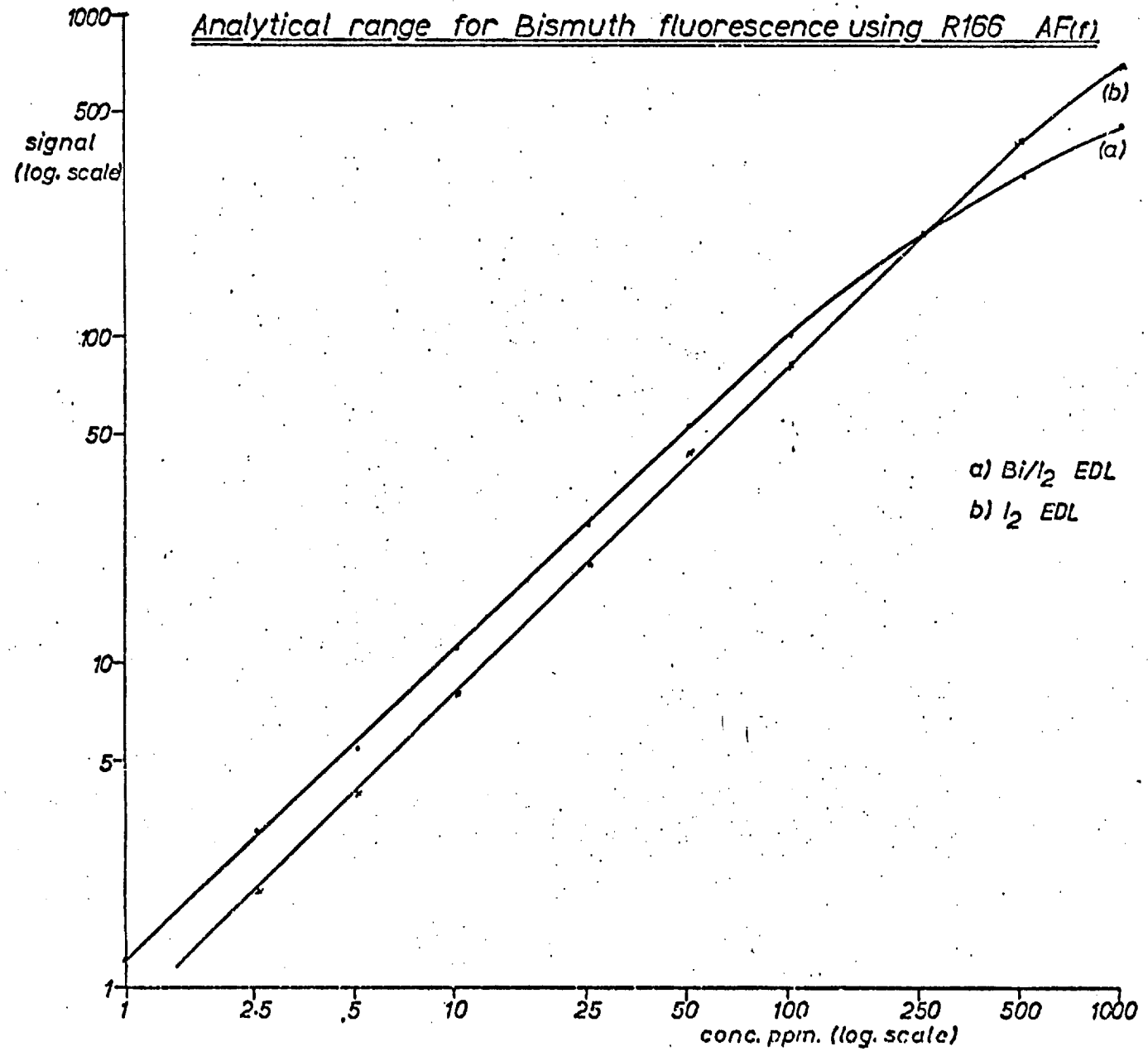
Analytical range for Bismuth fluorescence using R166 AF(f)
1000
500
signal
(log. scale)
100
50
10
5
1
(b)
(a)
a) Bi/I2 EDL
b) I2 EDL
1
2·5
5
10
25
50
100
250
500
1000
conc. ppm. (log. scale)

fig. 28

4.4.3. Interference studies AFf.

Of the selected ions, when present in a x100 excess over bismuth nitrate solution in nitric acid solution, only aluminium produced a variation greater than 5 % on the flourescence signal (see Table 8). This interference may be attributed to the formation of oxide particles which 'cage' the bismuth and which are not efficiently dissociated by the thermal energy available from the relatively cool flame at 1400K.

Table 8.

AFf	% Interference on 5 µg/ml Bismuth
ions	x100 excess
Ti IV	-4
Cr III	-2
Mo VI	-1.5
Fe III	0
Al III	-40
Ni II	0
Co II	0
Pb II	0
Sn II	-2.5
As III	0
Sb III	0

4.4.4. Optimisation of AFg parameters.

4.4.4.1. Source.

The optimum conditions of source operation were found to be identical to those reported for the flame (in section 4.4.1.1.)

4.4.4.2. Loop atomiser.

The 2 µl drop on the loop was dried for 40 secs. at a low temperature. It was then allowed to cool for 20 secs. During this period a higher temperature was selected. The loop was then flashed. The burn temperature was estimated to be 2,000C. The maximum fluorescence signal from the loop was obtained when the flow rate of argon was 4.5 1/min., and with a variable resistance setting 13.5 (see Fig. 29 a,b). The times in the loop events cycle quoted were the minimum consistent with a reproducible signal.

4.4.4.3. Instrumental.

The position of the loop in relation to the collimator slit of the PMT, and the source image have been previously discussed for mercury (section 3.4.4.3.). The optimum position was the same as shown (in Fig. 34a.b.c) for lead.

4.4.4.4. Detector.

The optimum EHT setting for the best S/N ratio for R431 PMT from fluorescence measurements was 1050 V.

4.4.5. Calibration studies AFg.

The stock solution was diluted to provide a range of concentrations and these solutions were used to construct an analytical curve (see Fig. 30). The results obtained are summarised in Table 9.

Table 9.

PMT	Source	Linear range µg/ml	Detection limit µg/ml	g.	Precision (10 readings) µg/ml	%
R166	I_2	0.05-100	0.043	2.2×10^{-10}	0.5	8.5
R166	Bi/I_2	0.05-500	0.016	8.0×10^{-11}	0.5	7.0
R431	I_2	0.01-50	0.007	3.5×10^{-11}	0.1	9.0
R431	Bi/I_2	0.01-50	0.0063	3.2×10^{-11}	0.1	6.5

fig. 29

a)

SIGNAL V. ARGON FLOW RATE (METERATE "F" TUBE 14 p.s.i.g.)

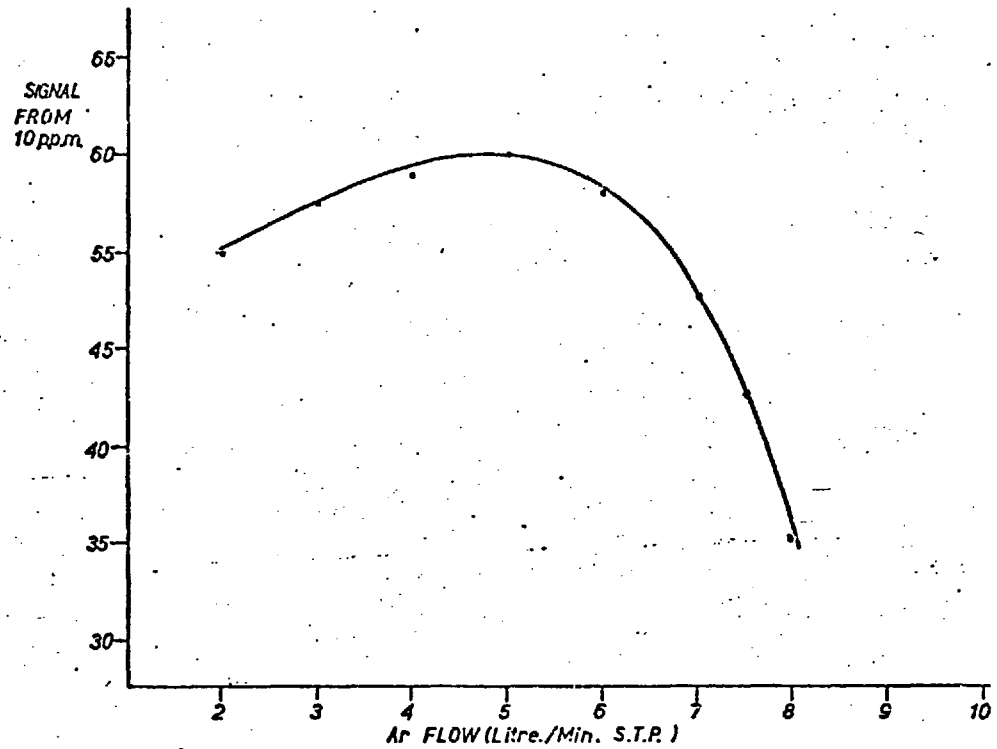

b)

Optimisation of 'loop' heating ramp for Bismuth fluorescence.

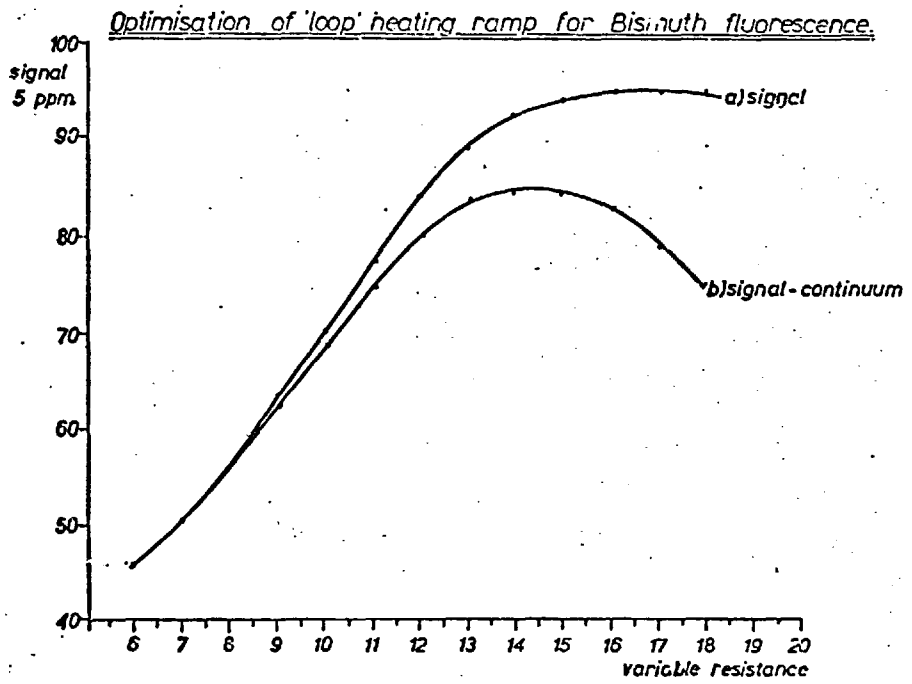

4.4.6. Interference studies AFg.

Study was made of x4 excess of various ions on a fluorescence signal from 5 µg/ml bismuth solution (see Table 10). This study was carried out under the previously optimised conditions for a Bi/I_2 EDL and R431 PMT.

Table 10.

AFg	% Interference on 5 µg/ml Bismuth
ions	x 4 excess
Ti IV	-42.0
Cr III	-39.0
Mo VI	-51.5
Fe III	-45.0
Al III	-60.0
Ni II	-15.5
Co II	-14.0
Pb II	- 1.0
Sn II	- 8.0
As III	-10.0
Sb III	- 5.0

4.5. Sample analysis.

In view of the complex nature of the samples (see Table 2) it was clearly impossible to determine the test elements directly in aqueous solution. Also solutions that contained sufficient amounts of the analyte element would be too viscous for efficient nebulisation in the AFf system and serious interference would result from the complex matrix in the AFg system. Moreover, in both cases, the preparation of complex blank and standard solutions would be required. It was therefore necessary to extract selectively and preconcentrate the analyte elements to overcome these difficulties, and also to increase the

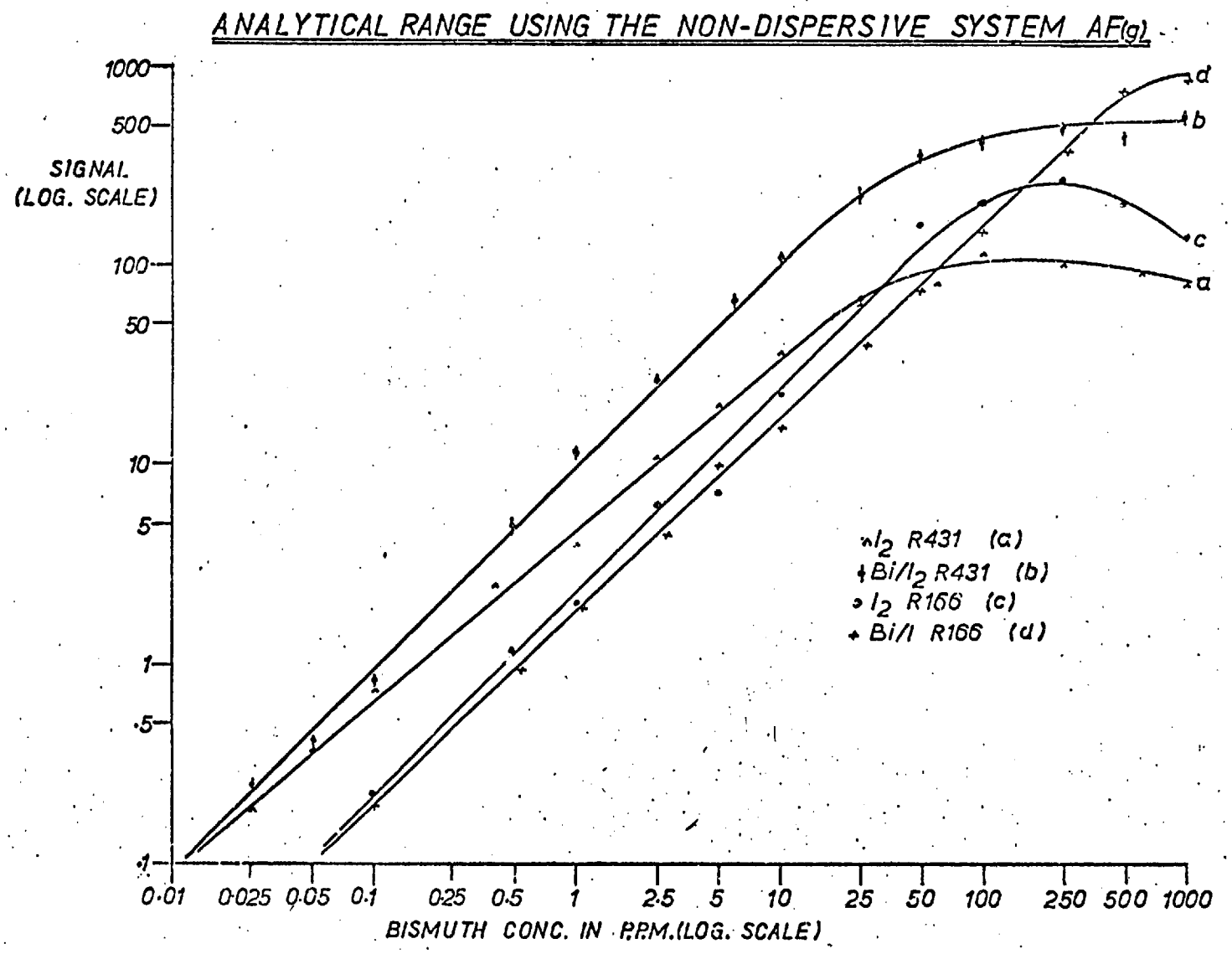
ANALYTICAL RANGE USING THE NON-DISPERSIVE SYSTEM AF(g)
SIGNAL (LOG. SCALE)
1000
500
100
50
10
5
1
·5
·1
0·01
0·025
0·05
0·1
0·25
0·5
1
2·5
5
10
25
50
100
250
500
1000
BISMUTH CONC. IN P.P.M.(LOG. SCALE)
I2 R431 (a)
Bi/I2 R431 (b)
I2 R166 (c)
Bi/I R166 (d)
a
b
c
d

fig. 30

sensitivity of the determination.

4.5.1. Sample preparation.

Both the nickel-cobalt alloys and the iron base samples were treated identically. The sample (0.5 g) was dissolved in a calculated minimum amount of hydrochloric acid. A few drops of concentrated nitric acid were added to aid dissolution and to obtain the higher oxidation state of the ions, eg ferrous to ferric.

4.5.2. Solvent extraction.

Several extraction processes have been discussed by Taylor (260) for a number of trace analytes including lead and bismuth in nickel-cobalt (Ni/Co) alloys and iron base samples. Taylor recomended an iodide/MIBK extraction system in preference to others which usually require a large excess of cyanide reagent. The iodide extraction system has been reported to be very efficient (99.9 %) by many authors (242-4, 251-61).

When an excess of potassium iodide was added to an acidic solution of bismuth, a yellow-orange colour was produced. This was due to the formation of the iodobismuthite ion (probably more than one species was formed). Because of their ionic nature, the complexes were extracted as the acids into oxygen-containing solvents (MIBK). Oxidising ions such as Fe (III) and Mo (VI) interfered by oxidising the iodide to iodine. However, iron (III) and molybdenum (VI) were pre-extracted from concentrated hydrochloric acid solution into oxygen-containing solvent MIBK without the loss of any lead or bismuth.

This solution was then separated from the organic phase and diluted to a 5 % solution with respect to the acid. The extract was shaken with 60 % potassium iodide solution, and lead and bismuth were extracted simultaneously into a fresh organic MIBK layer. The organic phase was then subjected to fluorescence measurements in the AFg system under optimised conditions.

The analysis of the iron base alloys by this method was successful, and the results are tabulated in Table 11. However, analysis of the Ni/Co alloys

was not successful by this method. The final aqueous solution in these samples was seeded with small amounts of cadmium. It was hoped that since the cadmium was also extracted under these conditions, a synergistic effect would result, (261). No improvement in the extraction efficiency was recorded.

Synthetic samples were investigated to test the efficiency of extraction, because the ratio of analyte to matrix was of the order of 1 to 10^6. It was found that with the analyte at the low levels and large matrix concentration present, the extraction system was not efficient. This was contrary to many reports in the literature.

Table 11.

Solvent extraction.

Sample	Bismuth content		Results AFg		Precision
Iron base	ppm solid	µg/ml	ppm solid	µg/ml	10 results %
A	20	0.2	18	0.18	6
B	10	0.1	9.5	0.095	7
C	40	0.4	39	0.39	5
D	80	0.8	80	0.80	5
Ni/Co	wt %	µg/ml	wt %	µg/ml	
R 3385	0.0002	0.02	-	ND	-
R 3386	0.0003	0.03	-	ND	-
R 3387	0.0012	0.12	0.00075	0.075	11
R 3388	0.0006	0.06	0.00035	0.035	19

1 µg/ml Bi in synthetic solution 60 % Ni 20 % Co 20% Cr

Bi can be detected with 80 % recovery efficiency.

0.1 µg/ml Bi in synthetic soln. 60 % Ni 20 % Co 20 % Cr

Bi can be detected with a 40 % recovery.

Addition of 1, 5, 10 µg/ml Cd acting as a synergist does not significantly effect the recovery of 0.1 µg/ml Bi soln.

4.5.3. Selective electrodepostion.

A number of recent reports (246-50) in the literature has used a voltammic stripping method to extract selectively and preoncentrate various analytes from different matrices, prior to spectroscopic determination. The technique of voltammic stripping is well established and the behaviour of many elements has been extensively reported (Meites, 245).

For the samples of interest, the analyte elements can be selectively extracted from the complex matrix in a saturated citric acid medium.

Element	Volts	
Bi III	-0.025	$w^{(o)}$
Pb II	-0.358	$w^{(o)}$
Co II	NR	
Cr VI	0	$w^{(III)}$
Cr III	-0.78	$i^{(II)}$
Fe III	+0.23	$w^{(II)}$
Fe II	NR	
Mo VI	-0.44	$w^{(V/III)}$
Ni II	-0.98	$i^{(o)}$
Ti IV	-0.37	$w^{(III)}$
Al III	NR	

where w is wave well defined
i is wave ill defined
() is the final oxidation state
NR is not reducible

The dissolved metal sample (0.5 g) was diluted with a saturated citric acid solution to 50 ml. The resulting solution was degassed with nitrogen prior to electrolysis. A three electrode system was employed. The working electrode was a mercury amalgamated platinum wire. The counter electrode was a platinum wire; the third was a saturated Calomel reference electrode. The solution was left over-night at a fixed potential of 0.400 V, and was continally stirred and also detassed via a nitrogen bleed.

The analyte elements were reverse-stripped from the mercury into 1.5 ml of dilute nitric acid sequentially, at their respective potentials. This solution was then analysed in the AFg system under the optimised conditions for lead and bismuth. The analysis of the Ni/Co alloys by this method was successful and the results are tabulated in Table 12.

Table 12.

Voltammic strippling.

Sample	Amount found		Amount found		Value quoted		% recovery	
Ni/Co	Bi µg/ml	Pb	Bi ppm	Pb	Bi ppm	Pb	Bi	Pb
R 3385	0.62	0.61	1.86	1.83	2	2	93	91.5
R 3386	0.93	0.925	2.79	2.775	3	3	93	92.5
R 3387	3.8	3.7	11.4	11.1	12	12	95	92.5
R 3388	1.85	1.9	5.55	5.9	6	6	92.5	98.3

4.6. Summary.

The studies made in this chapter have showed that the solar-blind PMT employed in both systems has adequately replaced the monochromator for conventional AF determinations.

For the flame cell, slightly poorer sensitivities were obtained in the non-dispersive mode, than those obtained with a monochromator. However, the results obtained are identical to those reported by Larkins (50), using a R166 PMT. The sensitivity obtained for bismuth from the loop was the same as that reported with a monochromator. In discussing sensitivity an allowance should be made for the fact that the most intense bismuth fluorescence emissions occurred at 302.5 and 306.7 nm. This corresponds to a region where the PMT has a poor response (Fig. 3b).

The determination of bismuth in the real samples was achieved. However,

careful and extensive sample pretreatment was required before the analyte could be determined in the system.

Chapter 5

Lead

5.1. Introduction.

Other workers in this Department have reported the determination of lead from a non-flame cell (CFAR) in the non-dispersive mode. King (235) reported a detection limit of 3×10^{-11} g and Sanz-Medel 5×10^{-12}g. There has only been one published report of AF determination of lead using a non-dispersive technique. Larkins (50) has obtained a detection limit of 0.15 µg/ml from a separated air/acetylene flame using the R166 PMT.

The best AF result for lead using a monochromator (405.8 nm line) and a flame was obtained by Browner (84). A detection limit of 0.06 µg/ml was reported from a premixed $Ar/O_2/H_2$ flame.

The only reported lead AF determination from a loop was reported by Bratzel (105). A monochromator (405.8 nm line) was used with an argon-sheathed tungsten loop. The detection limit obtained was 4×10^{-9}g (2 µg/ml). However, Chauvin (108) has reported lead AA from a rhenium alloy loop. The detection limit in an argon atmosphere was $1.2. \times 10^{-10}$g (0.06 µg/ml, 217 nm).

The work described in this chapter is a detailed investigation into the atomic fluorescence characteristics of lead measured in the non-dispersive mode. Both a flame and a non-flame atomiser were investigated. From this, optimum conditions for the determination of lead by the technique were established, and the method shown to be a viable technique for the analysis of real samples.

5.2. Fluorescence characteristics.

The fluorescence spectrum of lead was complex and possessed many lines. A comprehensive study has been reported by Browner (84), of the fluorescence emission from an $Ar/O_2/H_2$ flame excited by a lead EDL. The fluorescence signals obtained were as follows:-

Line nm	Relative fluorescence
283.3	52.5
364.0*	16.1
368.3*	7.61
405.8*	100
722.9*	65.2
217.0	3.21
261.4	4.0
280.2	2.65
282.3	2.23
287.3	1.31
402.0*	0.65
406.0*	-

* These lines would not be detected by the R166 PMT.

5.2.1. Mechanism.

The most intensely emitted line occurred at 405.8 nm - a direct line fluorescence emission. This was expected to be less intense than the resonance fluorescence line at 283.3 nm, but was not the case. This reversal has been partially elucidated by Browner (84). There was also resonance fluorescence at 217.0 nm; all the other emission lines may be attributed to stepwise and/or direct line fluorescence transitions.

5.3. Experimental.

5.3.1. Apparatus.

The apparatus has previously been described in section 3.3.1.

5.3.2. Reagents.

A stock solution (1000 µg/ml) of lead was prepared by dissolving lead nitrate in a 1 % nitric acid solution. Other reagents used were as reported in section 4.3.2.

5.4. Atomic fluorescence measurements.

5.4.1. Optimisation of AFf parameters.

5.4.1.1. Source.

The tube parameters, preparation and spectral characteristics of lead EDL have been reported in section 2.5.4. The optimum operating conditions of the lead EDL, after critical tuning of the $\frac{1}{4}$ wave cavity, were found to be 50 watts of microwave power and a thermal environment of 310 C (see Fig. 31 a.b). The optimum conditions that gave the best S/N ratio obtained from fluorescence measurements closely followed those from the integrated line intensity studies made in section 2.5.4.

5.4.1.2. Flame atomiser.

Optimum flame conditions for lead measurements were investigated and found to be as shown in Table 13. The optimum uptake rate of the nebuliser chamber was the same as that reported for mercury, (Fig. 23a).

Table 13.

Lead AFf flame conditions.

		Gas pressure		Flow rate
Premixed		Argon	30 psi	7.7 1/m
		Hydrogen	15 psi	8.0 1/m
		Oxygen	5 psi	0.651/m
	Sheath	Argon	15 psi	7.5 1/m
Diffusion		Hydrogen	15 psi	2.1 1/m
		Argon	30 psi	6.8 1/m

5.4.1.3. Instrumental.

The optimum positions were the same as those reported for mercury in section 3.4.1.3. The lead fluorescence signal showed little variation with height viewed in the separated region of the flame and the PMT viewing entrance was fixed nominally at three cm above the burner head.

fig. 31

a)

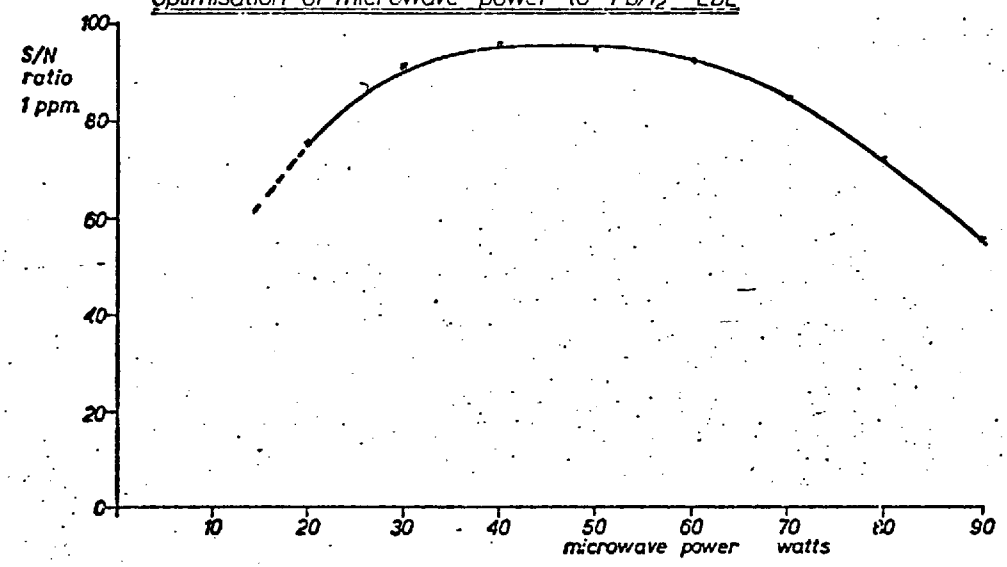
Optimisation of microwave power to Pb/I2 EDL
S/N ratio 1 ppm
100
80
60
40
20
0
10
20
30
40
50
60
70
80
90
microwave power watts

b)

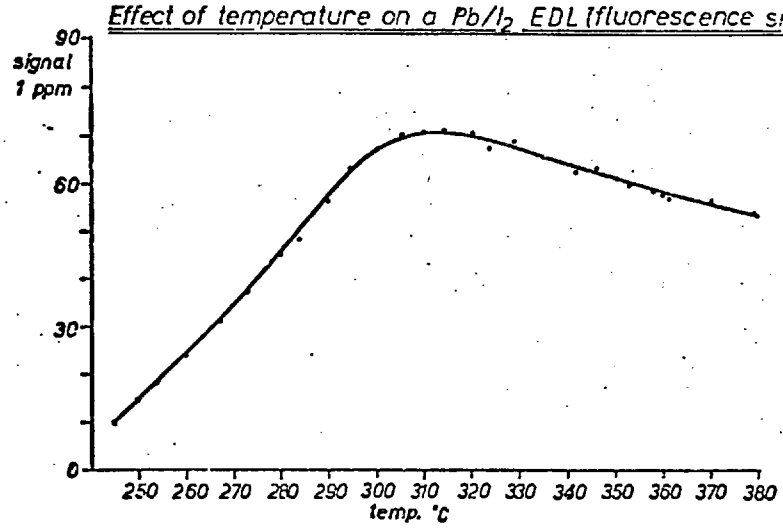
Effect of temperature on a Pb/I2 EDL (fluorescence signal)
90
signal 1 ppm
60
30
0
250 260 270 280 290 300 310 320 330 340 350 360 370 380
temp. °C

5.4.1.4. Detector.

The optimum conditions were the same as those reported for mercury previously in section 3.4.1.4.

5.4.2. Calibration studies AFf.

The stock solution of lead was diluted to provide a range of suitable concentrations. These solutions were used to construct an analytical growth curve (see Fig. 32). The linear portion covered the range 0.1 to 100 µg/ml. Larger concentrations of lead solutions resulted in a curvature towards the concentration axis. The detection limit was calculated to be 0.025 µg/ml (S/N = 2). The precision was found to be 8 % (10 readings) for a concentration of 0.25 µg/ml.

5.4.3. Interference studies AFf.

Of the selected ions, when present in excess x 100 over lead nitrate in nitric acid solution, only aluminium and bismuth produced a variation greater than 5 % on the fluorescence signal (see Table 14).

Table 14.

AFf ions	% Interference on 5 ug/ml Lead x 100 excess
Ti IV	-5
Cr III	-5
Mo VI	-2.5
Fe III	-3
Al III	-43.5
Ni II	-1
Co II	-1
Bi III	+20
Sn II	-1.5
As III	-2
Sb III	-1

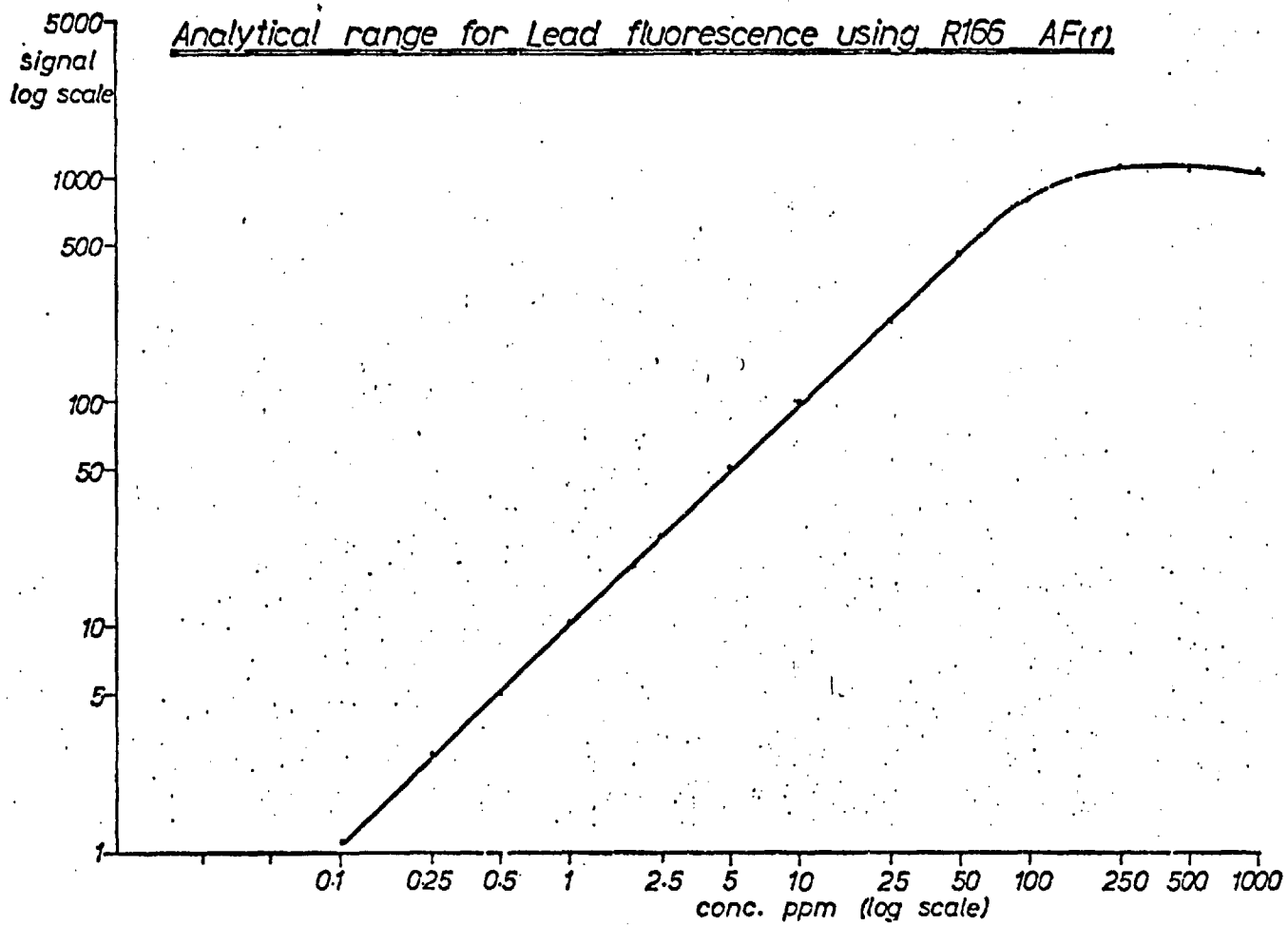
Analytical range for Lead fluorescence using R166 AF(f)
5000
signal
log scale
1000
500
100
50
10
5
1
0·1
0·25
0·5
1
2·5
5
10
25
50
100
250
500
1000
conc. ppm (log scale)

fig. 32

The aluminium interference has been previously discussed for bismuth in section 4.4.3. The increase in the lead signal by the presence of bismuth was expected, since the iodine line present in the lead source gave rise to bismuth fluorescence. A correction made for this effect showed that bismuth interfered very little with the lead signal.

5.4.4. Optimisation of AFg paramerers.

5.4.4.1. Source.

The optimum conditions of source operation was found to be identical to those reported for the flame in section 5.4.1.1.

5.4.4.2. Loop atomiser.

The 5 µl drop on the loop was dried for 30 secs. at a low temperature. It was then allowed to cool for 20 secs. During this period a higher temperature was selected. The loop was then flashed. The burn temperature was estimated to be 1400 C. The maximum fluorescence signal from the loop was obtained when the flow rate of argon was 2.5 1/min and with variable resistance setting 8 (see Fig. 33a,b). The times in the events cycle quoted, were the minimum consistent with reproducible signals.

5.4.4.3. Instrumental.

The position of the loop in relation to the collimator slit of the PMT and the source image have been previously discussed for mercury in section 3.4.4.3. The optimum position was that shown in (Fig. 34a.b.c).

5.4.4.4. Detector.

The optimum EHT setting for the best S/N ratio from the R431 PMT was 1050 V as shown in (Fig. 35a).

fig. 33

a)

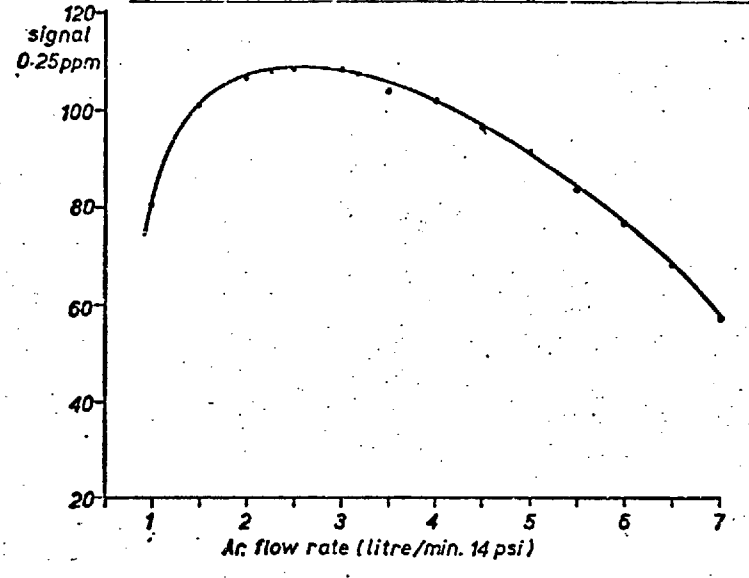
Optimisation of 'loop' gas flow for Lead fluorescence
120
signal
0·25ppm
100
80
60
40
20
1
2
3
4
5
6
7
Ar. flow rate (litre/min. 14 psi)

b)

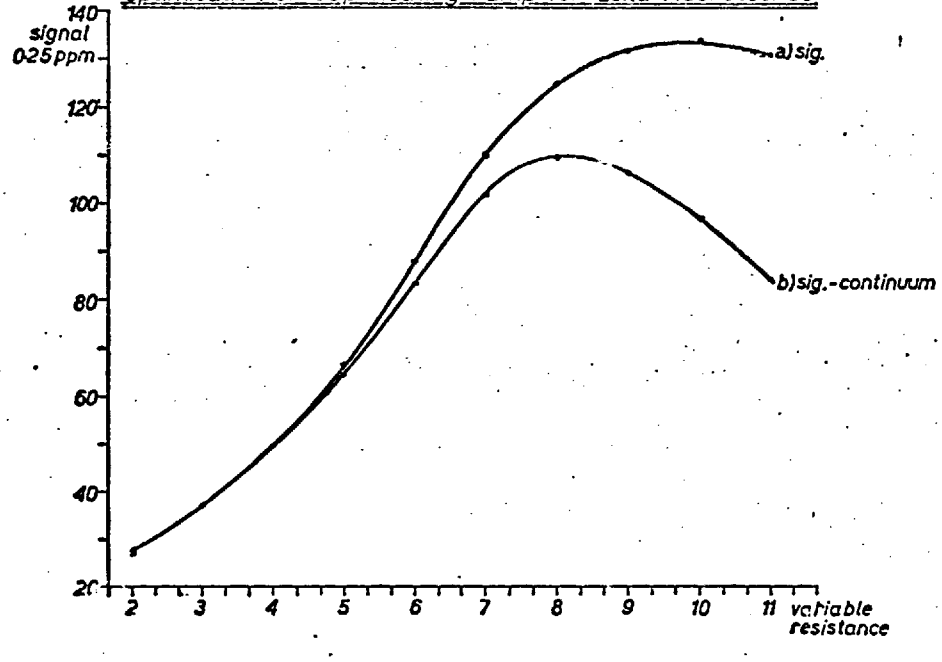
Optimisation of 'loop' heating ramp for Lead fluorescence
140
signal
0·25ppm
120
100
80
60
40
20
a) sig.
b) sig.-continuum
2
3
4
5
6
7
8
9
10
11
variable
resistance

fig. 34

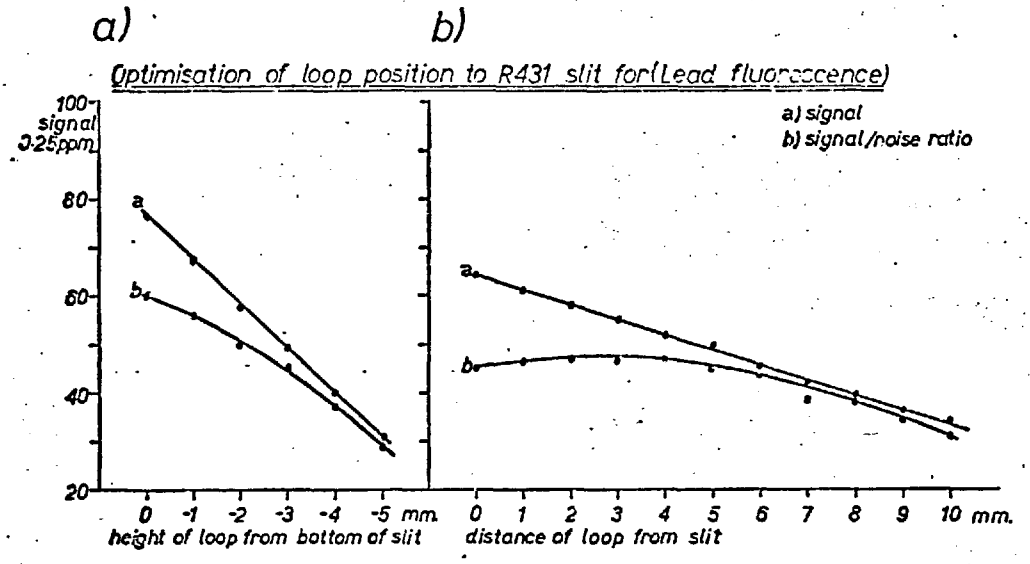
a)
b)
Optimisation of loop position to R431 slit for (Lead fluorescence)
100
signal
0.25ppm
80
60
40
20
a
b
a) signal
b) signal/noise ratio
0 -1 -2 -3 -4 -5 mm.
height of loop from bottom of slit
0 1 2 3 4 5 6 7 8 9 10 mm.
distance of loop from slit

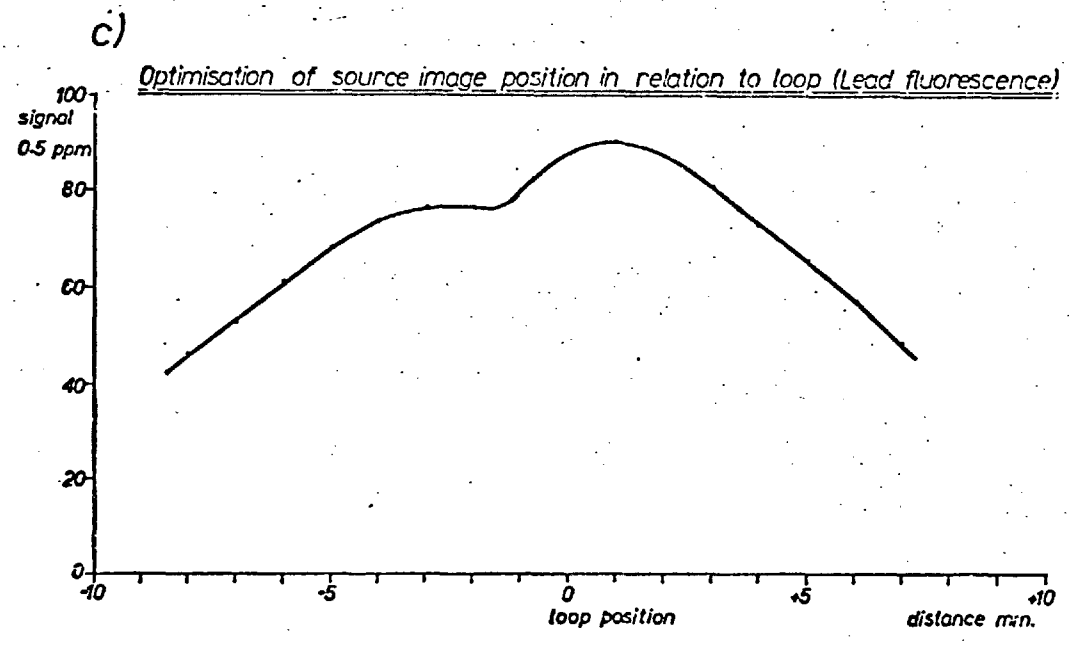
c)
Optimisation of source image position in relation to loop (Lead fluorescence)
100
signal
0.5 ppm
80
60
40
20
0
-10
-5
0
+5
+10
loop position
distance mm.

5.4.5. Calibration studies AFg.

The stock solution of lead was sutably diluted to provide a range of concentrations. These solutions were used to construct an analytical growth curve (see Fig. 35b). The linear portion extended from 0.005 to 10 µg/ml. Larger concentrations of lead solution caused a curvature towards the concentration axis. The limit of detection was calculated to be 7.5×10^{-12}g. (0.0015 µg/ml S/N = 2). The precision was found to be 7.5 % (10 readings) for a concentration of 0.05 µg/ml.

5.4.6. Interference studies AFg.

A study was made of x4 and x20 excess of various ions on a fluorescence signal from 0.25 µg/ml lead solutions (see Table 15).

Table 15.

AFg	% Interference on a 0.25 µg/ml Lead	
ions	x4	x20
Ti IV	-22	-48.5
Cr III	-14	-13.5
Mo VI	-15	-53.5
Fe III	- 0.95	-10.5
Al III	- 6.5	-40.5
Ni II	- 0	- 7
Co II	0	- 6
Bi III	+50	+80.5
Sn II	- 8.5	- 9.5
As III	-22	-49.5
Sb III	- 0.95	- 5

fig.35

a)

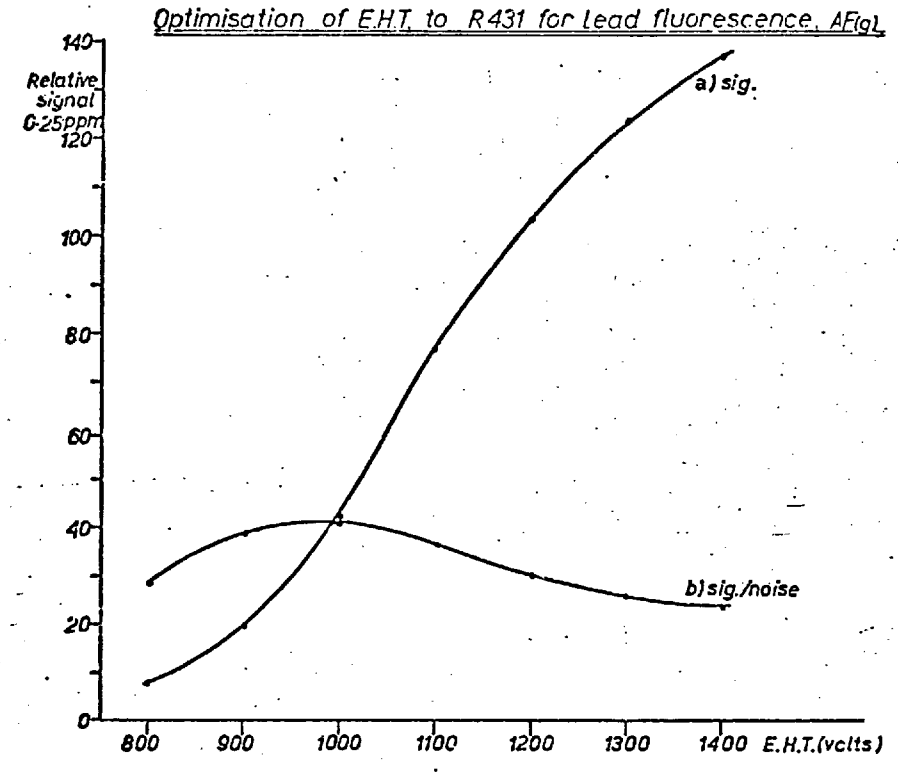
Optimisation of E.H.T. to R431 for Lead fluorescence, AF(g).
Relative signal 0·25ppm
140
120
100
80
60
40
20
0
a) sig.
b) sig./noise
800
900
1000
1100
1200
1300
1400
E.H.T.(volts)

b)

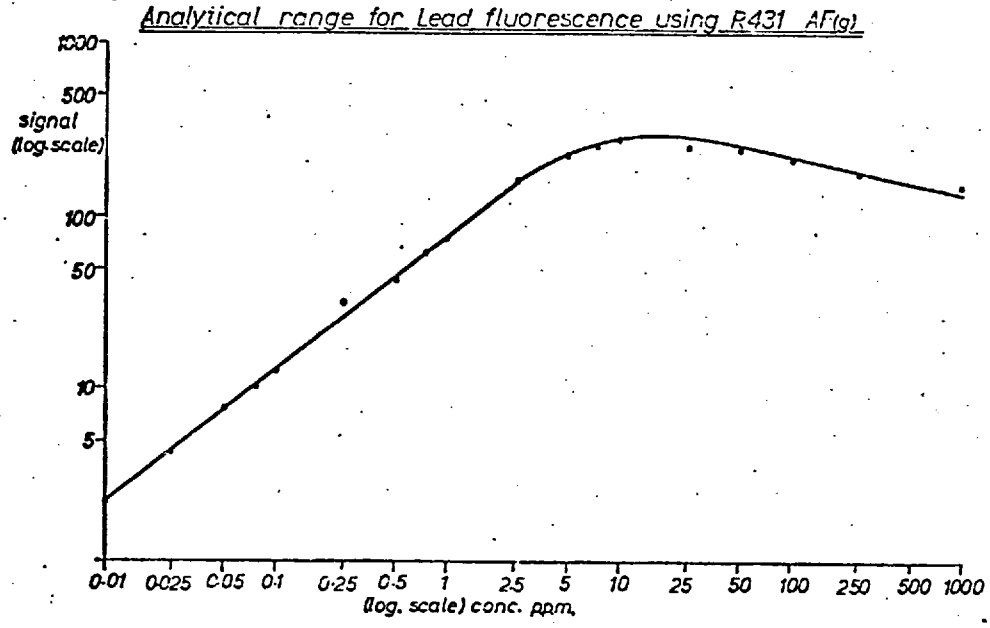
Analytical range for Lead fluorescence using R431 AF(g)
1000
500
signal (log scale)
100
50
10
5
0·01
0·025
0·05
0·1
0·25
0·5
1
2·5
5
10
25
50
100
250
500
1000
(log. scale) conc. ppm.

5.5. Samples analysis.

5.5.1. Sample treatment.

The samples were treated in the same manner as reported before in sections 4.5. and 4.5.1. for bismuth.

5.5.2. Solvent extraction.

The same extraction procedure was followed for bismuth in section 4.5.2. In this case, the excess of potassium iodide added to the lead solution in 5 % (w/v) hydrochloric acid formed the complex lead iodide PbI_4^{--}. This complex was extracted into an oxygen-containing solvent, MIBK.

5.5.3. Selective electrodeposition.

The lead content of the Ni/Co alloys was determined in the same manner as that discussed for bismuth in section 4.5.3. The results obtained can be found with those of bismuth in Table 12.

5.6. Discussion.

In the AFg system the linear portion of the analytical growth curve ended prematurely at a fairly low concentration level (Fig. 35b). This curvature of the growth curve towards the concentration axis was not due to the reason predicted from theory (sections 1.4.3.-4). An investigation was made of the lead fluorescence signal using a storage oscilloscope. This resulted in the detection of a double-peaked signal for all concentrations greater than 5 ug/ml (see Fig. 36D).

The ideal Gaussian-shaped signal was obtained from a 2.5 ug/ml lead solution (Fig. 36B). At a low burn temperature this signal was broadened, and at a much higher temperature the signal was distorted.

The analytical growth curves are plotted from peak height measurements; thus double peaks cause premature curvature from the linear range.

The oscilloscope traces also showed clearly that the signal event was completed before the continuum emission became appreciable. Traces made from the chart recorder (Fig. 36 E.G.G.), only showed separation of the signal event from the continuum rise, (Fig. 36 E) when the normal chart speed used was increased and the signal event duration was small, ie at low concentration of lead solution.

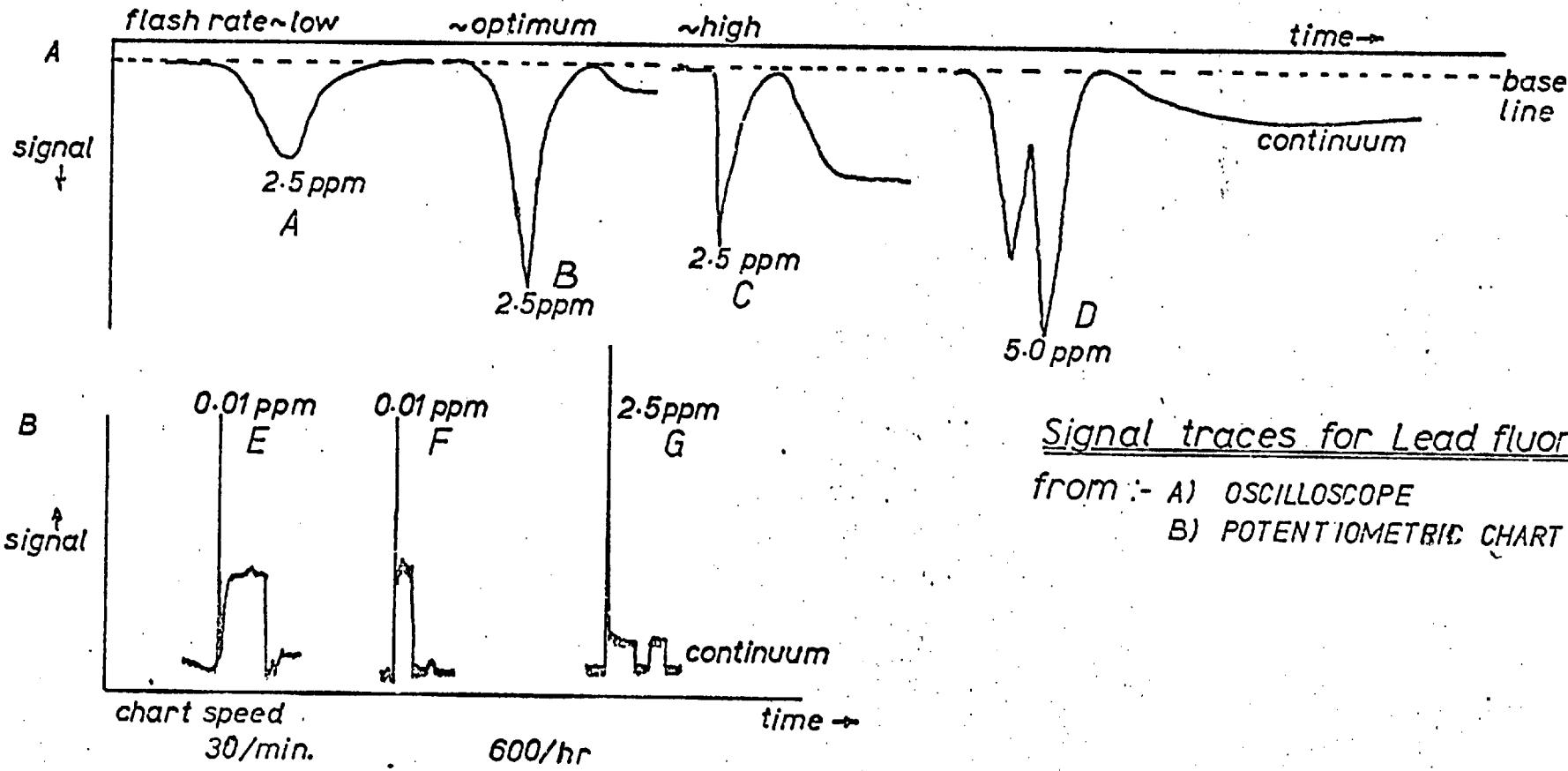

Signal traces for Lead fluorescence

from :- A) OSCILLOSCOPE
B) POTENTIOMETRIC CHART RECORDER

fig. 36.

However, with higher concentrations, the signal event duration (Fig. 36 G) was inseparable from the continuum emission with the recorder employed. This was a large contributing factor in the detection limits for bismuth and tin, where higher temperatures were required for atomisation. This meant that the emission brightness from the loop was greater and the continuum rise steeper.

The appearance of double peaks for a number of elements has been reported before (103, 105, 107). Williams (107) has proved conclusively for copper and manganese that the double peaking from the loop was not due to scattering by the matrix or refractive index change. Clark (262) suggested, with some evidence, that the multiple peaks for mercury in a Delves Cup were due to the vaporisation at different temperatures of the different valency salts. Both of these authors have stated that none of the peaks was due to molecular absorption, as both used the AA mode in their studies. They used a close non-resonance line to check for molecular absorption.

To verify that the recorded signal was a fluorescence signal and was not caused by scattering, the following procedure was used:
a zinc solution was atomised from the loop and irradiated with the lead lamp. No signal above the background resulted. A similar result was obtained with a lead solution and zinc irradiation.

The lead fluorescence signal from different types of lead solution was then investigated. The atomisation of lead nitrate and lead acetate from the loop resulted in the oscilloscope trace displaying a double peak, the first peak being smaller than the second. However, this situation was reversed when the analyte was lead chloride in concentrated hydrochloric acid, lead sulphide suspension in carbon tetra-chloride, and lead iodide in MIBK. A possible explanation for this reversal could be the different valency forms of lead compounds, Pb (II) and(IV), so giving rise to sequential (time resolved) peaks.

5.7. Summary.

The studies made in this chapter have showed that both of the non-dispersive systems employed can usefully be used for lead determinations. AF determinations were carried out using real samples. However, careful and extensive pretreatment was required before the analyte could be determined in the system.

For the flame, a similar sensitivity was obtained in the non-dispersive mode to those reported previously using a monochromator. The sensitivity obtained for lead AF determination from the loop was several orders of magnitude better than those reported using a monochromator. This increase in sensitivity was that expected from theory, as the particular combination of loop and solar-blind PMT makes full use of the potential sensitivity of the AF process.

Chapter 6.

Tin

6.1. Introduction.

There has only been one report published of AF determination of tin using the non-dispersive technique. Larkins(50) has obtained a detection limit of 3 µg/ml from a separated air/acetylene flame using the R166 PMT.

The best AF results for tin using a monochromator (303.4 nm line) and flame were obtained by Browner (83). The detection limit of 0.1 µg/ml was obtained in a nitrogen separated $Ar/H_2/O_2$ flame.

There has been no report of AF determinations from a loop. However, Williams (107) has reported tin AA from a tungsten loop. The detection limit in an argon atmosphere was 3×10^{-8} g (10 µg/ml) at the 286.3 nm line.

The work described in this chapter is a detailed investigation into the atomic fluorescence characteristics of tin measured in the non-dispersive mode. Both flame and non-flame atomisers were investigated. From this, optimum conditions for the determination of tin by the technique were established and the method shown to be a viable technique.

6.2. Fluorescence characteristics.

The fluorescence spectrum of tin showed many lines. An account has been previously reported by Browner (83). The fluorescence emission from a premixed $Ar/H_2/O_2$ and Ar/H_2 flame excited by a tin EDL has been studied. The fluorescence signals obtained were as follows:-

see over page.

Line (nm)	Relative fluorescence	
	$Ar/O_2/H_2$	Ar/H_2
224.65	3.70	-
235.48	3.61	-
242.95	7.42	6.30
254.66	5.92	4.75
326.23	8.14	35.5
270.65	81.5	58.5
284.00	215	58.5
333.00 **	37	4.74
286.33	237	122
300.91	200	94
303.41	519	130
317.51	482	213
380.10 *	66.7	39.6

* These lines would not be detected by the R166 PMT.

6.2.1. Mechanism.

Resonance fluorescence signals were obtained from three of the four tin lines arising from the ground state, 224.65, 270.65, 286.33 nm, but no signal from 207.31 nm because of its weak intensiity.

The strongest emission line was the stepwise transition at 303.4 nm. However, Browner states that this also contains a component from the resonance fluorescence transition 286.33 nm which was thermally assisted to the higher state.

The other emission lines can be attributed to direct line and /or stepwise transition. The line 254.66 nm was an intercombination line.

6.3. Experimental.

6.3.1. Apparatus.

The apparatus has previously been described in section 3.3.1.

6.3.2. Reagents.

A stock solution (1000 µg/ml) of tin was prepared by dissolving the pure metal in the minimum of concentrated hydrochloric acid in the presence of a platinum wire (catalyst), and accurately diluted further with 0.1M hydrochloric acid solution. Other stock solutions used were as reported in section 4.3.2.

6.4. Atomic fluorescence measurements.

6.4.1. Optimisation of AFf parameters.

6.4.1.1. Source.

The tube parameters, preparation and spectral characteristics of the tin EDL have been reported elsewhere, section 2.5.5. The optimum operating conditions of the tin EDL, after critical tuning of the $\frac{1}{4}$ wave cavity were found to be 60 watts of microwave power and a thermal environment of 40 C (see Fig. 36a,b). These optimum conditions that gave the best S/N ratio from fluorescence measurements, closely resemble those made from integrated line intensity studies in section 2.5.5.

6.4.1.2. Flame atomiser.

Optimum flame conditions for tin measurements were investigated and found to be shown in Table 18. The optimum uptake rate of the nebuliser chamber was the same as that reported for mercury (Fig. 23a).

Table 18.

Tin AFf flame conditions.

		Gas pressure		Flow rate
Premixed		Argon	30 psi	7.7 l/m
		Hydrogen	15 psi	8.0 l/m
		Oxygen	5 psi	1.1 l/m
	Sheath	Argon	15 psi	7.5 l/m

fig. 37.

a)

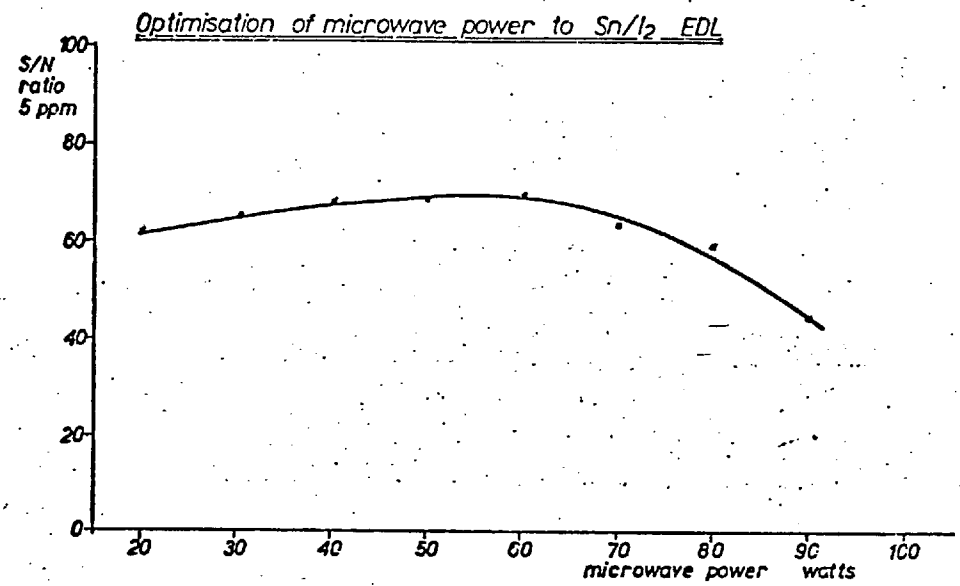
Optimisation of microwave power to Sn/I2 EDL
S/N ratio 5 ppm
100
80
60
40
20
0
20
30
40
50
60
70
80
90
100
microwave power watts

b)

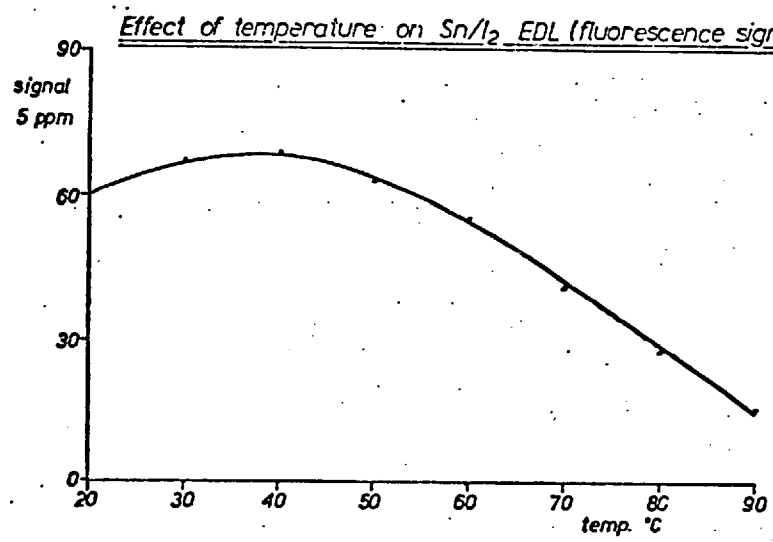
Effect of temperature on Sn/I2 EDL (fluorescence signal)
signal 5 ppm
90
60
30
0
20
30
40
50
60
70
80
90
temp. °C

Table 18 (cont'd)

	Gas pressure	Flow rate
Diffusion	Hydrogen 15 psi	4.5 l/m
	Argon 30 psi	7.7 l/m

6.4.1.3. Instrumental.

The optimum positions were the same as those reported for mercury in section 3.4.1.3. The tin fluorescence signal showed little variation with height in the separated region of the flame and the PMT viewing entrance was nominally fixed at 2 cm above the burner head.

6.4.1.4. Detector.

The optimum conditions of operation are the same as those reported previously in section 3.4.1.4.

6.4.2. Calibration studies AFf.

The stock solution was diluted to provide a range of concentrations and used to construct an analytical growth curve (see Fig. 38). The linear portion of the curve covered the range 2.5 to 1000 µg/ml. The limit of detection was calculated to be 0.75 µg/ml (S/N = 2). The precision was found to be 6.5 % (10 readings) for a concentration of 7.5 ug/ml.

6.4.3. Interference studies AFf.

Of the selected ions, when present in a x 100 excess over a tin solution, only molybdenum and bismuth produced a variation greater than 8 % on the fluorescence signal, see Table 19.

fig. 38.

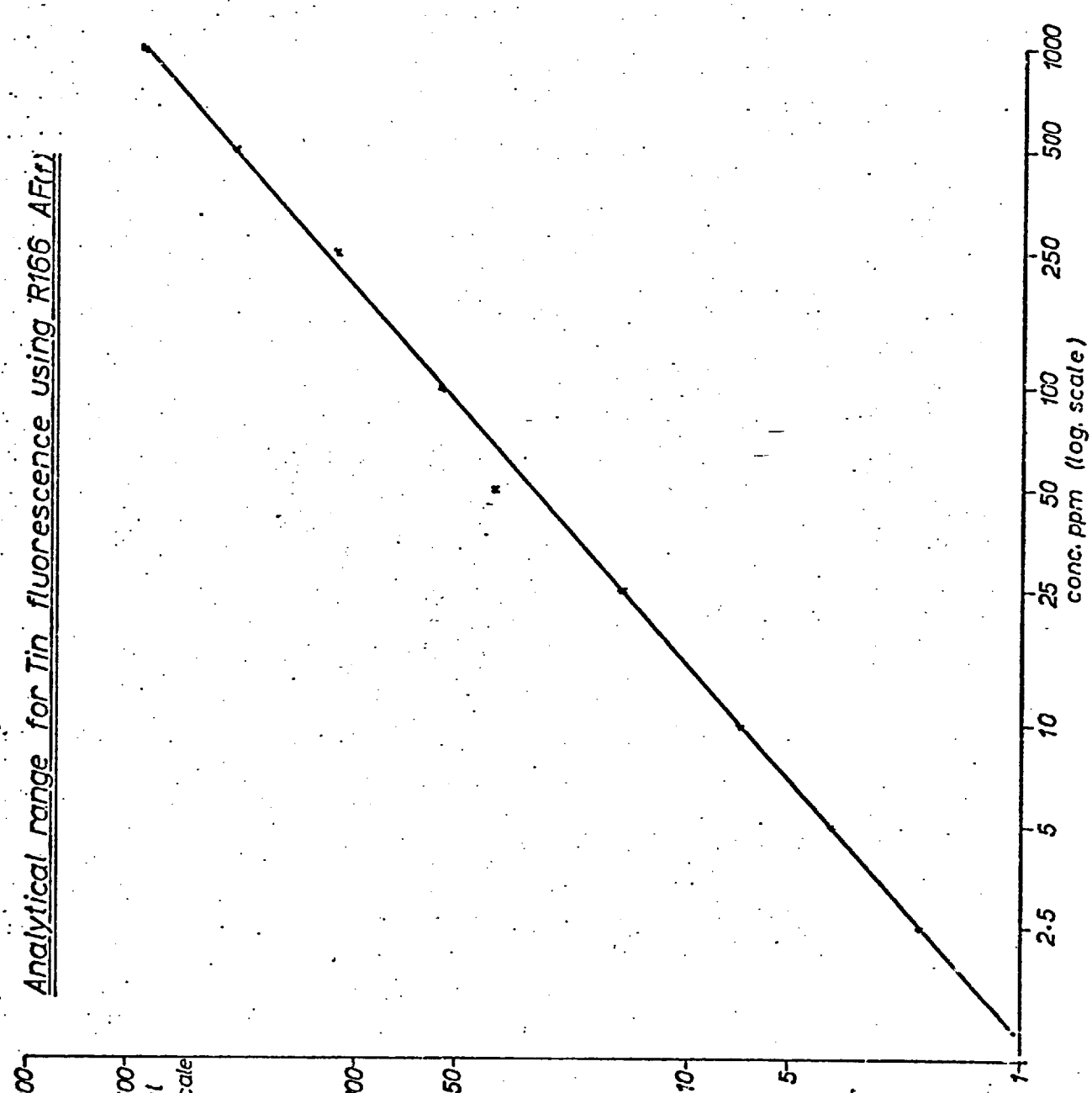
Analytical range for Tin fluorescence using R166 AF(t)
signal log. scale
1000
500
100
50
10
5
1
2.5
5
10
25
50
100
250
500
1000
conc. ppm (log. scale)

Table 19.

AFf ions	% Interference on 5 µg/ml Tin x 100
Ti IV	-6
Cr III	-4
Mo VI	-33
Fe III	-2
Al III	-8
Ni II	-3
Co II	-3
Bi III	+20
As III	-1
Sb III	-0.5
Pb II	0

The increase in the tin signal caused by the presence of bismuth was expected, since the iodine line present in the tin source gave rise to bismuth fluorescence. A correction made for this effect showed that bismuth interferes little with the tin signal.

6.4.4. Optimisation of AFg parameters.

6.4.4.1. Source.

The optimum conditions of source operation were found to be identical to those reported for the flame.

6.4.4.2. Loop atomiser.

The 5 µl drop on the loop was dried for 40 secs. at a low temperature. It was then allowed to cool for 20 secs. During this period a higher temperature was selected. The loop was then flashed. The burn temperature was estimated to be 2400 C. The maximum fluorescence signal from the loop was obtained, when the flow rate of argon was 4.5 l/min. and the variable resistance setting 15.5.

The times of the loop event cycle quoted, were the minimum consistent with a reprodicible signal.

6.4.4.3. Instrumental.

The position of the loop in relation to the collimator slit was lowered by 1 mm, to minimise the continuum glow of the loop during a burn period. Otherwise the loop position was similar to those already reported (see Fig. 34 abc).

6.4.4.4. Detector.

The optimum EHT setting for the best S/N ratio from the fluorescence signal was 1050 V from the R431 PMT.

6.4.5. Calibration studies AFg.

The stock solution of tin was diluted to provide a range of suitable concentrations and used to construct an analytical growth curve, (see Fig. 39). The linear portion extended from 0.5 to 250 µg/ml. Larger concentrations of tin caused a curvature towards the concentration axis.

The limit of detection was calculated to be 7.5×10^{-10}g (0.15 µg/ml S/N = 2). The precision was found to be 21 % (10 readings) for a concentration of 1.0 µg/ml.

6.4.6. Interefernce studies AFg.

A study was made of x4 and x20 excess of various ions on a fluorescence signal from 5 µg/ml signal (see table 20).

fig. 39.

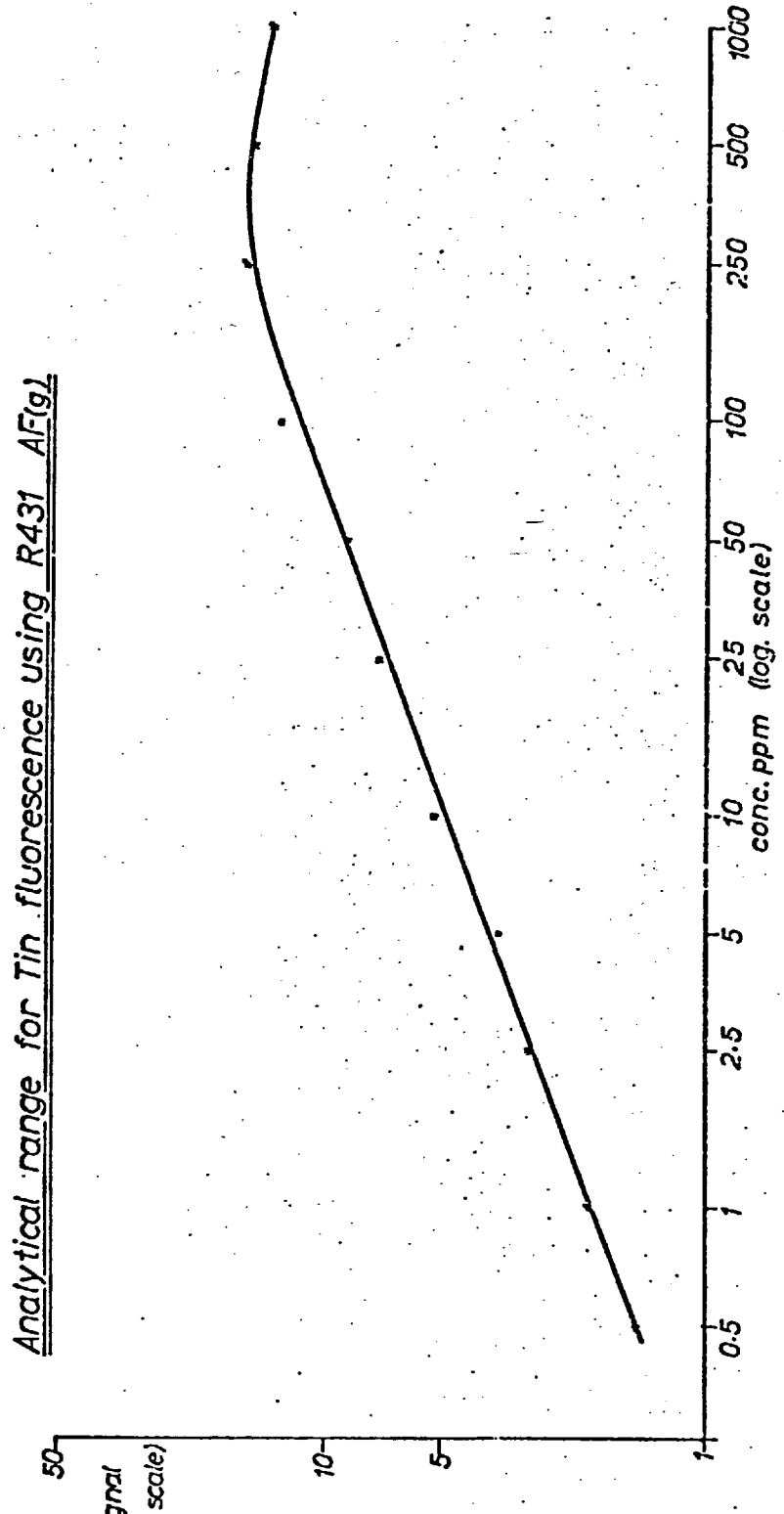
Analytical range for Tin fluorescence using R431 AF(g)
signal (log. scale)
50
10
5
1
0.5
1
2.5
5
10
25
50
100
250
500
1000
conc. ppm (log. scale)

Table 20.

AFg	% Interference on 5 µg/ml tin	
Ions	x4	x20
Ti IV	-15	-30
Cr III	-10	-12
Mc VI	-10	-20
Fe III	0	- 5
Al III	- 3	- 8
Ni II	- 0	- 0
Co II	0	-
Bi III	+13	+45
As III	-10	-14
Sb III	- 0	0
Pb II	0	0

6.5. Summary.

The studies made in this chapter have showed that both the non-dispersive systems employed can usefully be used for tin determinations.

Similar sensitivities for the flame cell, to those reported using a monochromator, were obtained for the tin AF determinations. The non-flame cell provided a very similar sensitivity to those reported for AA from the loop using a monochromator.

The small differences in sensitivities obtained for tin AF, between the loop and the flame atomisers, was unexpected. However, Browner (83) had previously reported that it is difficult to obtain the atomic state for tin, and the free atom state concentration was probably vastly improved in the flame. This is a result of the reducing nature of the flame, which was fuel rich when optimised for tin AF.

BIBLIOGRAPHY

1. R.W.Wood, Proc. Am. Acd. Arts & Sci. XL, 363 (1904)
2. A.C.G. Mitchell and M.W. Zemansly, Resonance Radiation and Excited Atoms, Univ. Press Camb. (1961)
3. A. Bogros, Compt. Rend. 183, 124 (1926)
4. C. Boeckner, Bureau of Stand. Journ. Res. 5, 13 (1930)
5. R.W. Wood, Researches in Physical Optics, I & II, Columbia Univ. Press, N.Y. (1913 & 1919)
6. A. Terenin, Z.f. Phys. 31, 26 (1925)
7. N. Ponomarev and A. Terenin, Z.f. Phys. 37, 95 (1926)
8. J. Fridrickson, Z.f. Phys. 64, 43 (1930)
9. A. Ellett, J. Opt. Soc. Amer. 10, 427 (1925)
10. H. Schuller, Z.f. Phys. 35, 323 (1926)
11. E.L. Nichols and H.L. Howes, Phys. Rev. 22, 425 (1923)
12. R.M. Badger, Z.f. Phys. 53, 56 (1929)
13. R. Mankopff, Verhandl, Deutsch. Phys. Ges. 14, 16 (1933)
14. A.L. Boers, C.Th.J. Alkemade and J.A. Smit, Physica, 22, 358 (1956)
15. H.P. Hooymayers and C.Th.J. Alkemade, J. Quant. Spec. Rad. Trans.6, 501 847 (1966)
16. D.R. Jenkins, Proc. Roy. Soc. A293, 493 (1966)
17. D.R. Jenkins, Proc. Roy. Soc. A303, 453 (1968)
18. D.R. Jenkins, Proc. Roy. Soc. A303, 467 (1968)
19. D.R. Jenkins, Proc. Roy. Soc. A306, 413 (1968)
20. D.R. Jenkins, Proc. Roy. Soc. A313, 551 (1969)
21. J.D. Winefordner and T.J. Vickers, Anal. Chem. 36, 161 (1964)
22. J.D. Winefordner and R.A. Staab, Anal. Chem. 36, 165 (1964)
23. J.D. Winefordner and R.A. Staab, Anal. Chem. 36, 1367 (1964)
24. J.D. Winefordner, J.M. Mansfield, and C. Veillon, Anal. Chem. 37, 1049 (1965)
25. J.W. Robison, Anal. Chim. Acta, 24, 254 (1961)
26. T.S. West, Lecture, Chemical Society, Burlington House, 6th Oct. (1965)

27. C.Th.J. Alkemade, International Conference on Spectroscopy, College Park, Md. June (1962)

28. N. Omenetto, and J.D. Winefordner, Appld. Spec. 26, 555 (1972)

29. H.P. Hooymayers, Spectrochim. Acta, 23b, 567 (1968)

30. V. Svoboda, R.F. Browner and J.D. Winefordner, Appld. Spec. 26, 505 (1972)

31. P.J.T. Zeegers, R. Smith and J.D. Winefordner, Anal. Chem. 40, 26a (1968)

32. G.F. Kirkbright and T.S. West, Chem. in Brit. 8, 428 (1972)

33. R.C. Elser and J. D. Winefordner, Anal. Chem. 43, 24a (1971)

34. J.D. Winefordner, Pure and Applied Chem. 23, 35 (1970)

35. J.D. Winefordner and T.J. Vickers, Anal. Chem. 36, 1939 (1964)

36. C.Th.J. Alkemade, Ph.D. Thesis, University of Utrecht, Netherlands (1954)

37. Le.de.Galan and J.D. Winefordner, J.Quant. Spec. Rad. Trans. 7, 251 (1967)

38. J.D. Winefordner, C.T. Mansfield and T.J. Vickers, Anal. Chem. 35, 1607 (1963)

39. C.Th.J. Alkemade, Proc. 10th. Spec. Colloq. Editor C.R. Lippinscott Spartan (1963)

40. H.P. Hooymayers and C.Th.J. Alkemade, J.Quant. Rad. Trans. 6, 501 (1966)

41. H.P. Hooymayers and C.Th.J. Alkemade, ibid, 6, 847 (1966)

42. D.R. Jenkins, Spectrochim. Acta. 23b, 167 (1968)

43. S.J. Pearce and Le.de Galan and J.D. Winefordner, Spectrochim. Acta, 23b 793 (1969)

44. W.J. McCarthy, M.L. Parsons and J.D. Winefordner, ibid, 23b, 25 (1967)

45. R. Smith, R.C. Elser and J.D. Winefordner, Anal. Chem. 43, 35 (1969)

46. M.P. Bratzel, R.M. Dagnall and J.D. Winefordner, ibid, 41, 713 (1969)

47. C. VanTright, T. Hollander and C.Th.J. Alkemade, J. Quant. Spec. Rad. Trans, 5, 813 (1965)

48. W.B. Barnett and H.L. Kahn, Anal. Chem. 44, 935 (1972)

49. T.S. West and X.K. Williams, Anal. Chem. 40, 335 (1972)

50. P.L. Larkins, Spectrochim. Acta, 26b, 477 (1971)

51. P.L. Larkins and J.B. Willis, ibid, 26b, 491 (1971)

52. P.L. Larkins, R.M. Lowe, J.V. Sullivan and A. Walsh, ibid, 24b, 187 (1969)

53. P.D. Warr, Talanta, 17, 543 (1970)

54. T.J. Vickers, P.JSlevin, V.I. Muscat and L.T. Farias, Anal. Chem. 44, 930 (1972)

55. T.J. Vickers, R.M. Vaught, V.I. Muscat and L.T. Farias, Anal. Chem. 41, 1477 (1969)

56. R.M. Dagnall, G.F. Kirkbright, T.S. West and R. Wood, ibid, 43, 1765 (1971)

57. P.W. Boumans, R.F. Rumphorst, L. Willemsen, F.J. DeBoer, Spectrochim. Acta, 28b, 227 (1973)

58. D.S. Gough, P. Hannaford and A. Walsh, ibid, 28b, 197 (1973)

59. D.G. Mitchell and A. Johanson, ibid, 25b, 175 (1970)

60. D.G. Mitchell and A. Johanson, ibid, 26b, 677 (1971)

61. A. Walsh, Pure and Applied Chem. 23, 1 (1970)

62. H.V. Malmstadt, 23rd Pittsburgh Con. Cleveland, Ohio (1972)

63. R.C. Elser and J.D. Winefordner, Appld. Spec. 25, 345 (1971)

64. Hamamatsu Photosensitive Devices Catalogue (1972)

65. R.M. Dagnall, K.C. Thompson and T.S. West, Anal. Chim. Acta. 36, 269 (1966)

66. C. Veillon, J.M. Mansfield, M.L. Parson and J.D. Winefordner, Anal. Chem. 38, 204 (1966)

67. D.W. Ellis and D.R. Demers, ibid, 38, 1943 (1966)

68. N. Omenetto and G. Rossi, Anal. Chim. Acta, 40, 195 (1968)

69. D.R. Demers and D.W. Ellis, Anal. Chem. 40, 860 (1968)

70. D.C. Manning and P. Heneage, At. Abs. News, 6, 124 (1967)

71. R.M. Dagnall, K.C. Thompson and T.S. West, Talanta, 15, 677 (1968)

72. R.M. Dagnall, K.C. Thompson and T.S. West, ibid, 14, 1467 (1967)

73. K.M. Aldous, R.F. Browner, R.M. Dagnall and T.S. West, Anal. Chem. 42, 939 (1970)

74. G.F. Kirkbright and T.S. West, Applied Optics, 7, 1305 (1968)

75. R.M. Dagnall, T.S. West and P. Young, Talanta, 13, 803 (1966)

76. P.J. Padley and T.M. Sugden, Proc. Roy. Soc. A248, 248 (1958)

77. R.M. Dagnall, K.C. Thompson and T.S. West, Analyst. 92, 506 (1967)

78. R. M. Dagnall , K.C. Thompson and T.S. West, ibid, 93, 72 (1968)

79. R.M. Dagnall, K.C. Thompson and T.S. West, ibid, 93, 518 (1968)

80. R.M. Dagnall, K.C. Thompson and T.S. West, ibid, 94, 64 (1969)

81. R.M. Dagnall, K.C. Thompson and T.S. West, At. Abs. Newsletter, 6, 117 (1967)

82. R. Jenkins, Spectrochim. Acta, 25b, 47 (1970)

83. R.F. Browner, R.M. Dagnall and T.S. West, Anal. Chim. Acta. 46, 207 (1969)

84. R.F. Browner, R.M. Dagnall and T.S. West, ibid, 50,375 (1970)

85. G.F. Kirkbright, A. Semb and T.S. West, Talanta, 14, 1011 (1967)

86. G.F. Kirkbright, A. Semb and T.S. West, ibid, 15, 441 (1968)

87. D.N. Hingle, G.F. Kirkbright and T.S. West, ibid, 15, 199 (1968)

88. J.D. Winefordner, C.T. Mansfield and T.J. Vickers, Anal. Chem. 35, 1607 (1963)

89. R.P. Mounce, R.M. Dagnall, B.L. Sharp and T.S. West, Proc. Soc. Anal. Chem. 10, 271 (1973)

90. L. Dunkelman, J. Opt. Soc. Am. 45, 134 (1955)

91. L. Dunkelman, ibid, 47, 1048 (1957)

92. L. Dunkelman, W.G. Fowler and J. Hennes, Appld. Optics, 1, 695 (1962)

93. T. Maruta and T. Takeuchi, Anal. Chim. Acta, 62, 253 (1972)

94. J.Y. Hwang, C.J. Mokeler and P.A. Ullucci, Anal. Chem. 44, 2018 (1972)

95. T. Takeuchi and M. Yanagisawa, Talanta, 19, 465 (1972)

96. H.M. Donega and T.E. Burges, Anal. Chem. 42, 1521 (1970)

97. J.Y. Hwang, P.A. Ullucci, S.B. Smith and A.L. Malenfant, Anal. Chem. 43, 1319 (1971)

98. T. Maruta and T. Takeuchi, Anal. Chim. Acta. 66, 5 (1973)

99. R. Bunsen, Justus Liebig's Annalen III, 257 (1859)

100. H. Brandenburger and H. Bader, Helv. Chim. Acta, 50, 1409 (1967)

101. H. Brandenburger and H. Bader, At. Abs. Newletter, 7, 53 (1963)

102. G.F. Kirkbright, Analyst, 96, 609 (1971)

103. K.M. Aldous, R.M. Dagnall, B.L. Sharp and T.S. West, Anal. Chim. Acta. 54, 233 (1971)

104. J.H. Runnels and J.H. Gibson, Anal. Chem. 39, 1398 (1967)

105. M.P. Bratzel, R.M. Dagnall and J.D. Winefordner, Appld. Spec. 24, 518 (1970)

106. R.M. Dagnall, B.L.Sharp and T.S. West, Nature Phys. Sci. 234, 69 (1971)

107. M. Williams and E.H. Piepmeier, Anal. Chem. 44, 1342 (1972)

108. J.V. Chauvin, M.P. Newton and D.O. Davis, Anal. Chim. Acta, 65, 291 (1973)

109. M.P. Bratzel, R.M. Dagnall and J.D. Winefordner, Anal. Chim. Acta. 48, 197 (1969)

110. K.M. Aldous, D.G. Mitchell and F.J. Ryan, Anal. Chem. 45, 1990 (1973)

111. S.R. Goode, A. Montaser and S.R. Crouch, Anal. Chem. in press

112. J.M. Mansfield, M.P. Bratzel, H.O. Norgordon, D.O.Knapp, K.E. Zacha and J.D. Winefordner, Spectrochim. Acta. 23b, 389 (1968)

113. M.D. Silvester and W.J. McCarthy, ibid, 25b, 229 (1969)

114. W. Mittorf, Wiedermann's Annalen, XXI, 138

115. J.J. Thompson, Phil. Mag. 32, 321 (1891)

116. D.A. Jackson, Proc. Roy. Soc. A121, 432 (1928)

117. W.F. Meggers, J. Opt. Soc. Am. 38, 7 (1948)

118. W.F. Meggers and F.O. Westfall, J. Res. Nat. Bur. Std. 44, 447 (1950)

119. W.F. Meggers and K.G. Kessler, J. Opt. Soc. Am. 40, 737 (1950)

120. L. Bovey and H. Wise, Aere-R 2976 (1959)

121. C.H. Corliss, W.R. Bozmann and F.O. Westfall, J. Opt. Soc. Am. 43, 398 (1953)

122. F.S. Tomkins and M. Fred, ibid, 47, 1087 (1957)

123. E.F. Worden, R.G. Gutmacher and J.G. Conway, Appld. Optics, 2, 707 (1968)

124. D.J. Hunt and G. Pish, J. Opt. Soc. Am. 46, 87 (1956)

125. R.J. Hull and H.H. Stroke, ibid, 51, 1203 (1961)

126. B. Budick, R. Norkick and A. Lurio, Appld. Optics, 4, 229 (1965)

127. W.E. Bell, A.L. Bloom and J. LYnch, Rev. Sci. Inst. 32, 688 (1965)

128. R.T. Atkinson, G.D. Chapman and L. Krause, J.Opt. Soc. Am. 53, 1269 (1965)

129. D.H. Burling, V. Czajkowski and L. Krause, ibid, 57, 1162 (1967)

130. N.S. Ham and A. Walsh, Spectrochim. Acta, 8, 12 (1958)

131. P. Warneck, Appld. Optics, 1,721 (1962)

132. Y. Tanaka and P.G. Wilkinson, J. Opt. Soc. Am. 45, 1044 (1955)

133. H. Okabe, ibid, 54, 478 (1964)

134. E.W. Schlag and F.J. Comes, ibid, 50, 866 (1960)

135. P.G. Wilkinson and E.T. Byram, Appld. Optics, 4, 581 (1965)

136. Y. Tanaka and M. Zelikoff, J. Opt. Soc. Am. 44, 254 (1954)

137. J,M. Vaughan, J. OPt. Soc. Am. 54, 318 (1964)

138. M. Zelikoff, H. Wyckoff, M. Aschenbrand and R. Loomis, ibid, 42, 818 (1952)

139. A. Davison, A. Giacchetti and R.W. Stanley, ibid, 52, 447 (1962)

140. E.B.M. Steers, Proc. Soc. Anal. Chem. 2, 108 (1965)

141. N.P. Ivanov, L.V. Minervina, S.V. Boranov and L.G. Porfralide, Zh. Analit. Khim. 21, 1129 (1966)

142. G.I. Goodfellow, Anal. Chim. Acta. 36, 132 (1966)

143. E.W. Richard, Spectrochim. Acta. 22, 158 (1966)

144. R.M. Dagnall, K.G. Thompson and T.S. West, Talanta, 14, 557 (1967)

145. R.M. Dagnall, K.C. Thompson and T.S. West, ibid, 14, 551 (1967)

146. R.M. Dagnall, K.C. Thompson and T.S. West, ibid, 14, 1151 (1967)

147. R.M. Daganall, and T.S. West, Appld. Optics. 7, 1287 (1968)

148. K.M. Aldous, D. Alger, R.M. Dagnall and T.S. West, Lab. Prac. 19, 587 (1966)

149. R.M. Dagnall, M.R.G. Taylor and T.S. West, Spec. Letters, 1, 397 (1968)

150. R.M. Dagnall, M.D. Silvester and T.S. West, Talanta, 18, 1103 (1971)

151. K.C. Thompson, Spec. Letters, 3, 59 (1970)

152. A. Fulton, K.C. Thomspn, T.S. West, Anal. Chim. Acta, 51, 373 (1970)

153. R.F. Browner, R.M. Dagnall and T.S. West, ibid, 45, 163 (1969)

154, C. Woodward, ibid, 51, 548 (1970)

155. A. Theodore-Forester, R.A. Gudmundsen and P.O. Johnson, J. Opt. Sco. Am. 39, 1054 (1949)

156. D. O. Cooke, R.M. Dagnall and T.S. West, Anl. Chim. Acta, 56, 17 (1971)

157. M.D. Silvester and W.J. McCarthy, Anal. Letters, 2, 305 (1969)

158. L. Ebdon, G.F. Kirkbright and T.S. West, Anal. Chim. Acta, 47, 563 (1969)

159. K.E. Zacha, M.P. Bratzel. J.D. Winefordner and J.M. Mansfield, Anal. Chem. 40, 1733 (1968)

160. D.O. Cocke, R.M. Dagnall and T.S. West, Anal. Chim. Acta, 54, 381 (1971)

161. F.C. Fehsenfeld, K.M. Evenson and H.P. Broida, Rev. Sci. Inst. 36, 294 (1965)

162. P.T. Cunningham and J.K. Link, J. Opt. Soc. Am. 57, 1000 (1967)

163. J.M. Mansfield, J.D. Winedordner and C. Veillon, Anal. Chem. 37, 1049 (1965)

164. R.F.Browner, R.M. Dagnall and T.S. West, Talanta, 16, 75 (1969)

165. G.B. Marshall and T.S. West, Talanta, 14, 823 (1967)

166. T.S. West, Pure and Applied Chem. 23, 99 (1970)

167. G.F. Kirkbright, A.B. Rao and T.S. West, Spec. Letters, 2, 69 (1969)

168. K.M. Aldous, R.M. Dagnall and T.S. West, Analyst, 94, 347 (1969)

169. B. Fleet, K.V. Liberty and T.S. West, Anl. Chim. Acta, 45, 205 (1969)

170. G.F. Kirkbright, A.P. Rao and T.S. West, Anal. Letters, 2, 465 (1969)

171. G.F. Kirkbright and R.M. Dagnall, Advances in Automated Analysis (1969)

172. R. Smith, C.M. Stafford and J.D. Winefordner, Anal. Chem. 41, 946 (1969)

173. G.B. Marshall and T.S. West, Anal. Chim. Acta. 51, 179 (1970)

174. B.M. Patel, R.F. Browner and J.D. Winefordner, Anal. Chem. 44, 2272 (1972)

175. B.M. Patel, R.F. Browner, T.H. Glen, M.E. Reitta, and J.D. Winefordner, Spec. Letters, 5, 311 (1972)

176. B.M. Patel, T. Reeves, R.F. Browner, D. Molvar and J.D. Winefordner, Appld. Spec. 27, 171 (1973)

177. R.F. Browner and J.D. Winefordner, Spectrochim. Acta. 28b. 263 (1973)

178. R.M. Dagnall, K.C. Thompson and T.S. West, Anal. Chim. Acta. 41, 551 (1968)

179. R.M. Dagnall, R.Pribil and T.S. West, Analyst, 93, 281 (1968)

180. E. Jacobsen. J. Opt. Soc. Am. 39, 1054 (1949)

181. S.V. Baranov, N.R. Ivanov, L.G. Pofrabils, V.V. Kayazev, B.M. Talalaer and E.N. Vasilev, J. Anal. Chem. U.S.S.R. 24, 1354 (1969)

182. C.F. Gallo, Appld. Optics, 10, 2517 (1971)

183. F.M. Hamm, T.L. Martin and P.B. Zeeman, Anal. Chem. 43, 491 (1971)

184. D.N. Hingle, G.F. Kirkbright and T.S. West, Analyst 93, 522 (1968)

185. A.G. Leiga, J.A. McInally, J. Opt. Soc. Am. 57, 317 (1967)

186. J.R. Brandenberger, Rev. Sci. Inst. 42. 1535 (1971)

187. L.F. Phillips, ibid, 42, 1078 (1971)

188. R. Smith, C.M. Stafford and J.D. Winefordner, Canadian Spec. 14, 38 (1969)

189. T.S. West, Endeavour, 26, 44 (1967)

190. G.O. Brink, R. Fluegge and R.J. Hull, Rev. Sci. Inst. 39, 1171 (1968)

191. B. McCarroll, ibid, 41, 279 (1970)

192. E. Jacobsen and G.R. Harrison, J. Opt. Soc. Am. 39, 1054 (1949)

193. J.B. Headridge and J. Richardson, Lab. Prac. 19, 372 (1970)

194. V.B. Gerrard, J. Sci. Inst. 39, 217 (1962)

195. R.G. Brewer, J. Sci. Inst. 32, 1356, (1961)

196. N.P. Penkin and L.N. Shabanova, Opts. and Spec. 14, 5 (1963)

197. K.C. Thompson and P.C. Wildy, Analyst, 95, 776 & 562 (1970)

198. M.J. AlAni, R.M. Dagnall and T.S. West, ibid, 92, 597 (1967)

199. C.F. Bruce and P. Hannaford, Spectrochim. Acta. 26b. 207 (1971)

200. L. Bovey, ibid, 10, 432 (1958)

201. H.E. Radford, Phys. Rev. 126, 1035 (1962)

202. C. Woodward, At. Abs. Newletter, 8, 121 (1969)

203. C.S. Rann, and A.N. Hambly, Anal. Chim. Acta. 32, 346 (1965)

204. G.B. Marshall and T.S. West ibid, 51, 179 (1970)

205. I. Kleinmann and V. Svoboda, Anal. Chem. 41, 1029, (1969)

206. J.I. Dinnin, ibid, 39, 1491 (1967)

207. C.G. Vurek, ibid, 39, 1599 (1967)

208. J. O'Haver and J.D. Winefordner, J. Chem. Ed. 46, 435 (1969)

209. J. O'Haver and J.D. Winefordner, ibid, 46, 241 (1969)

210. J.R. Hollahan, ibid, 43, A401, A497 (1966)

211. J. Norris and T.S. West, Anal. Chim. Acta. 59. 355 & 474 (1972)

212. A. King and D. Bartley, Private communication, Imperial College, England (1974)

213. K.C. Thompson, Ph.D. Thesis London University (1968)

214. R.S. Hobbs, G.F. Kirkbright and T.S. West, Talanta, 18, 859 (1971)

215. D.J. Rose and S.C. Brown, Phys. Rev. 98, 310 (1955)

216. R.H. Healy and J.W. Reed, Behaviour of Slow Electrons in Gases, Sydney Amalgamated Wireless, '41

217. S.C. Brown, Basic Data of Plasma Physics, J. Wiley and Sons, London (1967)

218. J.W. Lathrop, Ph.D. Thesis, M.I.T. (1952)

219. F. Llewellyn-Jones, Editor, The Glow Discharge, Methuen Co. Ltd., London (1966)

220. R.F. Baddour and R.S. Timmins, Editors, The Applicated of Plasmas Chemical Processes. Pergamon Press (1967)

221. W.S. Gleason, and R. Pertel, Rev. Sci. Inst. 42, 1638 (1971)

222. H. Kleiman and S.P. Davis, J. Opt. Sci. Am. 53, 822 (1963)

223. K.M. Aldous, R.M. Dagnall and T.S. West, Anal. Chim. Acta. 44, 457 (1969

224. K.M. Aldous, R.M. Dagnall, S.J. Pratt and T.S. West, Anal. Chem. 41, 1851 (1969)

225. C. Veillon and J.Y. Park, Anal. Chem. 44, 1473, (1972)

226. M.S. Cresser and T.S. West, Anal. Chim. Acta, 51, 530 (1970)

227. R.M. Dagnall, G.F. Kirkbright, T.S. West and R. Wood, Anal. Chem. 42, 1029 (1970)

228. R.M. Dagnall. G.F. Kirkbright, T.S. West and R. Wood, Analyst, 95, 425 (1970).

229. R.M. Dagnall, G.F. Kirkbright, T.S. West, and R. Wood, Anal. Chim. Acta. 47 ½ 407 (1969)

230. J.D. Norris and T.S. West, ibid, 55, 359 (1971)

231. J.D. Norris and T.S. West, ibid, 59, 355 (1972)

232. W.G. Schrenk, S.E. Valents and K.E. Smith, Appld. Spec. 26, 108 (1972)

233. D. Alger, R.M. Dagnall, H.D. Silvester and T.S. West, Anal. Chem. 44, 2255 (1972)

234. M. Hargreaves, Ph. D. Thesis, London University (1972)

235. A. King and A. Sanz-Medel, Private communication, Imperial College, England (1974)

236. D. Johnson, B.L. Sharp and T.S. West, in press (1974)

237. M.P. Bratzel, R.M. Dagnall and J.D. Winefordner, Anal. Chim. Acta 52, 157, (1970)

238. N.J. Prakash and W.W. Harrison, Anal. Chim. Acta, 53, 421 (1971)

239. Rains and Rush, N.B.S. Tech. Notes, 504

240. W.R. Brode, Chemical Spectroscopy, Wiley, N.Y. (1943)

241. J.E. Allan, Spectrochim. Acta, 18, 259, (1962)

242. A.A. Prokoshev, L.K. Chuchalin, B.Z. Iofa and Yu.A Zolotov, J. Anal. Chem. USSR. 27, 1364 (1972)

243. P.W.West, T.G. Lyons and J.K. Carlton, Anal. Chim. Acta. 6, 406 (1952)

244. P.W.West, P Senise and J,K. Carlton, Anal. Chim. Acta, 6, 488 (1952)

245. L. Meites, Polagraphic Techniques. J. Wiley and Sons, N.Y. (1965)

246. J.A. White, W.L. Harper, A.P. Friedman and V.E. Banas, Appld. Spec. 28, 192 (1974)

247. B. Metters and B.G. Cookey, Analyst in press

248. C. Fairless and A.J. Bard, Anal. Chem. 45, 2289 (1973)

249. J.A. Holocombe and R.D. Sacks, Spectrochim. Acta. 28b, 451 (1973)

250. J. Moorhead, Anal. Chem. 45, 2178 (1973)

251. K.E. Burke, Analyst, 97, 19 (1972)

252. B.T.N. Newlands and R.A. Mostyn, AA Newsletter, 10, 223 (1971-)

253. H.T. Delves, G. Shepherd and P. Vinter, Analyst, 96, 257 (1971)

254. J.B. Headridge and J. Richardson, Analyst, 95, 930 (1970)

255. R.C. Rooney, Analyst, 90, 545 (1965)

256. K. Tanaka, Japan Analyst, 10, 1087 (1961)

257. H. Goto and Y. Kakita, J. Chem. Soc. Japan, 82, 1212 (1961)

258. C.L. Luke, Anal. Chim. Acta, 39, 447 (1967)

259. I. Tsukahara and T. Yamamoto, Anal. Chim. Acta. 63, 464 (1973)

260. M.R.G. Taylor, R.M. Dagnall and T.S. West, Lab. Prac. 20, 209 (1971)

261. Y.A. Zolotov and V.I. Golovanov, J. Anal. Chem. USSR, 28, 1 (1973)

262. D. Clark, R.M. Dagnall and T.S. West, Anal. Chim. Acta. 60, 219 (1972)